Colloquium: Topological band theory

A. Bansil*

Department of Physics, Northeastern University, Boston, Massachusetts 02115, USA

Hsin Lin

Department of Physics, Northeastern University, Boston, Massachusetts 02115, USA, Centre for Advanced 2D Materials and Graphene Research Centre, National University of Singapore, Singapore 117546, and Department of Physics, National University of Singapore, Singapore 117542

Tanmoy Das

Centre for Advanced 2D Materials and Graphene Research Centre, National University of Singapore, Singapore 117546, Department of Physics, National University of Singapore, Singapore 117542, and Theoretical Division, Los Alamos National Laboratory, Los Alamos, New Mexico 87545, USA

(published 29 June 2016)

The first-principles band theory paradigm has been a key player not only in the process of discovering new classes of topologically interesting materials, but also for identifying salient characteristics of topological states, enabling direct and sharpened confrontation between theory and experiment. This review begins by discussing underpinnings of the topological band theory, which involve a layer of analysis and interpretation for assessing topological properties of band structures beyond the standard band theory construct. Methods for evaluating topological invariants are delineated, including crystals without inversion symmetry and interacting systems. The extent to which theoretically predicted properties and protections of topological states have been verified experimentally is discussed, including work on topological crystalline insulators, disorder and interaction driven topological insulators (TIs), topological superconductors, Weyl semimetal phases, and topological phase transitions. Successful strategies for new materials discovery process are outlined. A comprehensive survey of currently predicted 2D and 3D topological materials is provided. This includes binary, ternary, and quaternary compounds, transition metal and f-electron materials, Weyl and 3D Dirac semimetals, complex oxides, organometallics, skutterudites, and antiperovskites. Also included is the emerging area of 2D atomically thin films beyond graphene of various elements and their alloys, functional thin films, multilayer systems, and ultrathin films of 3D TIs, all of which hold exciting promise of wide-ranging applications. This Colloquium concludes by giving a perspective on research directions where further work will broadly benefit the topological materials field.

DOI: 10.1103/RevModPhys.88.021004

CONTENTS

*Corresponding author.
bansil@neu.edu

I. INTRODUCTION

Successful prediction of new topological insulator (TI) materials is perhaps the most spectacular triumph of the modern first-principles band theory (Hohenberg and Kohn, 1964; Kohn and Sham, 1965). TIs are an exotic state of quantum matter, which is distinct from the ordinary insulators in that even though electrons cannot conduct in the bulk of the material, surfaces of three-dimensional (3D) TIs and edges of two-dimensional (2D) TIs support metallic or conducting electronic states protected by constraints of time-reversal symmetry (TRS) (Kane and Mele, 2005a, 2005b; Bernevig, Hughes, and Zhang, 2006; Fu and Kane, 2007; Fu, Kane, and Mele, 2007; Moore and Balents, 2007; Roy, 2009). The gapless topological surface and edge states are forged when bonding forces involved in crystal formation are modified in a special manner through relativistic spin-orbit interactions. These metallic states are unique in that they exhibit chirality or locking of the directions of spin and momentum and are not allowed to scatter backward (no "U turns") in the absence of magnetic impurities. The experimental discovery of TIs (König *et al.*, 2007; Hsieh *et al.*, 2008, 2009a, 2009b; Chen *et al.*, 2009; Xia *et al.*, 2009) has focused attention on wide-ranging phenomena in materials driven by spin-orbit coupling (SOC) effects well beyond the traditional role of SOC in determining magnetic properties. In this sense topological materials represent the emergence of spin in quantum matter from being a "spectator" to a "driver," and a shift in focus from the Schrödinger equation to the Dirac equation as the controlling physics. TIs have brought topological considerations front and center in discussing the physics of materials, building on the earlier work on topology and topological orders in condensed matter systems (Thouless *et al.*, 1982; Haldane, 1988; Volovik, 1988; Wen, 1995; Zhang and Hu, 2001; Murakami, Nagaosa, and Zhang, 2004; Sinova *et al.*, 2004). The special symmetry protected electronic states in the TIs hold the exciting promise of providing revolutionary new platforms for exploring fundamental science questions, including novel spin textures and exotic superconducting states as well as for the realization of multifunctional topological devices for thermoelectric, spintronics, information processing, and other applications (Hasan and Kane, 2010; Mas-Ballesté *et al.*, 2011; Qi and Zhang, 2011; Butler *et al.*, 2013; Tsai *et al.*, 2013).

By examining how band structures evolve under spin-orbit interaction, many topologically interesting materials have been predicted. Theoretically predicted 3D TIs span binary, ternary, and quaternary compounds, transition metal and f-electron systems, Weyl and 3D Dirac semimetals, complex oxides, organometallics, skutterudites, and antiperovskites as summarized in the materials inventory given in the Appendix, Table I. In many cases, even though the pristine phase is found to be topologically trivial, computations show that the material could be coaxed into assuming a nontrivial phase through alloying, strain, or confinement. Among the practically realized materials, nontrivial compounds which were first predicted theoretically before experimental verification, include $Bi_{1-x}Sb_x$ (Fu and Kane, 2007; Hsieh *et al.*, 2008) for the Z_2 phase (Sec. IV.B.1), SnTe (Hsieh *et al.*, 2012; Dziawa *et al.*, 2012; Tanaka *et al.*, 2012; Xu *et al.*, 2012a) as a topological crystalline insulator (Sec. IV.B6), Cd_3As_2 and Na_3Bi (Z. Wang *et al.*, 2012, 2013; Ali *et al.*, 2014; Borisenko *et al.*, 2014; Liu *et al.*, 2014b; Neupane *et al.*, 2014b; Xu *et al.*, 2015c) as 3D Dirac-cone semimetals, and TaAs class (Huang *et al.*, 2015; Lv *et al.*, 2015; Weng *et al.*, 2015; Xu *et al.*, 2015a, 2015b; L. X. Yang *et al.*, 2015; Zhang *et al.*, 2016) as Weyl semimetals (Sec. IV.H). In the widely studied Bi_2Se_3 (Xia *et al.*, 2009; H. Zhang *et al.*, 2009) and $GeBiTe_4$ (Xu *et al.*, 2010) TIs, experimental verification and theoretical prediction occurred simultaneously. Many theoretically predicted TIs, however, have not been realized experimentally. The early experimental work on the first generation elemental TIs, Bi/Sb, quickly gave way to the second generation binary materials Bi_2Se_3, Bi_2Te_3, Sb_2Te_3, and their alloys, followed by work on ternary and quaternary materials, which offer greater flexibility and tunability with respect to lattice parameters, chemical compositions, band gaps, and transport properties.

Despite the progress made in synthesizing 3D TIs, the materials realization of 2D TIs or quantum spin Hall (QSH) insulators is still limited to the HgTe/CdTe (König *et al.*, 2007) and InAs/GaSb/AlSb (Knez, Du, and Sullivan, 2011) quantum well systems with small band gaps of ∼4–10 meV. In both these 2D materials, theoretical prediction preceded experimental verification (Bernevig, Hughes, and Zhang, 2006; Liu *et al.*, 2008). On the other hand, first-principles computations on atomically thin films of many elements and their alloys, and ultrathin films of most 3D TIs, yield numerous stable structures capable of supporting the QSH phase with band gaps large enough in many cases for room-temperature applications, see the Appendix (Table I) for an inventory. In sharp contrast to the case of graphene (Castro Neto *et al.*, 2009; Das Sarma *et al.*, 2011), which possesses a flat structure in its pristine form, the structure of most atomically thin films is naturally buckled so that their inversion symmetry can be broken by an external electric field (Mas-Ballesté *et al.*, 2011; Butler *et al.*, 2013).

A freestanding silicene sheet (one atom thick crystal of Si), for example, can harbor a rich phase diagram as a function of external electric and magnetic fields in which it transitions from being a band insulator, to a quantum anomalous or spin Hall insulator, to a valley polarized metal, to a spin valley polarized metallic phase (Liu, Feng, and Yao, 2011; Drummond, Zólyomi, and Fal'ko, 2012; Ezawa, 2012; Tabert and Nicol, 2013; Tsai *et al.*, 2013). A silicene nanoribbon could thus be used to manipulate spin-polarized currents (Tsai *et al.*, 2013; Gupta *et al.*, 2014; Saari *et al.*, 2014) via gating without the need to switch magnetic fields. Moreover, a rich tapestry of morphologies and topological characteristics is generated when we consider layer-by-layer growth of thin films on various substrates (Mas-Ballesté *et al.*, 2011; Butler *et al.*, 2013; Z.-Q. Huang *et al.*, 2013).

While a great deal of the existing literature on TIs has been concentrated on the Z_2 insulators in which the gapless surface and edge states are protected by the TRS, interest in exploring the role of crystal symmetries in creating protected states more generally has been growing. This has given birth to a new class of TIs called topological crystalline insulators (TCIs) (Fu, 2011; Hsieh *et al.*, 2012). In this connection, mirror symmetry has received special attention, on the basis of which band theory computations predicted SnTe and $Pb_{1-x}Sn_x(Se, Te)$ alloys to harbor a TCI state (Hsieh *et al.*, 2012), which was verified essentially immediately afterward by three different experimental groups (Dziawa *et al.*, 2012; Tanaka *et al.*, 2012; Xu *et al.*, 2012a). The Dirac-cone structure and the associated spin texture of surface states in a TCI is quite distinct from that in the more common TIs (Fu, 2011; Y. J. Wang *et al.*, 2013). For example, the TCI SnTe supports an even number (not an odd number that is a hallmark of a TI) of metallic Dirac-cone states on crystal surfaces, which are symmetric under reflections in the $\{110\}$ planes. The $Pb_{1-x}Sn_x(Se, Te)$ system is the first and still the only materials realization of a TCI; see the Appendix (Table I) for other materials predictions.

Topological materials practically realized to date are essentially "weakly correlated" in the sense that the standard density functional theory (DFT) based independent particle picture (Hohenberg and Kohn, 1964; Kohn and Sham, 1965) provides a reasonably robust description of their electronic structures, limitations of the local density approximation (LDA) and generalized gradient approximation (GGA) in correctly capturing the size of the band gap in semiconductors and insulators notwithstanding. Methods for treating strong electron correlation effects under the rubrics of LDA + U, *GW*, dynamical mean-field theory (DMFT), and various type of exchange-correlation functionals have been reviewed extensively in the literature (Maier *et al.*, 2005; Held *et al.*, 2006; Kotliar *et al.*, 2006; Capelle and Campo, 2013; Das, Markiewicz, and Bansil, 2014; Peverati and Truhlar, 2014). It is natural to expect that the combined effects of strong correlations and SOC would give rise to entirely new classes of TIs. Here, Mott (X. Zhang *et al.*, 2012; Deng, Haule, and Kotliar, 2013) and Kondo insulators (Dzero *et al.*, 2010; Weng *et al.*, 2014) provide a natural breeding ground for finding correlated TIs. The iridates, which exhibit many exotic phenomena through the interplay of $5d$ electrons and strong SOC, are drawing interest as candidate materials, although their topological nature remains elusive (Wan *et al.*, 2011; Yang, Lu, and Ran, 2011; Carter *et al.*, 2012). Among the f-electron systems, attention has been focused on SmB_6 (Cooley *et al.*, 1995; Frantzeskakis *et al.*, 2013; Jiang *et al.*, 2013; Neupane *et al.*, 2013; N. Xu *et al.*, 2013; Kim, Xia, and Fisk, 2014), which might support a topological Kondo insulator state as the bulk becomes insulating at low temperatures.

Many aspects of the electronic structures and properties of topological materials are difficult or impractical to model within a totally first-principles framework, and as a result, a variety of effective model Hamiltonians are invoked frequently in the field. Material specificity can be obtained by choosing parameters entering the model Hamiltonian to mimic appropriate first-principles results to varying degrees, although generic features can often be captured via minimal models consistent with the symmetries inherent in particular problems. In this way, new insights have been enabled in the characteristics of topological superconductors (Fu and Kane, 2008; Qi, Hughes *et al.*, 2009) and their interfaces with magnetic and nonmagnetic materials (Qi, Li *et al.*, 2009; Wray *et al.*, 2011; Oroszlány and Cortijo, 2012; Wei *et al.*, 2013), effects of external electric and magnetic fields on 2D and 3D TIs (Essin, Moore, and Vanderbilt, 2009; Cho *et al.*, 2011; Ojanen, 2012; H. Zhu *et al.*, 2013; Baasanjav, Tretiakov, and Nomura, 2014), evolution of electronic states with dimensionality (Y. S. Kim *et al.*, 2011; Bansal *et al.*, 2012; M.-X. Wang *et al.*, 2012; Glinka *et al.*, 2013; Vargas *et al.*, 2014), and various exotic quantum phenomena possible in the TIs, e.g., Majorana fermions (Fu and Kane, 2008; Roy and Kallin, 2008; Schnyder *et al.*, 2008; Kitaev, 2009; Elliott and Franz, 2015), axions (Essin, Moore, and Vanderbilt, 2009; Li *et al.*, 2010), magnetic monopoles (Qi, Li *et al.*, 2009), and fractional excitations (Wen, 1995; Grushin *et al.*, 2012; Li, Liu *et al.*, 2014; Teo and Kane, 2014), which are not amenable to treatment on a first-principles basis.

This review is organized as follows. Section II discusses underpinnings of the topological band theory. We delineate methods for characterizing the topology of the bulk band structure in terms of the Z_2 invariants, including surface and edge state computations and the treatment of interacting systems (Secs. II.A–II.D). The role of model Hamiltonians in addressing various classes of problems, which are not amenable to first-principles treatment, is pointed out (Sec. II.E), and the extent to which theoretically predicted properties and protections of topological states have been verified experimentally is discussed (Sec. II.F). Section III turns to topological phases and transitions in quantum matter more broadly and considers the following: topological crystalline insulators (Sec. III.A), disorder and interaction driven TIs (Sec. III.B), topological superconductors (Sec. III.C), Weyl and 3D Dirac semimetal phases (Sec. III.D), and topological phase transitions (TPTs) (Sec. III.E). Section IV provides a survey of currently predicted topological materials. Successful strategies for a new materials discovery process are summarized (Sec. IV.A), and salient features of different types of 3D and 2D topological materials are highlighted, including 2D thin-film materials (Sec. IV.D). The Appendix (Table I) provides an inventory of 2D and 3D topological materials reported in the literature, along with pertinent references in each case.

Although this review is focused on band theory work, we have made an effort to provide a broader perspective to the extent possible within space limitations.

Topological insulators have been reviewed previously in the *Reviews of Modern Physics* (Hasan and Kane, 2010; Qi and Zhang, 2011). A number of other reviews on various aspects of TIs have appeared elsewhere (Feng and Yao, 2012; Yan and Zhang, 2012; Ando, 2013; Bardarson and Moore, 2013; Beenakker, 2013; Dzero and Galitski, 2013; Fruchart and Carpentier, 2013; Okuda and Kimura, 2013; Zhang and Zhang, 2013; Wehling, Black-Schaffer, and Balatsky, 2014). The literature cited in this review should not be considered exhaustive, although it is fairly complete as of the submission date, and includes some subsequent updating. We have tended to cite more recent publications in many cases as entry points for accessing earlier literature.

II. UNDERPINNINGS OF TOPOLOGICAL BAND THEORY

The electronic spectrum of a crystal can be organized in the form of energy bands as a function of the crystal momentum $\mathbf{k}$, which is guaranteed to be a good quantum number due to the translational symmetry of the lattice. Practical band structure computations invoke a one-particle or an effective independent electron picture within the framework of the DFT proposed by Hohenberg and Kohn (1964) and its implementation by Kohn and Sham (1965). The DFT based band structure construct has provided a remarkable ordering principle for understanding wide-ranging properties of metals, semiconductors, and insulators, and an encoding of the materials "genome." In a metal, electrons occupy partially filled bands, which stretch across the Fermi energy; in an insulator filled and empty states are separated by a large band gap, while in a semiconductor this band gap is small enough to be bridged by thermal or other excitations. A band insulator, which is described by a gap in the one-particle band structure, is not the only type of insulator, and many other possibilities arise when additional broken or invariant symmetries are taken into account.

Lattice symmetries have always played a substantial role in the band theory of solids. Topological band theory, especially insofar as first-principles band structures are concerned, expands the consideration of symmetries to encompass the TRS. In the context of tight-binding model Hamiltonians, however, a further expansion is possible by including effects of the particle-hole symmetry characteristic of the superconducting state. Just as lattice symmetries have led to classification schemes based on point and space groups of the lattice, inclusion of time-reversal and/or particle-hole symmetries in the mix yields new schemes for classifying allowed exotic states of quantum matter (Schnyder *et al.*, 2008; Kitaev, 2009; Hasan and Kane, 2010; Hughes, Prodan, and Bernevig, 2011; Qi and Zhang, 2011; Fang, Gilbert, and Bernevig, 2012; Chiu, Yao, and Ryu, 2013; Slager *et al.*, 2013; Shiozaki and Sato, 2014).

Topological band theory in effect involves a layer of analysis and interpretation for assessing the topological characteristics of the bulk electronic spectrum, which sits on top of a standard band structure calculation. The spin-orbit interaction must be included in the computation. Nonrelativistic or semirelativistic treatment, which cannot mix up- and down-spin states, is generally not sufficient. Even when the existence of topological states can be inferred from symmetry considerations, appropriate surface and edge state computations must be undertaken to determine the number, spin texture, and location in energy and momentum of these states on specific surfaces and edges. Theoretical predictions along these lines are playing a key role in identifying particular topological states experimentally and in the discovery of new topological materials.

A. Characterizing a TI within the DFT

The telltale signature of the possibility that the band structure of an insulator might harbor a nontrivial topological phase is the inversion of energy levels with respect to their natural order around the band gap at high symmetry points in the Brillouin zone (BZ) as shown in the schematic drawing of Fig. 1. Several points should be clearly understood here: (1) Either the band inversion or the opening of the band gap must be driven by the SOC, and (2) "natural order" means the order of appropriate atomic levels. These are s and p orbitals in many semiconductors where the energy of the s level lies above that of the p level, but the s orbital experiences an attractive relativistic potential strong enough to pull it below the p orbitals in the solid. The inversion can, however, involve any pair of orbitals. Examples of materials, which involve orbitals with higher principal quantum numbers or with different magnetic quantum numbers in the inversion process, will be seen in Sec. IV. (3) Finally, an inverted band structure by itself does not prove the existence of a nontrivial phase, but further analysis is required to establish its topological nature.

Three different types of approaches, which are discussed at length in the following sections, can be used to assess the topological characteristics of the band structure: (1) Compute Z_2 topological invariants, which encode time-reversal invariance properties of the bulk band structure. (2) Use adiabatic continuity arguments where one attempts to connect the unknown band structure to a known topological or nontopological band structure via a series of adiabatic or slowly varying transformations of the Hamiltonian without closing the band gap. And (3) directly compute the spectrum of surface or edge states which connect the bulk conduction and valence bands.

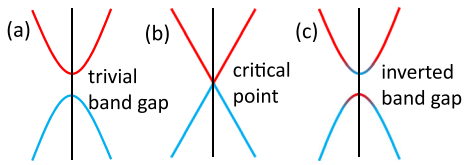

FIG. 1. Schematic band inversion between two bands derived from the natural order of atomic levels. The trivial band gap in (a) closes at a critical point in (b), and reopens inverted in (c) with the two states swapping their orbital characters at the symmetry point.

B. Computation of Z_2 topological invariants

Among the various formulations for the computation of Z_2 topological invariants (Kane and Mele, 2005a), the Fu-Kane criterion (Fu, Kane, and Mele, 2007) is especially well suited for analyzing band structures of crystals with inversion symmetry. Evaluation of Z_2 in systems without inversion symmetry and interacting systems is discussed next.

The Fu-Kane approach connects the Z_2 invariants to the matrix elements of Bloch wave functions at time-reversal invariant momentum (TRIM) points in the BZ. There are four TRIM points in the 2D BZ and eight in the 3D case. TRS yields one unique Z_2 invariant ν in 2D, but four distinct Z_2 invariants $(\nu_0;\nu_1\nu_2\nu_3)$ in 3D. In 2D, the two values of ν separate topological (or QSH) and nontopological states. The situation in 3D is more complicated with the involvement of four Z_2 invariants. Here $\nu_0 = 1$ identifies a "strong" TI in the sense that the system is robust against weak time-reversal invariant perturbations, and any of its surfaces is guaranteed to host gapless surface bands. An ordinary insulator is obtained when all four invariants are zero. In the mixed case where $\nu_0 = 0$ and at least one of the indices ν_1, ν_2, or ν_3 is nonzero, the 3D material can be viewed as a stacking of 2D TIs, and it is considered a "weak" TI in the sense that it is less robust against perturbations.

Formally, Fu and Kane introduced the quantities $\delta_i = \mathrm{Pf}[w(\Lambda_i)]/\sqrt{\mathrm{Det}[w(\Lambda_i)]} = \pm 1$, where Pf denotes the Pfaffian of unitary matrix $[w(\Lambda_i)]$ with components $w_{mn}(\mathbf{k}) = \langle u_m(\mathbf{k})|\Theta|u_n(-\mathbf{k})\rangle$. $u_m(\mathbf{k})$ are Bloch states for band m, Θ is the antiunitary time-reversal operator, and Λ_i are the TRIM points in the BZ. The Z_2 invariant ν_0 in 3D or ν in 2D is given by

$$(-1)^{\nu} = \prod_{i=1}^{n} \delta_i, \tag{1}$$

where n is 4 in 2D and 8 in 3D. In 3D, the other three Z_2 invariants are obtained from partial products of sets of four δ_i's, similar to that of Eq. (1), corresponding to TRIM points lying in three independent planes of the BZ. In a crystal with inversion symmetry, Bloch wave functions are also eigenfunctions of the parity operator with eigenvalues $\xi_m(\Lambda_i) = \pm 1$ and the formula for δ_i's simplifies to (Fu, Kane, and Mele, 2007)

$$\delta_i = \prod_m \xi_m(\Lambda_i), \tag{2}$$

where the product is over the parities of pairs of occupied Kramer's doublets resulting from TRS at the TRIM points Λ_i without multiplying the corresponding TR partners.

Figure 2 shows the band structure of a 2D bilayer of Bi (Z.-Q. Huang *et al.*, 2013) along with parities of the three valence bands at the four TRIM points (one Γ and three M) as an example of the application of Eq. (2). From Fig. 2(a), $\delta_\Gamma = -1$, as the product of $+1$, -1, and $+1$. Similarly, $\delta_M = +1$, so that from Eq. (1), $\nu = 1$, and we have a nontrivial TI or a QSH state. The same computation for the bands of Fig. 2(b) yields $\nu = 0$ or the trivial state. The QSH state is seen to result from the band inversion at M, which is accompanied

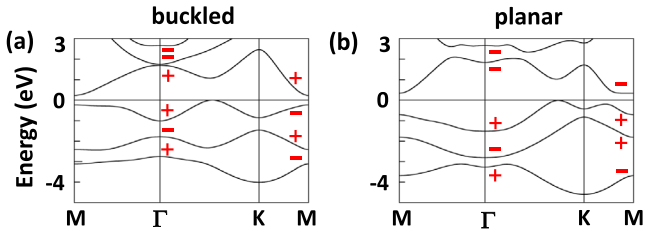

FIG. 2. Parities of bands at TRIM points in (a) buckled and (b) planar Bi thin films. Even (odd) parity is labeled + (−). Parity inversion between (a) and (b) is seen around the band gap at the M point. From Z.-Q. Huang *et al.*, 2013.

by a change in the parity of the two states involved and thus changes the value of ν.

1. Systems without inversion symmetry

The preceding parity analysis is not applicable to systems without a center of inversion symmetry. However, in 2D, Z_2 can be cast in the general form (Fu and Kane, 2006)

$$Z_2 = \frac{1}{2\pi}\left[\oint_{d\tau} \boldsymbol{A}(\mathbf{k})dl - \int_{\tau} F(\mathbf{k})d\tau\right] \mathrm{mod}2, \tag{3}$$

where $\boldsymbol{A}(\mathbf{k}) = i\sum_{n=1}^{N}\langle u_n(\mathbf{k})|\nabla_k|u_n(\mathbf{k})\rangle$ is the Berry connection (Berry, 1984; Xiao, Chang, and Niu, 2010) with a sum over occupied states, and $F(\mathbf{k}) = \nabla_k \times \boldsymbol{A}(\mathbf{k})$ is the corresponding Berry curvature. The integrals are over half of the 2D BZ surface τ and its boundary $d\tau$. The 3D extension involves computing Z_2 from Eq. (3) for six different 2D tori obtained by taking various pairs of TRIM points in the 3D BZ. Several half Heusler compounds were investigated by Xiao *et al.* (2010) along these lines using discrete $\mathbf{k}$ meshes (Fukui and Hatsugai, 2007).

Berry connection $\boldsymbol{A}(\mathbf{k})$ and Berry curvature $F(\mathbf{k})$ in Eq. (3) are important quantities that can be constructed from Bloch wave functions and enter the computation of topological properties of materials more generally. For example, an anomalous contribution to Hall conductivity is given by appropriate line and surface integrals of $\boldsymbol{A}(\mathbf{k})$ (Haldane, 2004). Also, the magnetoelectric response can be obtained from a BZ integral over a Chern-Simons 3-form involving $A_\mu^{mn}(\mathbf{k}) = -i\langle u_m(\mathbf{k})|\nabla_\mu|u_n(\mathbf{k})\rangle$ and its derivatives (Qi, Hughes, and Zhang, 2008). First-principle computations of magnetoelectric response along these lines have been carried out in trivial and nontrivial insulators (Coh *et al.*, 2011).

2. Interacting systems

The single-particle Bloch states are not eigenstates in an interacting system, and therefore the spectral function is no longer a δ function but develops a finite width as a function of E for a given $\mathbf{k}$, or equivalently, as a function of $\mathbf{k}$ for a given E. This is also the case in a disordered system due to disorder induced smearing of states (Schwartz and Bansil, 1974; Stocks, Temmerman, and Gyorffy, 1978; Bansil, 1979a, 1979b; Bansil *et al.*, 1999). Using field theoretic methods Z_2 can be evaluated in terms of just the zero frequency one-particle Green's function $G(0,\mathbf{k})$ of the interacting system

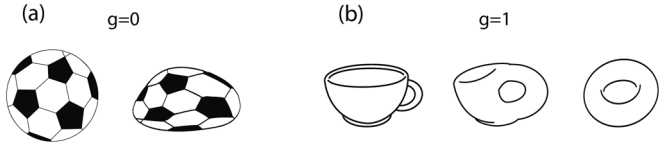

FIG. 3. Spherical and crumpled balls have the same genus of $g = 0$, in (a), but both the doughnut and the coffee cup with one hole in (b) are characterized by $g = 1$.

(Wang and Zhang, 2012, 2013). In inversion-symmetric crystals, the formulas become more tractable as Z_2 can be obtained from the parities of eigenvectors of the Hermitian matrices $G(0, \Lambda_i)$ at the TRIM points Λ_i in the spirit of Eq. (2).

C. Adiabatic continuation approach

Topological invariants are a manifestation of the overall geometry or curvature of the bulk system, and therefore two different systems with a similar bulk property or "genus" are topologically equivalent (Hasan and Kane, 2010; Essin and Gurarie, 2011). Figure 3(a) shows surfaces of spherical and crumpled balls, both with the genus $g = 0$, where the genus counts the number of holes (Nakahara, 1990). The doughnut and the coffee cup similarly have one hole or $g = 1$. The point is that we can obtain the genus of the crumpled ball from that of the spherical ball so long as we can smoothly or adiabatically deform one into the other without introducing holes. Similarly, changes in the Hamiltonian, which do not induce a band inversion anywhere in the BZ, will not change the value of Z_2. Examples of "deformations" are strains in the crystal structure, changes in the nuclear charges of constituent atoms while maintaining charge neutrality, or changes in the strength of the SOC.

Adiabatic continuity arguments provide a powerful tool for connecting different topological families and are used extensively for predicting new materials, especially systems without inversion symmetry, by starting from a known topological insulator (Al-Sawai *et al.*, 2010; Lin, Wray *et al.*, 2010; Chadov *et al.*, 2013; Lin, Das, Wang *et al.*, 2013). Figure 4 gives an illustrative example of how HgTe can be connected to the noncentrosymmetric half Heusler compound YPtSb as follows. Aside from changes in lattice constants, one first inserts Kr atoms into empty positions in the zinc-blende structure to obtain the hypothetical half Heusler compound KrHgTe, where the inert Kr atoms hardly affect the low-energy Hamiltonian. The nuclear charges on Kr, Hg, and Te are then adjusted slowly by setting $Z_{\mathrm{Kr}} = 36 + 2x + y$, $Z_{\mathrm{Hg}} = 80 - 2x$, and $Z_{\mathrm{Te}} = 52 - y$, and varying x and y. In

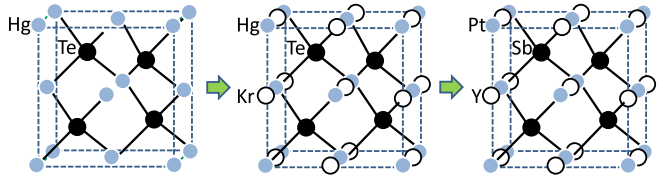

FIG. 4. Adiabatic transformation of the known topologically nontrivial HgTe into the half Heusler compound YPtSb. From Lin, Wray *et al.*, 2010.

the phase space of Hamiltonians defined by the parameters x and y, no band inversions are found numerically when one connects KrHgTe at $x = 0$, $y = 0$ to YPtSb at $x = 1$, $y = 1$, proving that YPtSb and HgTe are topologically equivalent (Lin, Wray *et al.*, 2010).

D. Surface and edge state computation

While the existence of gapless surface states on the interface of a TI with vacuum or another nontopological material is guaranteed by bulk-boundary correspondence considerations (Hasan and Kane, 2010; Essin and Gurarie, 2011), an actual computation must be carried out to ascertain the precise nature of these states. This can be done by considering a 2D slab of a 3D material or a 1D ribbon in 2D (Fu and Kane, 2007; Fu, Kane, and Mele, 2007; Xia *et al.*, 2009; H. Zhang *et al.*, 2009; Wang and Chiang, 2014). Topological surface states must connect valence and conduction bands by crossing the Fermi level (E_{F}) an odd number of times. The degeneracy of two surface bands at the TRIM points is protected by TRS, yielding linearly dispersing Dirac cones. The robustness of the gapless surface states has been demonstrated even when the dangling bond states dominate (Lin *et al.*, 2013). Topological surface states should be distinguished sharply from the well-known boundary states that arise in normal insulators with a long history in solid-state physics in that the latter type of states are less robust and can be removed by appropriate surface treatment (Hasan and Kane, 2010).

First-principles surface state calculations are computationally demanding, and the interpretation of results can be complicated by the spurious gaps resulting from interaction between the top and bottom surfaces of a finite slab. Figure 5 gives an illustrative example of a first-principles surface state computation of a Γ-centered Dirac cone. The constant energy contours on the right side of the figure are seen to be circular with a helical spin texture at 50 meV above the Dirac point, hexagonal at 150 meV, and snowflake-like at 200 meV with significant hexagonal warping and out-of-the-plane spin

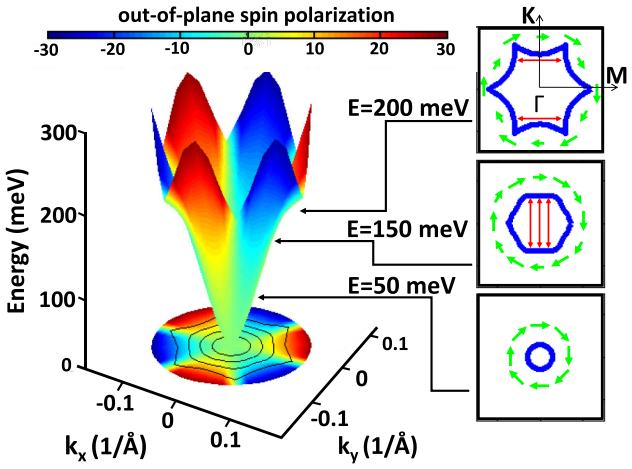

FIG. 5. First-principles surface state dispersion and out-of-the-plane spin polarization of the Dirac cone in Bi_2Te_3. Constant energy contours and the associated spin textures are shown at various energies above the Dirac point. From Hasan, Lin, and Bansil, 2009.

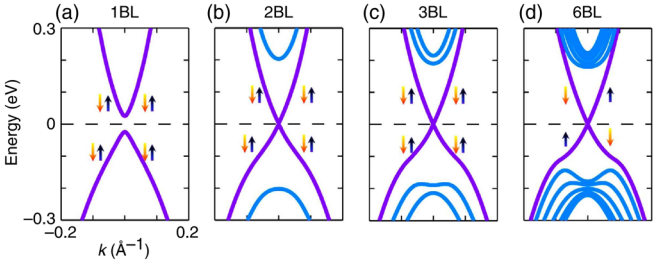

FIG. 6. Evolution of the electronic spectrum as a function of the number of bilayers (BLs). From Das and Balatsky, 2013.

component. There also are in-plane deviations in that the spin direction is not always perpendicular to **k** (Fu, 2009; Basak *et al.*, 2011).

E. Model Hamiltonians

A large variety of model Hamiltonians have been invoked for investigating 2D and 3D topological materials. For a few examples, see Haldane (1988), Kane and Mele (2005a), Bernevig, Hughes, and Zhang (2006), Fu (2009), H. Zhang *et al.* (2009), Dzero *et al.* (2010), Basak *et al.* (2011), and Das and Balatsky (2013). Some are minimal and generic while others attempt more realism and material specificity by appealing to first-principles results, including efforts to construct localized Wannier-type basis functions to reproduce bulk band structures (Marzari and Vanderbilt, 1997). Figure 6 gives an example of how the electronic spectrum evolves with film thickness using the model of Das and Balatsky (2013), which builds the 3D crystal by stacking 2D bilayers (BLs) with opposite Rashba-type SOC in adjacent layers. Emergence of the topological Dirac cone at six BLs (6BL) is seen from the nontopological 1BL and 2BL films. Model Hamiltonians become unavoidable for addressing the superconducting state and other problems where first-principles treatment is not practical.

F. Topological properties and protections

We now discuss the extent to which the unique theoretically predicted helical spin textures and suppression of backscattering of topological surface states, dimensional crossover in thin films, and unusual magnetoelectric and Hall effects have held up to experimental verification.

Dirac-cone dispersions and helical spin textures have been observed in angle-resolved photoemission spectroscopy (ARPES) experiments from a variety of topological materials in substantial accord with theoretical predictions, although the predicted position of E_F with respect to the Dirac point is often not in agreement with measurements due to uncertain doping of naturally cleaved surfaces (Xia *et al.*, 2009). It has been demonstrated experimentally that the position of E_F with respect to the Dirac point in the TIs can be manipulated via various dopings, which is important for reaching the topological transport regime, controlling carrier density, and achieving *n*- or *p*-type doping for developing applications (Hor *et al.*, 2009; Hsieh *et al.*, 2009a; Wray *et al.*, 2010; Kong *et al.*, 2011). Magnetic doping with Fe, Mn, and Cr dopants has also been carried out (Okada *et al.*, 2011; Wray *et al.*, 2011).

The predicted suppression of backscattering channels (Fu, 2009; Lee *et al.*, 2009; Zhou *et al.*, 2009) has been observed in quasiparticle interference (QPI) patterns obtained from measured scanning tunneling spectra (Roushan *et al.*, 2009). Moreover, as expected, the backscattering channels are seen to open up when magnetic impurities are introduced (Okada *et al.*, 2013). Although backscattering is the only channel available to 1D edge states, this is not the case for 2D surface states. Scattering in a 3D TI can be enhanced due to band structure effects on the Dirac-cone states such as hexagonal warping and deviation of dispersion from linearity, and the mixing of various orbitals, which can also reduce the spin polarization of surface states substantially (Fu, 2009; Basak *et al.*, 2011). Resonances can be created by disorder and impurities as shown theoretically (Biswas and Balatsky, 2009; Black-Schaffer and Balatsky, 2013), and observed in scanning tunneling microscopy (STM) and scanning tunneling spectroscopy (STS) experiments (Alpichshev *et al.*, 2012; Teague *et al.*, 2012). Stronger localization can be induced by strong scalar disorder (Li *et al.*, 2009; Guo *et al.*, 2010) and magnetic impurities (Biswas and Balatsky, 2009; Alpichshev *et al.*, 2012).

Topological surface states can be gapped by finite size effects in thin films, due to interactions between the top and bottom surfaces. Such gapped Dirac cones have been shown to appear via ARPES and STM experiments in Bi_2Se_3 films of thickness less than 6 quintuple layers (Y. Zhang *et al.*, 2010; M.-X. Wang *et al.*, 2012; Neupane *et al.*, 2014b), where the critical thickness depends on the size of the bulk band gap. Notably, the 2D QSH phase is predicted to emerge in thin films of many 3D TIs (Lin, Markiewicz *et al.*, 2010; Liu *et al.*, 2010; Ebihara *et al.*, 2012; Singh *et al.*, 2013).

Topological surface states exhibit novel magnetoelectric effects and non-Abelian axion dynamics described by the term $(\theta/4\pi)\mathbf{E}\cdot\mathbf{B}$ in the electromagnetic action (Wilczek, 1987). The axion field or axion angle θ is related to the magnetoelectric polarization $P_3 = \theta/2\pi$ (Qi, Hughes, and Zhang, 2008). In a gapped surface state, changes in θ are associated with a surface Hall conductivity (Hasan and Kane, 2010), which has been verified by Shubnikov–de Hass oscillation measurements in Bi_2Te_3 (Qu *et al.*, 2010; Xu *et al.*, 2014). Another interesting effect first predicted theoretically in Bi_2Se_3, Bi_2Se_3, and Sb_2Te_3 films doped with Cr and Fe is the quantum anomalous Hall effect (Yu *et al.*, 2010), which has been observed in thin films of Cr-doped $(Bi, Sb)_2Te_3$ (Chang *et al.*, 2013). The heterostructure of a TI with a magnetic insulator can lead to a large magnetic gap in the topological surface state (Eremeev *et al.*, 2013; Luo and Qi, 2013).

III. OTHER TOPOLOGICAL STATES OF QUANTUM MATTER

Although this section discusses many prominent phases of quantum matter, a large number of other exotic possibilities exist in principle (Thouless *et al.*, 1982). The classification can be based on various combinations of TRS, crystal space-group symmetries, and particle-hole symmetry in superconductors (Schnyder *et al.*, 2008; Kitaev, 2009; Hasan and Kane,

2010; Hughes, Prodan, and Bernevig, 2011; Fang, Gilbert, and Bernevig, 2012; Chiu, Yao, and Ryu, 2013; Slager *et al.*, 2013; Shiozaki and Sato, 2014).

A. Topological crystalline insulator

In a TCI, spatial crystalline symmetries are the source of protection of topological states (Fu, 2011). TCIs are a natural extension of the Z_2 TIs in which topological states are protected by the TRS. The hallmark of a TCI is the existence of metallic surface states with novel characteristics on high symmetry crystal faces. These surface states form a highly tunable 2D electron gas in which the band gap can be opened and tuned by external electric field or strain with potential applications in field-effect transistors, photodetectors, and nanoelectromechanical systems (J. Liu *et al.*, 2014). SnTe and $Pb_{1-x}Sn_x(Se, Te)$ alloys were the first TCI system driven by SOC predicted theoretically and subsequently realized experimentally (Hsieh *et al.*, 2012; Dziawa *et al.*, 2012; Tanaka *et al.*, 2012; Xu *et al.*, 2012a).

It is possible to realize a TCI without SOC. An example is the model of Fu (2011) in which topological surface states are protected by the combination of TRS and point-group symmetries for spinless fermions. For analyzing the topological invariant, note that for spinless fermions, $(TU)^2 = -1$ in a TCI, where U is the unitary operator for the point-group symmetry operation, and T is the antiunitary time-reversal operator. This is equivalent to the time-reversal operator Θ for spinfull fermions. Therefore, although T itself does not guarantee twofold degeneracy, the combination TU for C_4 symmetry gives fourfold degeneracy at the four momentum points: $\Gamma = (0, 0, 0)$, $M = (\pi, \pi, 0)$, $Z = (0, 0, \pi)$, and $A = (\pi, \pi, \pi)$. The topological invariant ν_0 is given by

$$(-1)^{\nu_0} = \delta_{\Gamma M}\delta_{AZ}, \tag{4}$$

where

$$\delta_{\boldsymbol{k}_1\boldsymbol{k}_2} = e^{i\int_{k_1}^{k_2} d\mathbf{k}\cdot\mathbf{A}_\mathbf{k}} \frac{\mathrm{Pf}[w(\boldsymbol{k}_2)]}{\mathrm{Pf}[w(\boldsymbol{k}_1)]} \tag{5}$$

in terms of the Berry connection $\mathbf{A}_{\boldsymbol{k}}$, see Eq. (3), and Pfaffians of antisymmetric matrices $w(\boldsymbol{k}_i)$, where $w_{mn}(\boldsymbol{k}_i) = \langle u_m(\boldsymbol{k}_i)|UT|u_n(-\boldsymbol{k}_i)\rangle$. The line integrals are between the points $\boldsymbol{k}_1$ and $\boldsymbol{k}_2$ in the corresponding 2D planes.

B. Disorder or interaction driven TIs

Anderson's pioneering work showed that disorder can lead to a metal-insulator transition (Anderson, 1958). For a variety of tight-binding models, the existence of a disorder induced inverted insulating gap has been shown in 2D as well as 3D systems and supported by the observation of quantized conductance when the E_F lies in the gap (Li *et al.*, 2009; Guo *et al.*, 2010).

An axion insulator has a quantized magnetoelectric response given by the axion angle θ, which assumes a quantized value of π in the topological state (Essin, Moore, and Vanderbilt, 2009). For a commensurate antiferromagnetic insulator, the $\theta = \pi$ state can be obtained through the combination of time-reversal and lattice translational symmetries (Mong, Essin, and Moore, 2010). The axion insulator state is theoretically predicted in magnetic systems such as the iridates (Wan *et al.*, 2011) and the osmium compounds in the geometrically frustrated spinel structure (Wan, Vishwanath, and Savrasov, 2012). Since TRS is broken, axion insulators lack protected surface states.

A quantum anomalous Hall (QAH) insulator is another example of a TRS breaking state in which band inversion between the majority and minority spin states is driven by the magnetic exchange energy. This state is theoretically predicted in a number of models, following the original proposal of Haldane with bond currents on a honeycomb lattice (Haldane, 1988). These models include localization of band electrons (Onoda and Nagaosa, 2003), a two-band model of a 2D magnetic insulator (Qi, Wu, and Zhang, 2006), and magnetically doped topological (crystalline) insulator thin films (Yu *et al.*, 2010; Wang, Liu, and Liu, 2013b; Fang, Gilbert, and Bernevig, 2014) or even trivial thin films (Doung *et al.*, 2015).

C. Topological superconductors

The form of the low-energy Hamiltonian of a fully gapped superconductor is similar to that of a TI in many ways. A topological superconductor is obtained when the bulk system has a pairing gap, but supports gapless Majorana modes at the boundary (Roy and Kallin, 2008). For instance, the TRS breaking (chiral $p + ip$) and TRS preserving $p \pm ip$ pairing states are analogous to the integer quantum Hall and quantum spin Hall states, respectively. The former case supports chiral propagating Majorana edge modes, while the latter supports the counterpropagating Majorana edge modes (Elliott and Franz, 2015) which are topologically protected against time-reversal invariant perturbations.

Chiral superconductivity has been predicted in Sr_2RuO_4 (Mackenzie and Maeno, 2003), doped graphene (Pathak, Shenoy, and Baskaran, 2010; Nandkishore, Levitov, and Chubukov, 2012), and other systems (F. Liu *et al.*, 2013; Hsu and Chakravarty, 2014). The B phase of ^{3}He may harbor a time-reversal-invariant topological superfluid state, although the corresponding surface states are yet to be identified (Chung and Zhang, 2009; Qi and Zhang, 2011). Superconductivity seen experimentally by doping Bi_2Se_3 with Cu (Wray *et al.*, 2010) is argued to be the signature of a parity-odd superconducting state (Sato, 2009; Fu and Berg, 2010). A fully gapped state is also observed in In-doped TCI SnTe (Novak *et al.*, 2013). Fu and Kane (2008) proposed an alternative approach in which the topological state is induced via proximity effects between the topological and trivial s-wave superconductors. This proximity effect has been observed in Bi_2Se_3 on a $NbSe_2$ conventional superconductor substrate (M.-X. Wang *et al.*, 2012) as well as an unconventional d-wave $Bi_2Sr_2CaCu_2O_{8+\delta}$ superconducting substrate (E. Wang *et al.*, 2013). A new type of topological mirror superconductor has been predicted (Tsutsumi *et al.*, 2013; Zhang, Kane, and Mele, 2013), where the protection is through the combination of mirror and time-reversal symmetries like a TCI.

A number of proposals have been made for realizing a Majorana state (Elliott and Franz, 2015) leading to the general

principle that Majorana edge modes are inherited by the ends of a one-dimensional chain of magnetic impurities or adatoms or a helical Shiba chain on a superconducting substrate (Pientka, Glazman, and von Oppen, 2013; Heimes, Kotetes, and Schön, 2014). Such bond states have been reported by STM in Fe chains on superconducting Pb (Nadj-Perge *et al.*, 2014).

D. Weyl and 3D Dirac semimetal phases

Gapless conelike dispersions can exist in the 3D bulk electronic spectrum described by the Hamiltonian $H(\boldsymbol{k}) = v_{ij}k_i\sigma_j$, which is similar to the Weyl equation (Weyl, 1929), with the associated Chern number given by $\mathrm{sgn}(\det[v_{ij}]) = \pm 1$. If the TRS or the inversion symmetry is broken, these cones can become nondegenerate except at the (Weyl) nodes or points, yielding a topologically protected Weyl semimetal phase. Weyl nodes can be created or annihilated only when two nodes with opposite signs of Chern numbers come together (Vafek and Vishwanath, 2014). The total number of Weyl nodes can be shown to come in multiples of 4 for TRS preserved and 2 for TRS broken systems (Burkov and Balents, 2011; Ojanen, 2013). The Weyl semimetal phase may sometimes be viewed as a bridge between a Z_2 TI with broken inversion symmetry and a trivial band insulator (Murakami, 2007), or alternatively as a bridge between an axion insulator with broken TRS and a trivial Mott insulator (Wan *et al.*, 2011). It is possible to have two degenerate Weyl points with the same sign of Chern numbers or to have multiple degenerate Weyl points protected by point-group symmetry (Fang, Gilbert, and Bernevig, 2012).

Spin degenerate 3D Dirac cones, which consist of two gapless Weyl nodes, are also possible. Accidental gapless Dirac cones can occur at the topological phase transition between a TI and a trivial insulator if both inversion and time-reversal symmetries are intact (Xu *et al.*, 2011), although cases where the Dirac nodes are protected by space-group symmetry are more interesting (Z. Wang *et al.*, 2012; Young *et al.*, 2012; Z. Wang *et al.*, 2013).

Weyl and 3D Dirac semimetal phases have important applications including the realization of an anomalous Hall effect (Burkov and Balents, 2011; Xu *et al.*, 2011; Yang, Lu, and Ran, 2011), nontrivial electromagnetic responses (Turner and Vishwanath, 2013), Majorana excitations (Meng and Balents, 2012), a disconnected, yet protected, Fermi surface (FS) or a "Fermi arc" (Wan *et al.*, 2011), and possible Weyl superconductors (Meng and Balents, 2012).

E. Topological phase transition

A TPT, which is driven by changes in the topology of the bulk band structure, is very different from the familiar phase transitions such as the melting of a solid, which are characterized by broken symmetries and sharp anomalies in thermodynamic properties. Many theoretical studies show that TPTs can be induced by tuning the band structure using chemical substitution, strain, or pressure, or via electron correlation effects (Sato, 2009; Pesin and Balents, 2010; Wan *et al.*, 2011; Wray *et al.*, 2011; Xu *et al.*, 2011; L. Wu *et al.*, 2013).

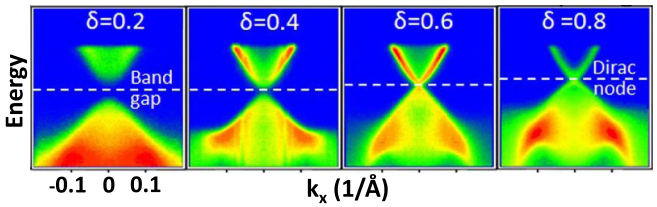

FIG. 7. ARPES spectra of $TlBi(S_{1-\delta}Se_\delta)_2$ showing a TPT as δ increases from 0.2 to 0.8. From S.-Y. Xu *et al.*, 2011.

TPTs have been observed experimentally in $TlBi(S_{1-\delta}Se_\delta)_2$ (Sato *et al.*, 2011; G. Xu *et al.*, 2011) as well as in the TCI $Pb_{1-x}Sn_xSe$ (Dziawa *et al.*, 2012; Zeljkovic *et al.*, 2014). An example is given in Fig. 7, which shows the evolution of the spectrum in $TlBi(S_{1-\delta}Se_\delta)_2$ with Se content δ. The band gap is trivial at $\delta = 0.2$, closes around $\delta = 0.6$, and reopens at $\delta = 0.8$ with the appearance of linearly dispersing bands connecting valence and conduction bands. Similar results are found in a time-domain terahertz spectroscopy study of $(Bi_{1-x}In_x)_2Se_3$ (L. Wu *et al.*, 2013). TPTs can be induced via laser or microwave pumping to produce a nonequilibrium topological state or a Floquet TI (Kitagawa *et al.*, 2010; Gu *et al.*, 2011; Lindner, Refael, and Galitski, 2011; Dóra *et al.*, 2012; Katan and Podolsky, 2013; Kundu and Seradjeh, 2013; Rechtsman *et al.*, 2013; Y. H. Wang *et al.*, 2013; Perez-Piskunow *et al.*, 2014; R. Wang *et al.*, 2014).

IV. SURVEY OF TOPOLOGICAL MATERIALS

A. Materials discovery strategies

A key ingredient for realizing a topologically nontrivial state is the presence of an SOC driven band inversion as discussed in Sec. II.A. Therefore, natural candidates for the topological materials discovery process are traditional semiconductors and insulators containing heavy elements. The size of the band gap here is not important because it could be inverted and/or extended throughout the BZ via controls of strain, alloying, and/or confinement, so that semimetals also provide viable base materials. For example, a Bi/Sb alloy was the first materials realization of a 3D TI in which the parent Sb is a semimetal with a nontrivial band topology (Fu and Kane, 2007; Hsieh *et al.*, 2008, 2009c). In nonmagnetic compounds, the search for new topological materials should typically start thus by considering systems with an even number of electrons per unit cell, which could in principle be accommodated in completely filled bands. (This of course does not apply to magnetic or strongly correlated systems.) Large gap ionic compounds in which the conduction and valence bands are formed from distinct atomic orbitals can be ruled out. Intermetallics and covalent bonded materials are more appropriate. Since strong SOC resides in the bottom part of the periodic table, by excluding metallic Pb and group IIIA elements, we arrive at Sn in group IVA and Bi/Sb in group VA, which are not too ionic, as the elemental ingredients of choice for creating new topological materials.

The crystal structure is also a key player in controlling band topology. For example, a hypothetical simple cubic Sb or Bi crystal [Fig. 8(a)] will be metallic as it contains an odd number

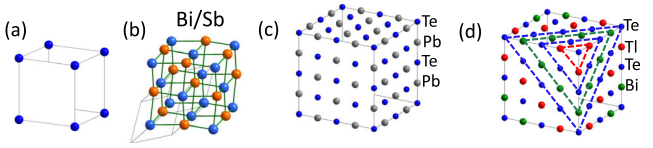

FIG. 8. (a) Simple cubic and the (b) related pseudocubic rhombohedral structure. (c) Rock salt and the (d) related pseudo-rock-salt rhombohedral structure.

of valence electrons (3 or 5 in group VA). Sb and Bi, however, occur naturally in a rhombohedral lattice with two basis atoms, which can be viewed as a pseudocubic structure (Hofmann, 2006) [Fig. 8(b)], yielding an even number of electrons in the unit cell, and opening up the possibility of an insulating phase. An even number of electrons in the unit cell is maintained when we replace Sb by Sn and Te in alternate layers since Sn and Te lie on the left- and right-hand sides of Sb in the periodic table, giving a rock salt-type face-centered-cubic (fcc) lattice with two basis atoms [Fig. 8(c)]. This strategy has been useful in manipulating $Pb_{1-x}Sn_xTe$, which undergoes inversions at four equivalent L points in the BZ with increasing x, and thus remains Z_2 trivial for all x. (Section IV.B.6 discusses how a TCI phase emerges in $Pb_{1-x}Sn_xTe$.) But, a strong TI can be realized via a rhombohedral distortion along [111], which limits band inversion to just one of the four L points. This approach successfully predicted $TlBiTe_2$ with pseudo PbTe structure to be a TI where the rhombohedral distortion is induced chemically by replacing alternate layers of Pb by Tl and Bi [Fig. 8(d)] (Lin, Markiewicz *et al.*, 2010; Hsieh *et al.*, 2012).

Note that out of a total of 230 available crystallographic space groups, the three TI families of $TlBiSe_2$ and distorted (Pb/Sn)Te and (Bi/Sb) alloys belong to the same space group #166 (R-3m), which transforms into #164 (P-3m1) when a conventional hexagonal cell is considered. Bi_2Se_3, ternary tetradymites, $Ge_mBi_{2n}Te_{m+3n}$ series, $(Bi_2)_m(Bi_2Te_3)_n$, and BiTeCl TIs all belong to the same or similar space groups. Interestingly, their structures can be viewed as being more or less pseudocubic with most atoms having essentially a coordination of 6. We may thus consider Bi/Sb to be a prototype TI for a variety of Bi/Sb based layered TIs as well as for the (Pb/Sn)Te alloys. In contrast, gray Sn, which is connected adiabatically to several zinc-blende–type TIs, presents a second distinct structural branch favored by topological materials. These observations point to the value of space groups in searching for new topological materials. Yet other classes of TIs involving d and f electrons highlight the role of strong electron correlations in producing new topological phases. Notably, some topological phases are not driven by the SOC (Fu, 2011; Alexandradinata *et al.*, 2014).

Standard band theory techniques can be deployed for treating the electronic structure and topological properties of 2D films, see Sec. IV.D, by constructing an effective 3D "crystal" obtained by stacking replicas of the 2D film separated by vacuum layers. While weakly correlated materials can be modeled in a parameter free manner within the band theory framework, this is generally not the case when electronic correlations are strong, and a variety of parameters are often invoked in order to make headway (e.g., a value of U in an LDA + U computation or the strength of the SOC); we refer to the discussions of Secs. IV.E–IV.I and the cited literature for the specifics in various cases.

B. Bi/Sb-based materials

1. $Bi_{1-x}Sb_x$: First 3D TI

Although Bi and Sb are both semimetals, the ordering of conduction and valence bands in Bi and Sb at the three L points in the rhombohedral BZ is different. In $Bi_{1-x}Sb_x$ alloys, as x increases, band gaps close and reopen at the three L points with a critical point at $x \approx 4\%$, and the system becomes a direct-gap semiconductor at $x \approx 8\%$. These considerations led to the theoretical prediction that Bi-Sb alloys harbor a TI phase (Fu and Kane, 2007), and to the experimental discovery of the first 3D TI in $Bi_{0.9}Sb_{0.1}$, which was established by observing the hallmark topological surface states via ARPES on the [111] surface (Hsieh *et al.*, 2008). Gapless surface states have been observed on the [110] surface as well (X.-G. Zhu *et al.*, 2013). Also, the QPI patterns in STS experiments show the expected suppression of the backscattering channels, while scattering channels between different pieces of the FSs remain open (Gomes *et al.*, 2009; Roushan *et al.*, 2009). Interestingly, STS experiments show Landau levels as well as QPI patterns of nontrivial surface states in the topological semimetal Sb (Soumyanarayanan *et al.*, 2013).

2. Bi_2Se_3, Bi_2Te_3, and Sb_2Te_3: Second generation TIs

Bi_2Se_3, Bi_2Te_3, and Sb_2Te_3 are strong TIs, which share a rhombohedral structure containing blocks of quintuple layers (QLs). Nontrivial topology results from band inversions driven by SOC in the p-orbital manifold at the Γ point. The band gap in Bi_2Se_3 is as large as 0.3 eV. Unlike the multiple surface states in $Bi_{1-x}Sb_x$, these materials possess the advantage of exhibiting only a single Dirac cone on their naturally cleaved [111] surfaces (Chen *et al.*, 2009; Hsieh *et al.*, 2009a; Xia *et al.*, 2009; H. Zhang *et al.*, 2009). As a result, they have become the workhorse materials of the field with many ARPES (Chen *et al.*, 2009; Hsieh *et al.*, 2009b; Xia *et al.*, 2009), STM (Hor *et al.*, 2009; T. Zhang *et al.*, 2009; Okada *et al.*, 2011; Alpichshev *et al.*, 2012), transport (Qu *et al.*, 2010; Xiong *et al.*, 2012), and optical (Jenkins *et al.*, 2010, 2012; Valdés Aguilar *et al.*, 2012; L. Wu *et al.*, 2013) studies.

An experimental challenge has been to practically realize the bulk insulating state and to manipulate the position of the E_F. Since bulk Bi_2Se_3 is an n-type semiconductor, many studies attempt doping with extra holes. 0.25% Ca doping and NO_2 surface deposition tunes E_F to the Dirac point and fully removes the bulk conducting band from E_F (Hor *et al.*, 2009; Hsieh *et al.*, 2009b), while Sb doping in Bi_2Te_3 (Kong *et al.*, 2011; J. Zhang *et al.*, 2011) and Bi_2Se_3 (Analytis *et al.*, 2010) has been shown to control the carrier density and E_F. In $(Bi_{1-x}Sb_x)_2Te_3$ alloy, increasing Sb content shifts E_F down from an n- to a p-type regime. On a nanotemplate of this sample, ambipolar gating effects have been reported (Chen *et al.*, 2010b; Steinberg *et al.*, 2010; Kong *et al.*, 2011). In-doped $(Bi_{1-x}In_x)_2Se_3$ thin films exhibit a metal-insulator

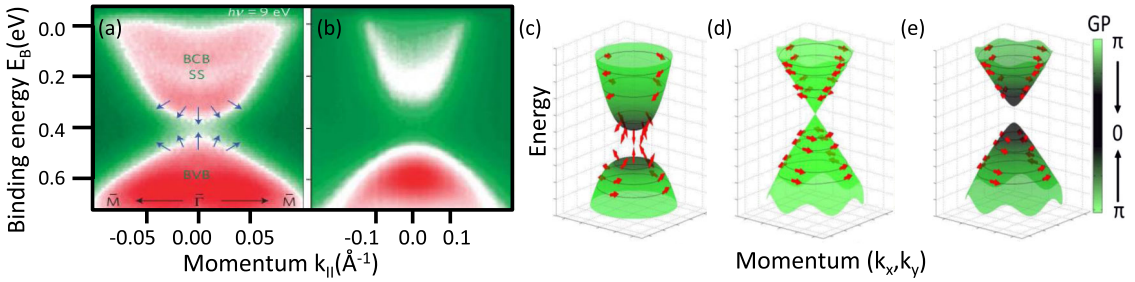

FIG. 9. Band dispersion via ARPES in (a) magnetically doped Bi_2Se_3 and its (b) 3QL thick film. (c) Schematic spin texture for a TRS breaking gapped Dirac cone, (d) a gapless Dirac cone, and (e) a gapped Dirac cone. From S.-Y. Xu *et al.*, 2012b.

transition (Brahlek *et al.*, 2012; L. Wu *et al.*, 2013). DFT calculations predict that the position of the topological surface state can be tuned in heterostructures of a TI with various band insulators (Q. Zhang *et al.*, 2012; Menshchikova *et al.*, 2013; G. Wu *et al.*, 2013).

Doping with magnetic impurities is interesting as it gives insight into the effects of TRS breaking perturbations (Okada *et al.*, 2011; Schlenk *et al.*, 2013; Jiang *et al.*, 2015). The opening of a magnetic gap at the Dirac node is suggested by ARPES measurements on Fe/Mn doped Bi_2Se_3 (Chen *et al.*, 2010a). However, other factors such as spatial fluctuations and surface chemical disorder (Beidenkopf *et al.*, 2011; J. Zhang *et al.*, 2011) could be responsible since a gap-like feature is also observed in doped nonmagnetic samples (Xu *et al.*, 2012b). Spin-resolved ARPES reveals a hedgehog spin texture of the gapped Dirac cones in Mn-doped Bi_2Se_3 [Figs. 9(a) and 9(c)], which is distinct from that of a gapped Dirac cone due to confinement effects in thin films [Figs. 9(b) and 9(e)]. Finally, the long-sought quantum anomalous Hall effect has been demonstrated in $(Bi,Sb)_2Te_3$ thin films (Chang *et al.*, 2013; J. Zhang *et al.*, 2013), where the surface state tunneling gap in the undoped system can be closed and reopened via Cr doping, and a quantized Hall signal of the expected value is seen.

Topological superconductivity could be induced via doping or pressure, although this has not been confirmed experimentally. In $Cu_xBi_2Se_3$, the transition temperature T_c goes up to 3.8 K with Cu doping (Wray *et al.*, 2010), and superconductivity occurs through an unusual doping mechanism in that the spin-polarized topological surface states remain intact at the E_F. Low-temperature electrical resistivity and Hall effect measurements (S. J. Zhang *et al.*, 2012; Kirshenbaum *et al.*, 2013) on Bi_2Se_3 and Bi_2Te_3 single crystals under pressures $\lesssim$50 GPa show the onset of superconductivity above 11 GPa. T_c and the upper critical field H_{c2} both increase with pressure up to 30 GPa, where they peak with values of 7 K and 4 T, respectively. With further increase in pressure, T_c remains anomalously flat even though the carrier concentration increases tenfold, pointing to an unusual pressure induced topological pairing state in Bi_2Se_3.

3. Ternary tetradymites, $Ge_mBi_{2n}Te_{(m+3n)}$ series

The large family of tetradymitelike layered TIs with formulas B_2X_2X', AB_2X_4, $A_2B_2X_5$, and AB_4X_7 (A = Pb, Sn, Ge; B = Bi, Sb; X, X' = S, Se, Te) offers substantially greater chemical and materials tunability compared to its binary cousins discussed previously. Many of these compounds have been synthesized and ARPES (Xu *et al.*, 2010; J. Zhang *et al.*, 2011; Eremeev *et al.*, 2012b; Neupane *et al.*, 2012; Okamoto *et al.*, 2012) and transport measurements (Ren *et al.*, 2010; Taskin *et al.*, 2011; Xiong *et al.*, 2012) are available. Theoretically predicted single surface Dirac cones have been observed in several of these materials via ARPES as well as pump-probe spectroscopy of unoccupied surface states (Niesner *et al.*, 2012, 2014).

The crystals of this series are built by stacking layers. We highlight the materials flexibility by considering the example of $Ge_mBi_{2n}Te_{(m+3n)}$. It reduces to Bi_2Te_3 for $m = 0$ and $n = 1$. By increasing m, we get $GeBi_2Te_4$, which can be viewed as an insertion of a GeTe layer into Bi_2Te_3, yielding 7-layer blocks. An increase in n now gives $GeBi_4Te_7$ with alternating stacks of 5-layer blocks of Bi_2Te_3 and 7-layer blocks of $GeBi_2Te_4$, which resembles a heterostructure. Many variations in stacking and composition can thus be made to tune properties of the surface Dirac cone (Eremeev *et al.*, 2012b). The bulk gap varies over a wide range from 0 to 0.5 eV. A fully isolated Dirac cone at the E_F can be obtained in $Sb_xBi_{2-x}Se_2Te$ for $x = 1.67$ (Neupane *et al.*, 2012).

4. Thallium based ternary chalcogenides

Although Pb and Sn based chalcogenides were studied extensively in the 1980s in search of Dirac fermions (Fradkin, Dagotto, and Boyanovsky, 1986), Tl-based III-V-VI_2 chalcogenides $MM'X_2$ (M = Tl, M' = Bi or Sb, and X = Te, Se, or S) have been recognized as TIs very recently. Their rhombohedral lattices [see Fig. 8(d)] can be embedded in a 2×2 supercell of the fcc lattice. Figure 10 gives insight into how nontrivial phases evolve from the trivial band structures of PbTe and SnTe (Lin, Markiewicz *et al.*, 2010; Hsieh *et al.*, 2012; Safaei, Kacman, and Buczko, 2013). The analysis is simplified greatly by choosing the M atom (Pb, Sn, or Tl), which is a center of inversion symmetry, to lie at the origin of the real space lattice. Bands are plotted using black and gray (red) dots where the size of the gray (red) dots is proportional to the weight of the s orbital on the M atom. This representation is easily generated in band structure codes and allows a straightforward analysis of parities. Since the s orbital on the M atom is even, its weight must be strictly zero for a state with odd parity. The parities of wave functions at TRIM points in the BZ are thus easily obtained from the colors of the dots, being gray (red) for even and black for odd parity, and changes in the Z_2 invariants of the band structure can be

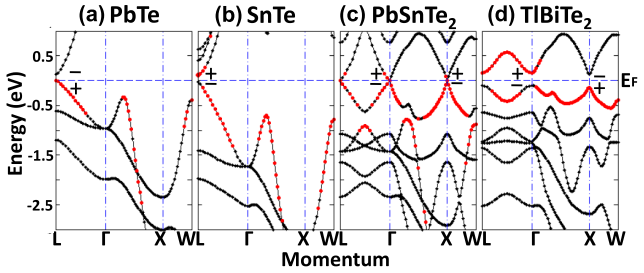

FIG. 10. Band structures of fcc (a) PbTe and (b) SnTe, and rhombohedral (c) $PbSnTe_2$ and (d) $TlBiTe_2$, all plotted in the BZ of an fcc lattice. Parities at TRIM points are shown. The size of the gray (red) dots is proportional to the weight of the s orbital on the metal atoms. From Lin, Markiewicz *et al.*, 2010.

monitored simply by counting the number of inversions of gray (red) and black dots at TRIM points around the E_F.

In order to understand how the topology of bands evolves in Fig. 10, it is useful to plot all bands in the BZ of the fcc lattice, so that bands in Figs. 10(c) and 10(d) for rhombohedral lattices refer to an extended zone scheme (Lin, Markiewicz *et al.*, 2010). The top of the valence bands in PbTe lies at the L points with a small gap, Fig. 10(a). The band structure of the hypothetical ternary compound $PbSnTe_2$ obtained by replacing one of the Pb atoms by Sn in the supercell is shown in Fig. 10(c). Pb-to-Sn replacement is seen to induce band inversions at both the Γ and the three X points around E_F. Because the total number of inversions is even, as is the case in SnTe at the four L points in Fig. 10(b), there is no change in Z_2, and $PbSnTe_2$ remains topologically trivial like PbTe. In fact, the band inversion in going from PbTe to $PbSnTe_2$ can be adduced to occur first at Γ and then at X, suggesting that a small rhombohedral lattice distortion or chemical tuning by replacement of Pb and Sn with other elements could prevent the band inversion associated with the three X points and produce a nontrivial phase. This indeed is seen to be the case in Fig. 10(d) when Pb is replaced by Tl and Sn by Bi.

Band theory calculations predict (Eremeev, Koroteev, and Chulkov, 2010; Lin, Markiewicz *et al.*, 2010; Yan, Liu *et al.*, 2010; Eremeev *et al.*, 2011) that four Tl-based chalcogenides $MM'X_2$ ($M = \mathrm{Tl}$, $M' = \mathrm{Bi/Sb}$, and $X = \mathrm{Te/Se}$) are topologically nontrivial. These theoretical predictions were verified experimentally soon after they were made by observing single-Dirac-cone surface states in $TlBiTe_2$ and $TlBiSe_2$ (Chen *et al.*, 2010b; Kuroda *et al.*, 2010b; Sato *et al.*, 2010). Notably, $TlBiTe_2$ could be a topological superconductor (Chen *et al.*, 2010b; Yan, Liu *et al.*, 2010). On the other hand, $TlSbS_2$ does not crystallize in the rhombohedral structure, but the trivial $TlBiS_2$ does. The correct prediction of different topological phases between two isostructural compounds ($TlBiS_2$ and $TlBiSe_2$) suggests the possibility of a topological phase transition in $\mathrm{TlBi(Se,S)_2}$ alloys, which has been realized experimentally (G. Xu *et al.*, 2011); see Sec. III.E. On the other hand, because the structure of Sb_2Se_3 is different from Bi_2Se_3 or Sb_2Te_3, it will be difficult to realize such a transition in $\mathrm{(Bi,Sb)_2Se_3}$ or $\mathrm{Sb_2(Se,Te)_3}$ alloys.

5. Noncentrosymmetric Bi compounds

Bi-based noncentrosymmetric compounds BiTeX ($X = $ Cl, I, and Br) show the presence of giant Rashba-type SOC (Bahramy, Arita, and Nagaosa, 2011; Ishizaka *et al.*, 2011; Eremeev *et al.*, 2012a). Band structure computations on BiTeCl find oppositely polarized layers of Bi and Te (Chen *et al.*, 2013) so that the system resembles a topological p-n junction. A single V-shaped Dirac cone is reported via ARPES on the n-type, but not the p-type surface in BiTeCl (Chen *et al.*, 2013). The nature of surface states, however, remains uncertain with DFT predicting BiTeCl to be a trivial insulator (Eremeev *et al.*, 2012a; Landolt *et al.*, 2013), although BiTeI is predicted to become a nontrivial TI under pressure (Bahramy *et al.*, 2012).

6. First topological crystalline insulator: (Pb,Sn)Te

As discussed in Sec. III.A, surface states in a TCI are protected by the combined effects of time-reversal and crystal symmetries. A TCI supports an even number of Dirac cones and band inversions in sharp contrast to a TI. (Pb/Sn)Te and related compounds were first predicted theoretically to host the TCI phase (Hsieh *et al.*, 2012). The experimental realization followed almost immediately (Dziawa *et al.*, 2012; Tanaka *et al.*, 2012; Xu *et al.*, 2012a). To date this remains the only known TCI family verified by experiments.

Crystal structure of this system is based on the rock-salt fcc structure [Fig. 8(c)]. The band gaps at four equivalent L points in the BZ in SnTe are inverted relative to PbTe [Figs. 10(a) and 10(b)]. The band gap in $Pb_{1-x}Sn_xTe$ alloys closes and reopens with an even number of inversions between the two end compounds, so that even though neither SnTe nor PbTe can be a Z_2 TI, we obtain a TCI phase driven by the mirror symmetry of the fcc lattice. Note that standard parity analysis cannot be used here for the identification of an intrinsic band inversion because parity eigenstates depend on the choice of origin. For example, if the inversion center is shifted from Pb or Sn to a Te atom, the states at L would change parity but those at Γ will not. Obviously, one cannot identify a TCI by comparing the sequence of parity eigenstates at L and Γ. The trick of plotting the weight of the key orbital involved in the inversion discussed in connection with the gray (red) dots in Fig. 10 can, however, still be used. Here the relevant orbital is the Te p orbital, which gets inverted in going from PbTe to SnTe. Specifically, SnTe at ambient pressure is a TCI with mirror Chern number $n_M = -2$, where the nonzero value of n_M indicates the existence of surface states on any crystal surface symmetric about the $\{110\}$ mirror planes.

The practical situation in SnTe is complicated by the rhombohedral distortion of the structure (Iizumi *et al.*, 1975), which breaks the mirror symmetry to produce gapped surface Dirac cones (Hsieh *et al.*, 2012). Moreover, the SnTe surface is heavily p doped by naturally occurring Sn vacancies, which lower the chemical potential below the bulk valence band maximum (Burke *et al.*, 1965) and push the Dirac cone into the valence bands (Littlewood *et al.*, 2010). But, this p doping is absent in Pb-rich samples (Takafuji and Narita, 1982), and indeed, in topological compositions of $Pb_{1-x}Sn_xTe$ the Dirac cone is seen via ARPES, and its expected spin structure is verified by spin-resolved ARPES experiments (Xu *et al.*, 2012a).

The commonly studied surface is the $\{001\}$ surface where the $\Gamma L_1 L_2$ plane of the bulk BZ projects onto the ΓX_1

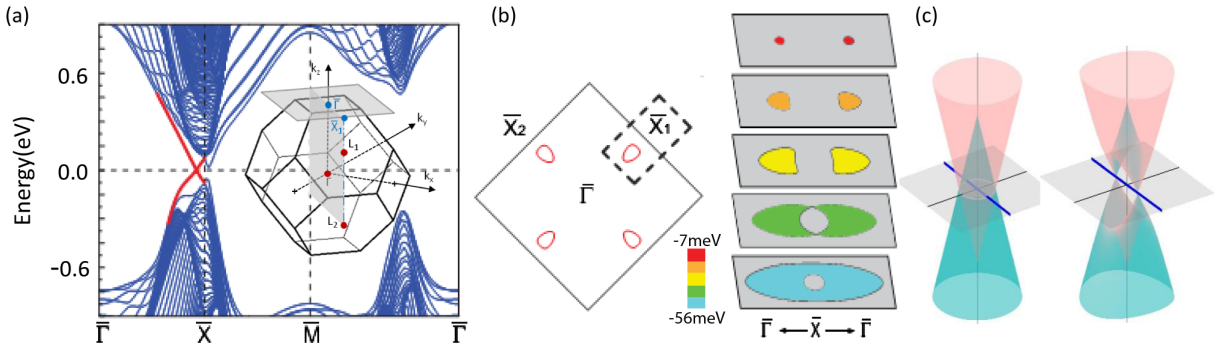

FIG. 11. [001] surface states of SnTe. (a) Surface (red lines) and bulk (blue lines) bands. BZ is shown in the inset. (b) FS (left) and a set of constant energy surfaces showing the Lifshitz transition (right). (c) Model of two noninteracting (left) and interacting (right) Dirac cones. From Hsieh *et al.*, 2012, and Y. J. Wang *et al.*, 2013.

symmetry line in the surface BZ with both L_1 and L_2 projecting onto X_1; see the inset in Fig. 11(a). The mirror Chern number $n_M = -2$ dictates the existence of two pairs of counterpropagating, spin-polarized surface states with opposite mirror eigenvalues along the $X_1 - \Gamma - X_1$ line, replicated along the $X_2 - \Gamma - X_2$ line via rotational symmetry. We thus obtain four Dirac points located on the four equivalent ΓX lines. As E_F decreases from the Dirac point, the FS initially consists of two disconnected hole pockets away from X, which subsequently reconnect to form a large hole and a small electron pocket, both centered at X, undergoing a Lifshitz transition in FS topology as depicted in Fig. 11(b). The role of surface passivations in destroying trivial surface states on the (111) polar surface of SnTe has been discussed (Eremeev *et al.*, 2014).

The complicated surface band structure and spin textures discussed in the preceding paragraph can be understood in a model involving two coaxial Dirac cones where one starts with two noninteracting "parent" Dirac cones centered at X, which are vertically offset in energy [Fig. 11(c)]. Hybridization between these two parent cones opens a gap at all points except along the mirror line, leading to a pair of lower-energy "child" Dirac points away from X. The parent Dirac nodes are protected by TRS and cannot be gapped by removing the mirror symmetry, but the child Dirac nodes can be gapped by breaking mirror symmetry. Notably, the two parent Dirac cones must have different orbital characters since they belong to different eigenvalues of the mirror operation. In SnTe, the lower (higher) parent Dirac cone is primarily composed of Sn-p_z(Te-p_x) orbital around the $(\pi, 0)$ point. Y. J. Wang *et al.* (2013) presented a 4×4 model Hamiltonian along these lines based on up- and down-spin Sn-p_z and Te-p_x orbitals, which captures salient features of the corresponding first-principles surface states and their spin textures.

The aforementioned orbital textures would be expected to yield intensity asymmetries in the QPI patterns obtained from STS spectra. The scattering between the p_z-like hole branch will be strong while that between different orbitals on the electron branch will be suppressed. Also, if mirror symmetry is broken along only one of the two mirror planes, then we will obtain massive Dirac cones along one direction, while the Dirac cones along the other direction will remain massless. Such a coexistence of massive and massless Dirac cones has been adduced via the observation of three nondispersive features in the STS spectra, including the mapping of the associated dispersions in substantial accord with theoretical predictions (Okada *et al.*, 2013; Zeljkovic *et al.*, 2014). Experiment and theory should, however, be compared at the level of spectral intensities including matrix element effects, which are important in STS, ARPES, and other highly resolved spectroscopies (Mader *et al.*, 1976; Mijnarends and Bansil, 1976; Smedskjaer *et al.*, 1991; Lindroos and Bansil, 1996; Bansil and Lindroos, 1999; Huotari *et al.*, 2000; Bansil *et al.*, 2005; Sahrakorpi *et al.*, 2005; Nieminen *et al.*, 2009, 2012).

The surface of a TCI provides an especially rich sandbox for exploring how spin and orbital textures play out in the presence of many different types of carriers and van Hove singularities in the densities of states.

C. Gray-tin variants as 3D TIs

Gray Sn may be considered the parent of several families of TIs discussed in this section that occur in the zinc-blende–type structure, and to which gray Sn is connected adiabatically. Among the group IVA elements, gray Sn with an inversion-symmetric diamond structure possesses a nontrivial band topology (Fu and Kane, 2007), while the lighter elements Si and Ge with the same structure are trivial insulators. Topology of bands in Si, Ge, and Sn is controlled by states near E_F at Γ. The $j = 1/2$ s-like doublet lies above the p-like fourfold degenerate $j = 3/2$ levels in Si/Ge, but in gray Sn this natural order is inverted through a single band inversion at Γ [Figs. 12(a) and 12(b)], yielding a nontrivial zero-gap semiconductor or semimetal. A TI phase in Sn can be realized by lifting the degeneracy of the $j = 3/2$ states via a lattice distortion [Fig. 12(c)]. Notably, the band gap in the III-V zinc blendes generally decreases for heavier constituent atoms with larger lattice constants, suggesting the presence of an inverted band gap. For example, first-principles computations predict TlP and TlAs to be stable in the zinc-blende structure with inverted bands at Γ. Similarly, the band gap of the trivial insulator InSb becomes nontrivial when the lattice is expanded sufficiently (Ciftci, Colakoglu, and Deligoz, 2008; Lin, Das, Wang *et al.*, 2013).

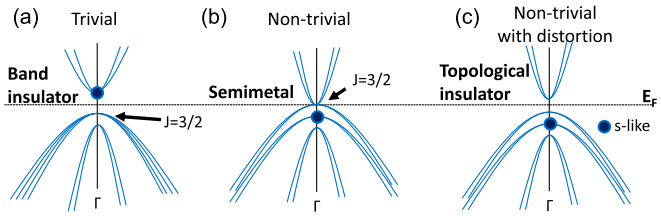

FIG. 12. Schematic band structures at (a) Γ in Si/Ge, (b) band inversion in Sn, and (c) a TI realized by a distortion. From Lin, Das, Wang *et al.*, 2013.

1. Ternary half Heusler compounds

Chemically, the ternary half Heuslers $MM'X$ for $M = (\mathrm{Lu, La, Sc, Y})$ and $M'X = (\mathrm{PtBi, AuPb, PdBi, PtSb, AuSn, NiBi, PdSb})$ involve a total of 18 valence electrons per formula unit obtained by combining ten d orbitals of M' atom with two s and six p orbitals of the X atom (Al-Sawai *et al.*, 2010; Chadov *et al.*, 2010; Lin, Wray *et al.*, 2010; Xiao *et al.*, 2010). These 18 electrons can be accommodated in closed $d^{10}s^2p^6$ shells with zero total spin and angular momentum, and can thus, in principle, support a nonmagnetic insulating band gap. Because M' and X atoms $[(M'X)^-]$ form a zinc-blende–type sublattice, the half Heusler compounds resemble 3D HgTe and InSb. As discussed in Sec. II.C, the half Heusler compounds with inverted band structure at Γ are connected adiabatically with nontrivial HgTe. The band topology in half Heusler compounds is determined by the relative energies of the s-like Γ_6 and p-like Γ_8 levels, and the energy difference $\Delta = E_{\Gamma_8} - E_{\Gamma_6}$ can be considered a measure of the band inversion strength. Figure 13 shows the relationship between Δ and $t = (Z_{M'} + Z_X)V$, where V is the cell volume and $Z_{M'}$ (Z_X) is the atomic number of M' (X) atom. t captures effects on Δ of changes in the $(M'X)^-$ unit as well as the overall cell volume. Effects of disorder or nonstoichiometry could be modeled using a variety of approaches (Bansil *et al.*, 1981; Huisman *et al.*, 1981; Khanna *et al.*, 1985; Lin *et al.*, 2006). The $\Delta = 0$ line separates trivial and nontrivial phases. Materials near the zero line will be amenable to switching between trivial and nontrivial states with external perturbations.

Insight is gained by framing the four compounds containing the same binary $(M'X)^-$ unit with a triangle (Fig. 13) (Al-Sawai *et al.*, 2010; Lin, Wray *et al.*, 2010). Remarkably, for all seven subgroups, Sc, La, and Lu lie at corners of the triangle while Y lies inside. The "orientation" of all seven triangles is the same in that it runs counterclockwise from La to Lu to Sc, where the element with the largest atomic mass Lu occupies the corner with the largest Δ, except for the MAuSn and MAuPb subgroups. Moreover, the volume of compounds in each subgroup is ordered as Sc > Lu > Y > La, except for the MAuPb subgroup. The center of gravity for each triangle is seen to increase with t for all subgroups. All compounds, whether physically realized or artificial, follow the aforementioned trends independent of the sign of Δ. These relationships between Δ and t may thus be valid more generally and useful in ascertaining the nature of the topological phase in other nonmagnetic half Heusler compounds. Δ would constitute a viable metric for genomic searches in this class of materials. YPtBi is a candidate for a topological superconductor (Butch *et al.*, 2011).

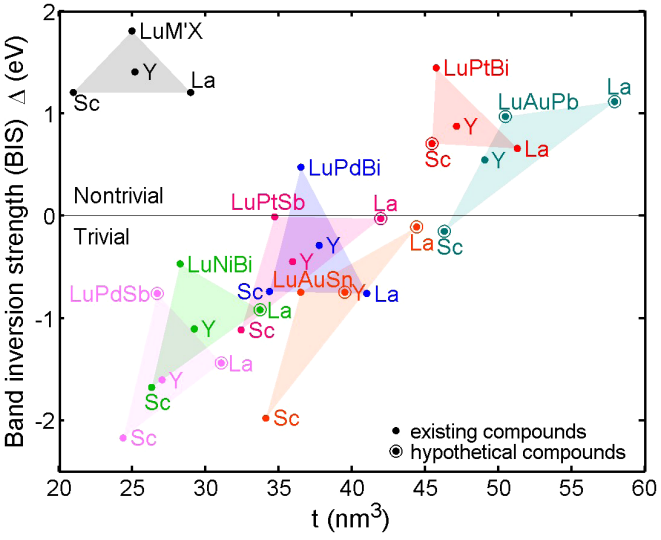

FIG. 13. Band inversion strength $\Delta = \Gamma_8 - \Gamma_6$ for various half Heusler compounds vs $t = (Z_{M'} + Z_X)V$, where $Z_{M'}$ (Z_X) is the atomic number of the M' (X) atom and V is the unit-cell volume. From Al-Sawai *et al.*, 2010, and Lin, Wray *et al.*, 2010.

2. Li_2AgSb class semiconductors

Like the half Heusler compounds, M' and X atoms in the ternary intermetallics (Lin, Das, Wang *et al.*, 2013) $Li_2M'X$ (M' = Cu, Ag, Au, or Cd; X = Sb, Bi, or Sn) form a zinc-blende sublattice with a total of 18 valence electrons in closed $d^{10}s^2p^6$ shells. The electronic structure is similar to the half Heusler compounds or gray Sn, and the band topology is controlled by the ordering of Γ_6 and Γ_8 levels. Band calculations predict Li_2AgBi and Li_2AuBi to be nontrivial semimetals, and Li_2AgSb to be close to a critical point. The TI phase can be stabilized by a rhombohedral distortion with expansion along the hexagonal a-b plane, which lifts the degeneracy of $j = 3/2$ states and also induces a band inversion. Li_2AsSb based compounds are connected adiabatically to nontrivial gray Sn. The phase diagram of Fig. 14 identifies Li_2CdSn and InSb with expanded lattice as possible new nontrivial candidate TIs, demonstrating the value of band inversion strength and adiabatic continuity arguments as useful materials discovery tools.

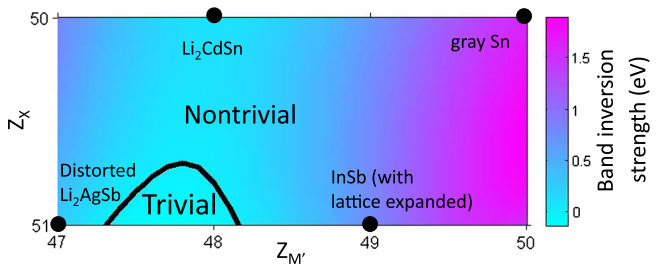

FIG. 14. Band inversion strength and topological phase diagram of $Li_2M'X$ as a function of atomic numbers of M' and X atoms. From Lin, Das, Wang *et al.*, 2013.

3. Ternary chalcopyrites, famatinites, and quaternary chalcogenides

Ternary I-III-VI_2 and II-IV-V_2 chalcopyrites (Feng *et al.*, 2011), I_3-V-VI_4 famatinites, and quaternary I_2-II-IV-VI_4 chalcogenides (Y. J. Wang *et al.*, 2011) can be regarded as superlattices of distorted zinc-blende structure. Famatinites obey the octet rule and form a $(\text{I-VI})_3(\text{V-VI})$ superlattice. Famatinites evolve into quaternary chalcogenides when one of their group-I elements is replaced by group-II and group-V elements by group-IV. The structure can be viewed as $(\text{I-II})_2(\text{II-VI})(\text{IV-VI})$ sublattice with two zinc-blende formula units. Substitution with larger atoms expands the lattice and increases both the tetragonal distortion and the crystal-field splitting. In contrast to the cubic zinc-blende–type compounds in Sec. IV.C, the materials in this section naturally acquire a tetragonal distortion along the c axis ($c < 2a$) through strong interlayer coupling between the two cation planes. This also results in a mismatch between the cation-anion bond lengths in the two zinc-blende formula units and helps lower the total energy. Tetragonal compression along the c axis lifts the degeneracy of p states in the zinc-blende lattice at Γ, and a subsequent inversion between the s and p states as in Fig. 12(c) yields a TI or semimetal phase (Feng *et al.*, 2011).

4. LiAuSe honeycomb lattice

Like the ternary cubic semiconductors, topological phases can be expected among the closed-shell relatives of graphene with graphite-type XYZ structure for 8 or 18 valence electrons. Suitable combinations are (i) $X =$ Li, Na, K, Rb, or Cs, $Y =$ Zn, Cd, or Hg, and $Z =$ P, As, Sb, or Bi; (ii) $X =$ K, Rb, or Cs, $Y =$ Ag or Au, and $Z =$ Se or Te; (iii) $X =$ rare earth, $Y =$ Ni, Pd, or Pt, and $Z =$ P, As, Sb, or Bi. Among these numerous possibilities, H.- J. Zhang *et al.* (2011) considered LiAuSe, LiAuTe, CsAuTe, KHgBi, and CsHgBi due to the likelihood of being synthesized. Electronic structures are similar to their cubic counterparts except that in the binary semiconductors or C_{1b} Heusler compounds, the bonds within the YZ tetrahedrons are of sp^3 or sd^3 type, while in the planar graphite-type layers the σ-type bonding occurs between the sp^2 and sd^2 orbitals. The remaining p orbitals provide π bonding similar to graphite. LiAuSe and KHgSb are both semimetals, although KHgSb is topologically trivial while LiAuSe is nontrivial.

5. β-Ag_2Te

Ag-based chalcogenide Ag_2Te undergoes a transition below 417 K from the α to the β phase, which is a narrow gap nonmagnetic semiconductor (Dalven, 1966; Dalven and Gill, 1967; Junod *et al.*, 1977) with an unusually large and nonsaturating quasilinear magnetoresistance (Xu *et al.*, 1997). Such a large magnetoresistance cannot be explained within a conventional quadratic band structure, and a gapless linear dispersion driven by disorder effects was proposed (Abrikosov, 1998). First-principles calculations, however, predict β-Ag_2Te to be a TI (W. Zhang *et al.*, 2011). The high temperature α phase of Ag_2Te, on the average, possesses an inversion-symmetric antifluorite structure with three interpenetrating fcc sublattices of Te, Ag(1), and Ag(2) with Te and Ag(1) forming a zinc-blende sublattice. Band structure of α-Ag_2Te is similar to that of HgTe with an inverted band ordering at Γ. In the β phase, Ag_2Te assumes a distorted antifluorite structure in which the structural distortion removes the degeneracy at Γ and opens a nontrivial insulating gap with the Dirac cone lying inside the gap. The emergence of metallic surface states is confirmed by the experimental observation of pronounced Aharonov-Bohm oscillations and a weak Altshuler-Aronov-Spivak effect in electron transport measurements on β-Ag_2Te nanoribbons (Sulaev *et al.*, 2013). The pressure dependence of topological phase transitions in Ag_2Te at room temperature was discussed by Zhao, Wang *et al.* (2013).

D. 2D topological materials

Conducting electrons at the edges of a 2D TI with single-Dirac-cone edge states can move only parallel or antiparallel to the edges with opposite spins. In a 3D TI, on the other hand, although the surface states are free from backscattering, they can still scatter at other angles. 2D TIs with single Dirac-cone edge states are thus more promising for spintronics applications since the only scattering channel (backscattering) is prohibited. In the 2D TIs realized experimentally so far (HgTe/CdTe, InAs/GaSb quantum wells) (König *et al.*, 2007; Knez, Du, and Sullivan, 2011), the band gap is very small so that transport measurements below 10 K are required to see topological states. The need for finding 2D TIs with larger band gaps is thus clear, and DFT calculations are playing a major role in predicting possible new 2D TI materials.

To date, most predicted 2D TIs have been obtained by reducing dimensionality in quantum wells or in slabs of 3D TIs. In particular, 2D TIs are predicted in thin films of almost every class of 3D TIs [e.g., Bi/Sb, Sn, Bi_2Se_3, Bi_2Te_3, $Ge(Bi,Sb)_2Te_4$, and Tl-based chalcogenides] (Lin, Markiewicz *et al.*, 2010; Liu *et al.*, 2010; Wada *et al.*, 2011; Chuang *et al.*, 2013; Singh *et al.*, 2013). The topological characteristics are sensitive to thickness, composition, and strain and are tunable by electrical gating. Substrates can modify the electronic structure and change the band topology. For example, Bi thin films are predicted to be 2D TIs, but Sb thin films are trivial and become nontrivial under applied strain (Wada *et al.*, 2011; Chuang *et al.*, 2013; M. Zhou *et al.*, 2014). Some of these thin films have been synthesized in various experiments but there still is no transport evidence for their being QSH insulators (Y. Zhang *et al.*, 2010; Chun-Lei *et al.*, 2013; S. H. Kim *et al.*, 2014).

A number of strategies for engineering topological states in 2D systems or their heterostructures have been proposed. Examples are (i) adding adatoms of heavy elements in the graphene structure to induce a stronger SOC for driving a topological phase transition (Kane and Mele, 2005a; Weeks *et al.*, 2011), (ii) applying a circularly polarized laser field on a 2D electronic system where the light field acts like a Rashba-type SOC to generate a nontrivial gap in an optical lattice (Inoue and Tanaka, 2010), (iii) stacking two Rashba-type spin-orbit coupled 2D electron gases with opposite signs of Rashba coupling in adjacent layers in heterostructure geometry (Das and Balatsky, 2013), and (iv) GaAs/Ge/GaAs heterostructure with opposite semiconductor interfaces acting as Rashba bilayers to allow a band inversion yielding a 15 meV or larger insulating gap (D. Zhang *et al.*, 2013).

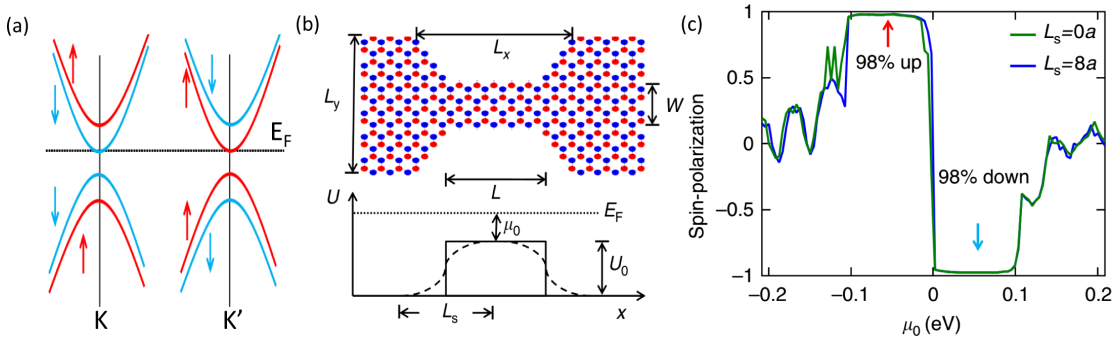

FIG. 15. (a) Schematic band structure of silicene in an external electric field. (b) Design of a spin filter as a quantum point contact with barrier potential $U(x)$. (c) Spin polarization of the filter as a function of the barrier height μ_0. From Tsai *et al.*, 2013.

1. III-V HgTe/CdTe quantum well structures

HgTe/CdTe quantum well is the first materials realization of a 2D topological phase (Bernevig, Hughes, and Zhang, 2006; König *et al.*, 2007). HgTe and CdTe both possess the zinc-blende structure. HgTe is a topologically nontrivial semimetal with a single band inversion at Γ [Fig. 12(b)], while CdTe is topologically trivial [Fig. 12(a)]. However, the HgTe/CdTe heterostructure exhibits a thickness-dependent QSH state (Kane and Mele, 2006) as first predicted theoretically (Bernevig, Hughes, and Zhang, 2006) and then verified experimentally (König *et al.*, 2007). This system has been reviewed extensively (Hasan and Kane, 2010; Qi and Zhang, 2011); see the materials inventory in the Appendix (Table I) for recent literature on HgTe/CdTe and InAs/GaSb/AlSb quantum well systems.

2. Graphene

Graphene is the natural starting point for discussing 2D systems considered in this section. Properties and applications of graphene have been reviewed extensively in the literature (Beenakker, 2008; Castro Neto *et al.*, 2009; Peres, 2010; Das Sarma *et al.*, 2011; Goerbig, 2011; Kotov *et al.*, 2012), and, therefore, we make only a few remarks here. Graphene is the simplest 2D topological system in which the theoretically predicted SOC gap is too small to be accessible experimentally. If the SOC is turned off, graphene becomes gapless with Dirac cones centered at the BZ corners K and K', which are not TRIM points. SOC opens only a band gap, but does not induce changes in the parity of eigenstates or band inversions at the TRIM points Γ and M. Notably, any 2D electron gas can be transformed into a host for Dirac fermions via patterning with a periodic array of gates (Kotov *et al.*, 2012). In particular, a 2D electron gas under an external hexagonal periodic potential or optical lattice has been shown to develop graphene-like massless Dirac cones both theoretically (Wunsch, Guinea, and Sols, 2008; Park and Louie, 2009) and experimentally (Gomes *et al.*, 2012; Shikin *et al.*, 2014). Introduction of adatoms on a graphene sublattice or sandwiching a graphene sheet between two Bi_2Se_3 slabs is an alternative route for inducing a topological gap (Hu *et al.*, 2012; L. Kou *et al.*, 2013).

3. "Beyond" graphene atomically thin films: Silicene, germanene, and stanene

Like a single layer of C atoms (graphene), Si, Ge, and Sn can also form atomically thin crystals yielding silicene, germanene, and stanene. Freestanding silicene and its Ge and Sn counterparts are "beyond" graphene 2D materials with advantages over graphene of a stronger SOC and atomic bonds that are buckled and not flat like graphene (Mas-Ballesté *et al.*, 2011; Butler *et al.*, 2013). First-principles calculations show these materials to be QSH insulators. Aside from being gapped, their band structures are similar to graphene with conduction and valence band edges located at the K and K' corners of the BZ. The SOC induced gaps in germanene and stanene are predicted to be 25 and 70 meV, respectively, large enough for room-temperature applications (Liu, Feng, and Yao, 2011; Tsai *et al.*, 2013). The band gap can be tuned with a perpendicular electric field, which breaks the inversion symmetry due to the buckling of the honeycomb structure (Drummond, Zólyomi, and Fal'ko, 2012; Tsai *et al.*, 2013), and topological phase transitions can be realized by gating control. The resulting field-tunable nondegenerate states possess nearly 100% spin polarization, providing a basis for designing high efficiency spin filters (see Fig. 15), and other devices for manipulating spin currents (Chuang *et al.*, 2013; Tsai *et al.*, 2013; Gupta *et al.*, 2014). Although silicene has been grown on various substrates, the resulting electronic and geometric structures may be quite different from those of freestanding silicene films (Feng *et al.*, 2012; Fleurence *et al.*, 2012; Vogt *et al.*, 2012; Meng *et al.*, 2013). Honeycomb III-V thin films are a natural extension of silicene, and low-buckled GaBi, InBi, and TlBi thin films are predicted to be 2D TIs (Chuang *et al.*, 2014).

First-principles calculations predict films of Sn compounds SnX (X = H, I, Br, Cl, F, or OH) to be in the QSH phase (Y. Xu *et al.*, 2013), with the hydrogenated version called stanane. Hybridization with the X atom removes p_z bands from the E_F, so that low-energy states are dominated by the s and p orbitals, and the band topology is controlled by band inversion at Γ as in 3D gray Sn. An insulating gap as large as 300 meV is predicted in SnI. Similar results are found in films of other compounds. GeI also shows a gap of 300 meV. PbX (X = H, F, Cl, Br, or I) is predicted to be a 2D TI, but phonon calculations suggest that the structure is not stable (Si *et al.*, 2014). A study of band topology and stability of the multilayer stanane indicates that one to three layer thick films are TIs, and films with greater thickness are metallic (Chou *et al.*, 2014). Functional thin films of Bi and Sb have also been predicted to be large gap TIs with band gaps ranging from 0.74–1.08 eV (Song *et al.*, 2014).

E. Organometallic compounds

Computations indicate the presence of TI phases in 2D triphenyl-lead $Pb(C_6H_5)_3$ (Wang, Liu, and Liu, 2013a) and 2D organometallics such as π-conjugated Ni-bis-dithiolene $Ni_3Cl_2S_{12}$ (Wang, Su, and Liu, 2013). Triphenyl-Pb has a buckled hexagonal structure in which the para-Pb atoms are displaced alternately up and down out of the plane of the benzene rings. Without SOC, the band structure displays a gapless Dirac cone at the K point, but a gap of $\sim$8.6 meV opens up when SOC is turned on. When Pb is replaced by magnetic Mn this family can exhibit a QAH effect (Wang, Liu, and Liu, 2013b). In contrast to triphenyl-Pb, 2D $Ni_3Cl_2S_{12}$ adopts a kagome lattice. The band structure now contains two Dirac bands near E_F with a gap of $\Delta_1 = 13.6$ meV, and a flat band, which is a distinctive feature of the kagome lattice, lying $\Delta_2 = 5.8$ meV above the upper Dirac band. Both Δ_1 and Δ_2 vanish in the absence of SOC. Z. Liu *et al.* (2013) predicted 2D In-phynylene to have a quasiflat Chern band near E_F in its ferromagnetic phase.

F. Transition metal compounds

1. Iridates

5*d* orbitals of Ir in iridium oxide provide a playground for unfolding the interplay between electron correlation and SOC effects. In addition to the Ir skutterudites, topological materials have been proposed in iridates with pyrocholore, perovskite, and layered honeycomb structures. Ir pyrochlores, $R_2Ir_2O_7$ (R = Nd, Sm, Eu, and Y), exhibit metal-insulator transitions (Matsuhira *et al.*, 2007). LDA + U calculations predict the magnetic phase of $Y_2Ir_2O_7$ to be a Weyl semimetal (Wan *et al.*, 2011). A phase diagram of Ir pyrochlores with varying strengths of electron-electron interaction and SOC harbors a variety of topological phases (Pesin and Balents, 2010). Crystal-field splittings induced by lattice distortion of the IrO_6 octahedra can lead to topological insulator (Kargarian, Wen, and Fiete, 2011) and topological Mott insulator (Yang and Kim, 2010) states in pyrocholore iridates. In the honeycomb lattice of Na_2IrO_3, a QSH insulator phase and a fractionalized QSH state have been proposed (Young, Lee, and Kallin, 2008; Shitade *et al.*, 2009). Ir perovskites $Sr_{n+1}Ir_nO_{3n+1}$ undergo a transition from a Mott insulator (Kim *et al.*, 2008) to a correlated metal with increasing n, while orthorhombic perovskite $SrIrO_3$ is metallic. Because of strong SOC, band structures of Ir perovskites display narrow $J_{\text{eff}} = 1/2$ bands near E_F. $SrIrO_3$ with a staggered potential in alternating layers could be a strong TI (Carter *et al.*, 2012). The presence of topological phases in the iridates has not yet been confirmed experimentally (Q. Li *et al.*, 2013; Ye *et al.*, 2013).

2. Osmium compounds

Os compounds involve 5*d* electrons like the iridates, but the SOC is stronger in Os compared to Ir. Os compounds are thus natural candidates to search for correlated topological phases. Os oxides AOs_2O_4, where A is an alkali atom such as Mg, Ca, Sr, or Ba, have a metastable spinel structure which is predicted by DFT + U calculations to host a plethora of exotic phases depending on the strength of U (Wan, Vishwanath, and Savrasov, 2012). In particular, ferromagnetic $CaOs_2O_4$ and $SrOs_2O_4$ are predicted to be magnetic axion insulators with $\theta = \pi$, protected by inversion symmetry with a gapped surface state. Yan *et al.* (2012) proposed that Ce-filled skutterudite compounds $CeOs_4As_{12}$ and $CeOs_4Sb_{12}$ are zero-gap TIs with an inverted band gap between Os-*d* and Ce-*f* orbitals. When the Kondo effect is included between these orbitals, the systems could yield a topological Kondo insulator.

G. Heavy *f*-electron materials

1. Topological Kondo insulator (TKI) SmB_6

SmB_6 is a mixed valence compound whose insulating gap arises from *f*-*d* hybridization (Martin and Allen, 1979). Optical (Gorshunov *et al.*, 1999) and transport (Flachbart *et al.*, 2001) studies give evidence of two gaps of $\sim 3-5$ and $\sim 10-20$ meV. The transition to the insulating state starts below 50 K, but the conductivity remains finite and saturates below 4 K suggesting the presence of metallic states within the gap (Allen, Batlogg, and Wachter, 1979; Cooley *et al.*, 1995). These observations led to renewed interest in SmB_6 as a possible TKI system (Dzero *et al.*, 2010, 2012; Kim, Xia, and Fisk, 2014; G. Li *et al.*, 2014). Other predicted TKIs include SmS (Li, Li *et al.*, 2014; Y. Zhao *et al.*, 2014), and YB_6 and YB_{12} as topological Kondo crystalline insulators (Weng *et al.*, 2014).

ARPES experiments on SmB_6 show a spin-polarized surface state at Γ lying inside the bulk band gap (Denlinger *et al.*, 2013) and X-centered electronlike bands spanning the gap, (Jiang *et al.*, 2013; Neupane *et al.*, 2013; N. Xu *et al.*, 2013), including earlier hints of in-gap states (Miyazaki *et al.*, 2012). An ionic character of bonding in SmB_6 implies the possibility of surface terminations with opposite polarity, which could drive surface reconstructions, a variety of which are seen in STM measurements (Yee *et al.*, 2013; Rößler *et al.*, 2014). Other explanations for the observed in-gap states in SmB_6 suggest these to be of bulk origin (Frantzeskakis *et al.*, 2013) or as being polarity driven nontopological states (Z.-H. Zhu *et al.*, 2013). Transport results such as the observed linear magnetoresistance (Thomas *et al.*, 2013) and quantum Hall effect (D. J. Kim *et al.*, 2013) in SmB_6 have been interpreted within a TKI framework.

2. Topological Mott insulators in actinides

In going from 4*f* electrons in Sm to 5*f* electrons in U, Pu, or Am, Kondo physics becomes too weak to support an insulating phase (Das *et al.*, 2012; Das, Zhu, and Graf, 2012), but a Mott insulator can be induced via strong Coulomb interaction. LDA + U calculations (X. Zhang *et al.*, 2012) predict AmN and PuY, which crystallize in the rock-salt structure, to be TIs where the low-energy electronic spectrum is governed by the actinide *f* and *d* orbitals. The 6*d* states split into Γ_7^+ and Γ_8^+ and 5*f* into $5f^{5/2}$ and $5f^{7/2}$ due to effects of SOC and crystal field. At a certain value of the Coulomb interaction $U = 2.5$ eV, the $5f^{7/2}$ states shift away from E_F and create a nontrivial insulator with band inversion along the Γ-X direction.

LDA + DMFT calculations predict PuB_6, which crystallizes in the same CsCl-type structure as SmB_6, to be a topological Mott insulator (Deng, Haule, and Kotliar, 2013). The band orderings are similar to PuY or AmN with

a surface Dirac cone located in the inverted band gap at the X point. (The size of the insulating gap depends on the value of U used in the computations.) A quantum phase transition in the spin-orbit channel is predicted in URu_2Si_2 yielding a topological metal (Das, 2012). An experimental confirmation of a topological Mott insulator in the actinides has not been reported.

H. Weyl and 3D Dirac semimetals

Weyl and 3D Dirac semimetal phases have been predicted in a variety of existing or tailored systems as follows: (i) pyrochlore iridates could host 24 Weyl nodes through the interplay of SOC and strong electron correlations (Wan *et al.*, 2011), (ii) ferromagnetic $HgCr_2Se_4$ spinel with nodes protected by C_4 point-group symmetry (G. Xu *et al.*, 2011; Fang *et al.*, 2012), (iii) crystalline Cd_3As_2 (Z. Wang *et al.*, 2013) and A_3Bi (A = Na, K, and Rb) (Z. Wang *et al.*, 2012), (iv) β cristobalite BiO_2 (Young *et al.*, 2012), (v) strained $Hg_{1-x-y}Cd_xMn_yTe$ under magnetic field (Bulmash, Liu, and Qi, 2014), (vi) $TlBiSe_2$ (Singh *et al.*, 2012), (vii) heterostructure of magnetically doped 3D TI and normal insulator (Burkov and Balents, 2011), and (viii) a superlattice of alternating layers with odd and even parity orbitals (Das, 2013). Experimentally realized 3D Dirac semimetals so far are Cd_3As_2 (Neupane *et al.*, 2014b; Ali *et al.*, 2014; Borisenko *et al.*, 2014) and Na_3Bi (Liu *et al.*, 2014b; Xu *et al.*, 2015c). Bulk Dirac cones have also been reported in $SrMnBi_2$ and $CaMnBi_2$ (Feng *et al.*, 2014). Attempts to obtain Weyl fermions by breaking TRS in 3D Dirac semimentals have been undertaken in Cd_3As_2 (Jeon *et al.*, 2014). By breaking inversion symmetry rather than the TRS, Weyl semimetals have been predicted and then realized in the TaAs family (Huang *et al.*, 2015; Lv *et al.*, 2015; Weng *et al.*, 2015; Xu *et al.*, 2015a, 2015b; L. X. Yang *et al.*, 2015; Zhang *et al.*, 2016).

I. Other topological materials

1. Complex oxides

Complex oxides are widely studied in the context of magnetism, metal-insulator transitions, superconductors (Pickett, 1989; Imada, Fujimori, and Tokura, 1998; Gardner, Gingras, and Greedan, 2010), and as platforms for oxide electronics (Tokura and Hwang, 2008; Heber, 2009). First-principles calculations indicate that the electronic structures of bulk $YBiO_3$ (Jin *et al.*, 2013), $BaBiO_3$ (Yan, Jansen, and Felser, 2013), (111) bilayer of $LuAlO_3$ (Xiao *et al.*, 2011), and a superlattice of CrO_2/TiO_2 (Cai *et al.*, 2015) are potential TI and QAH candidates. (Iridates are related materials discussed in Sec. IV.F.1.) The band inversion between Bi- and O-p states in $YBiO_3$ upon the inclusion of SOC occurs at TRIM points R, rather than at Γ (Jin *et al.*, 2013). $BaBiO_3$ is a known superconductor with $T_c \sim 30$ K (Sleight, Gillson, and Bierstedt, 1975; Cava *et al.*, 1988), which is predicted by DFT to have a large topological band gap of 0.7 eV (Yan, Jansen, and Felser, 2013). Although the treatment of electron correlation effects is a source of uncertainty in band structure computations, Okamoto *et al.* (2014) showed that the TI phase survives in DMFT computations on a $LuAlO_3$ bilayer.

2. Skutterudites, antiperovskites, and other structures

We note a variety of other theoretically predicted topological materials as follows: (i) IrBi3 (Yang and Liu, 2014) and $CoSb_3$ (Smith *et al.*, 2011) in their skutterudite crystal structure are predicted to have a nontrivial topological phase by DFT + U calculations. (ii) Antiperovskite compounds $(M_3N)Bi$ (M = Ca, Sr, and Ba) (Sun *et al.*, 2010) and the Ca_3PbO family (Kariyado and Ogata, 2011), (iii) cubic perovskites $CsXI_3$ (X = Pb, Sn) under strain (Yang *et al.*, 2012), (iv) strain induced topological phase transition in Zintl compounds Sr_2X (X = Pb, Sn) (Sun *et al.*, 2011), (v) single-layer $ZrTe_5$ and $HfTe_5$ in a layered structure as 2D TIs with a band gap as large as 0.4 eV (Weng, Dai, and Fang, 2014), (vi) β-GaS and GaS-II family under uniaxial strain (X. Huang *et al.*, 2013), and (vii) $Cs(Sn, Pb, Ge)(Cl, Br, I)_3$ ternary halides (Yang *et al.*, 2012).

V. OUTLOOK AND CONCLUSIONS

Although considerable progress has been made in discovering new topological materials during the last few years, the menu of choices available currently is still quite limited, especially when it comes to 2D systems and to materials where topological states are protected through combinations of time-reversal, crystalline, and particle-hole symmetries. Implementation of robust tools for assessing topological characteristics of band structures (e.g., Z_2 invariants, Chern numbers, Berry connection, Berry curvature) in widely available open source band structure codes will help accelerate the discovery process, and the development of viable materials with flexibility and tunability necessary for fundamental science investigations and as platforms for various applications. Limitations of the band theory in strongly correlated materials apply to the topological band theory as well, but extensions of the weak coupling band theory to reliably treat the intermediate coupling regime with predictive capabilities should be possible. Realistic modeling of the spectral intensities, including matrix element effects, is needed for reliable identification of the key topological states and their spin textures, especially for the surface sensitive angle-resolved photoemission and scanning tunneling spectroscopies, which are the most relevant spectroscopies in connection with topological materials. In this vein, realistic modeling of transport properties of topological materials, including effects of external fields, electron-phonon couplings, defects, and impurities, is another area that needs attention for developing practical spintronics and other applications. There are many experimental challenges as well in synthesizing materials, which can reach the topological transport regime. A related challenge is realizing a high degree of theoretically predicted spin polarization of the topological surface states, which is reduced by various intrinsic and extrinsic effects. There are exciting possibilities for observing in a solid-state setting non-Abelian particles associated usually with high-energy physics such as axions, Majorana fermions, magnetic monopoles, and fractional excitations. The challenge here is to control correlated physics of magnetism and superconductivity within the topological matrix. Nevertheless, there can be little doubt that vast treasures of riches and surprises await us in the gold mine of 3D and 2D topological materials,

and their interfaces and heterostructures involving magnetic, nonmagnetic, and superconducting materials.

ACKNOWLEDGMENTS

It is a great pleasure to acknowledge our collaborations and discussions on various aspects of topological materials with the following colleagues: J. Adell, N. Alidoust, J. M. Allred, T. Balasubramanian, A. Balatsky, L. Balicas, B. Barbiellini, S. Basak, I. Belopolski, G. Bian, M. Bissen, J. Braun, R. S. Cava, H. R. Chang, T.-R. Chang, J. G. Checkelsky, Y. Chen, F. C. Chou, F. C. Chuang, Y.-T. Cui, J.-W. Deng, J. D. Denlinger, C. Dhital, J. H. Dil, H. Ding, K. Dolui, W. Duan, T. Durakiewicz, H. Ebert, A. V. Fedorov, Z. Fisk, L. Fu, D. R. Gardner, Q. Gibson, M. J. Graf, D. Grauer, G. Gupta, M. Z. Hasan, Y. He, J. Hoffman, Y. S. Hor, D. Hsieh, T. H. Hsieh, C.-H. Hsu, C.-Yi Huang, Y.-B. Huang, Z.-Q. Huang, E. Hudson, Z. Hussain, Y. Ishida, M. B. Jalil, H.-T. Jeng, H. Ji, S. Jia, Y. Jo, S. Kaprzyk, S. Khadka, D.-J. Kim, T. Kondo, J. W. Krizan, S. K. Kushwaha, G. Landolt, M. Leandersson, J. Lee, Y. S. Lee, G. C. Liang, M. Lindroos, C. Liu, J. Liu, Y.-T, Liu, Z. Liu, V. Madhavan, D. Marchenko, A. Marcinkova, R. S. Markiewicz, F. Meier, P. E. Mijnarends, J. Minár, K. Miyamoto, S.-K. Mo, R. Moore, E. Morosan, M. Neupane, J. Nieminen, Y. Ohtsubo, Y. Okada, T. Okuda, N. P. Ong, J. Osterwalder, A. Pal, L. Patthey, A. Petersen, R. Prasad, C. M. Polley, D. Qian, O. Rader, A. Richardella, N. Samarth, J. Sánchez-Barriga, F. Schmitt, M. R. Scholz, M. Serbyn, M. Severson, R. Shankar, A. Sharma, Z. X. Shen, S. Shin, B. Singh, B. Slomski, A. Soumyanarayanan, A. Taleb-Ibrahimi, W.-F. Tsai, A. Varykhalov, A. Volykhov, F. von Rohr, D. Walkup, Y. Wang, Y.-J. Wang, Z. Wang, S. D. Wilson, L. A. Wray, D. Wu,Y. Xia, J. Xiong, S. Xu, H. Yan, L. V. Yashina, M. M. Yee, D. Zhang, Y. Zhang, Bo Zhou, and W. Zhou. The work of A. B. was supported by the U.S. Department of Energy, Basic Energy Sciences, Division of Materials Sciences Grants No. DE-FG02-07ER46352 (core research), No. DE-AC02-05CH11231 (computational support at NERSC), and No. DE-SC0012575 (work on layered materials). The work of H. L. and T. D. was supported by the National Research Foundation, Prime Minister's Office, Singapore under its NRF fellowship (NRF Award No. NRF-NRFF2013-03).

APPENDIX: INVENTORY OF 2D AND 3D TOPOLOGICAL MATERIALS

TABLE I. An inventory of 2D and 3D topological materials. Although we have attempted to separate the references in the table as being theoretical (Th) or experimental (Exp) in their focus, many articles involve both components. This inventory should not be considered exhaustive, although it should be fairly complete as of the submission date, and includes some subsequent updating.

Material	References
Bi/Sb variants Sb; $Bi_{1-x}Sb_x$	Th: Fu and Kane (2007), Teo, Fu, and Kane (2008), Zhu and Hofmann (2014), and Sahin and Flatte (2015). Exp: Hsieh *et al.* (2008), Gomes *et al.* (2009), D. Hsieh *et al.* (2009a), Roushan *et al.* (2009), Nishide *et al.* (2010), Guo *et al.* (2011), Soumyanarayanan *et al.* (2013), X.-G. Zhu *et al.* (2013), and Tian *et al.* (2015).
As	Th: Campi, Bernasconi, and Benedek (2012).
Bi_2Se_3; Bi_2Te_3; Sb_2Te_3	Th: Xia *et al.* (2009), H. Zhang *et al.* (2009), Wang, Wang, and Zhang (2010), Menshchikova, Eremeev, and Chulkov (2011), M. S. Bahramy *et al.* (2012), Chis *et al.* (2012), Henk, Ernst *et al.* (2012), Henk, Flieger *et al.* (2012), Hinsche *et al.* (2012), Luo, Sullivan, and Quek (2012), Niesner *et al.* (2012), J.- M. Zhang *et al.* (2012), Eremeev *et al.* (2013), Koleini, Frauenheim, and Yan (2013), X. Kou *et al.* (2013), Luo and Qi (2013), W. Wang *et al.* (2013), G. Wu *et al.* (2013), L. Wu *et al.* (2013), C. H. Li *et al.* (2014), Wan and Savrasov (2014), Wang and Chiang (2014), Hinsche *et al.* (2015), and Wang *et al.* (2015). Exp: Chen *et al.* (2009), Hor *et al.* (2009), Hsieh *et al.* (2009a, 2009b), Xia *et al.* (2009), T. Zhang *et al.* (2009), Analytis *et al.* (2010), J. Chen *et al.* (2010), Jenkins *et al.* (2010), Kuroda *et al.* (2010a), Qu *et al.* (2010), Steinberg *et al.* (2010), Y. Zhang *et al.* (2010), S. Kim *et al.* (2011), L. Zhu *et al.* (2011), X. Zhu *et al.* (2011), Alpichshev *et al.* (2012), Crepaldi *et al.* (2012), Jenkins *et al.* (2012), Kim *et al.* (2012), Okada *et al.* (2012), Pauly *et al.* (2012), Qu, Hor, and Cava (2012), Valdés Aguilar *et al.* (2012), Y. Wang *et al.* (2012), J.- M. Zhang *et al.* (2012), P. Zhang *et al.* (2012), Aitani *et al.* (2013), Chiu and Lin (2013), Fauqué *et al.* (2013), Jozwiak *et al.* (2013), D. Kim *et al.* (2013), Kirshenbaum *et al.* (2013), Kong *et al.* (2013), Luo and Qi (2013), Luo *et al.* (2013), Ning *et al.* (2013), Rischau *et al.* (2013), Tian *et al.* (2013), Wang, Su, and Liu (2013), Yan *et al.* (2013), J. Zhu *et al.* (2013), X.- G. Zhu *et al.* (2013), Bansal *et al.* (2014), Boschker *et al.* (2014), Deshpande *et al.* (2014), Edmonds *et al.* (2014), Fu *et al.* (2014), Hoefer *et al.* (2014), Hong *et al.* (2014), D. Kim *et al.* (2014), N. Kim *et al.* (2014), Lang *et al.* (2014), C. H. Li *et al.* (2014), Y. Liu *et al.* (2014), Mellnik *et al.* (2014), Neupane *et al.* (2014a), Nomura *et al.* (2014), Sessi, Bathon *et al.* (2014), Sung *et al.* (2014), Tsipas *et al.* (2014), Vargas *et al.* (2014), Yan *et al.* (2014), L. Zhao *et al.* (2014), Y. Zhao *et al.* (2014), Cacho *et al.* (2015), Kastl *et al.* (2015), Park *et al.* (2015), and Seibel *et al.* (2015).

(*Table continued*)

TABLE I. (*Continued*)

Material	References
Bi_2Te_2Se; B_2X_2X' (B = Bi, Sb; X, X' = S, Se, Te)	Th: Chang *et al.* (2011), Lin *et al.* (2011), Menshchikova, Eremeev, and Chulkov (2011), Wang and Johnson (2011), Eremeev *et al.* (2012b), and Gehring *et al.* (2013). Exp: Ren *et al.* (2010), Bao *et al.* (2012), Miyamoto *et al.* (2012), Ren *et al.* (2012), Xiong *et al.* (2012), Barreto *et al.* (2014), Hajlaoui *et al.* (2014), and Wang, Graf, and Petrovic (2014).
Alloy $(Bi, Sb)_2(S, Se, Te)_3$	Th: Niu, Dai, Zhu, Ma *et al.* (2012). Exp: Kong *et al.* (2011), Taskin *et al.* (2011), J. Zhang *et al.* (2011), Ji *et al.* (2012), Ando *et al.* (2014), Lee *et al.* (2014), Ou *et al.* (2014), Shikin *et al.* (2014), J. Tang *et al.* (2014), Yoshimi *et al.* (2014), F. X. Yang *et al.* (2015), and Yoshimi *et al.* (2015).
Mn/Fe/Cr/Gd/V magnetically doped	Th: H. B. Zhang *et al.* (2012). Exp: Y. L. Chen *et al.* (2010a), Hor *et al.* (2010), Beidenkopf *et al.* (2011), Okada *et al.* (2011), Wray *et al.* (2011), Checkelsky *et al.* (2012), Xu *et al.* (2012b), D. Zhang *et al.* (2012), Chang *et al.* (2013), Jiang *et al.* (2013), X. Kou *et al.* (2013), Schlenk *et al.* (2013), Zhang, Kane, and Mele (2013), Z. Zhao *et al.* (2013), Checkelsky *et al.* (2014), Fan *et al.* (2014), Harrison *et al.* (2014), Sessi, Reis *et al.* (2014), Bestwick *et al.* (2015), Chang *et al.* (2015), Lee *et al.* (2015), and M. Li *et al.* (2015).
Cu doped	Exp: Wray *et al.* (2010), Kriener *et al.* (2012), and Lawson, Hor, and Li (2012).
$(Bi_{1-x}In_x)_2Se_3$	Exp: Brahlek *et al.* (2012) and L. Wu *et al.* (2013).
$Ge_mBi_{2n}Te_{m+3n}$; $A_mB_{2n}X_{m+3n}$ (A = Pb, Sn, Ge; B = Bi, Sb; X, X' = S, Se, Te)	Th: Kim, Kim, and Jhi (2010), Xu *et al.* (2010), Jin *et al.* (2011), Sa *et al.* (2011), Singh *et al.* (2013), and Sa *et al.* (2014). Exp: Xu *et al.* (2010), Taskin *et al.* (2011), Neupane *et al.* (2012), Okamoto *et al.* (2012), Marcinkova *et al.* (2013), Muff *et al.* (2013), Okuda *et al.* (2013), Niesner *et al.* (2014), Nomura *et al.* (2014), and Sa *et al.* (2014).
$(PbSe)_5(Bi_2Se_3)_{3m}$	Exp: Nakayama *et al.* (2012), Fang *et al.* (2014), and Sasaki, Segawa, and Ando (2014).
$TlBiSe_2$; $MM'X_2$ (M = Tl, M' = Bi or Sb, and X = Te, Se, or S)	Th: Eremeev, Koroteev, and Chulkov (2010), Lin, Markiewicz *et al.* (2010), Yan, Liu *et al.* (2010), Chang *et al.* (2011), Eremeev *et al.* (2011), Niu, Dai, Zhu, Lu *et al.* (2012), and Singh *et al.* (2012). Exp: Chen *et al.* (2010b), Kuroda *et al.* (2010b), Sato *et al.* (2010), Sato *et al.* (2011), S.-Y. Xu *et al.* (2011), Novak *et al.* (2015), Shoman *et al.* (2015), and Xu *et al.* (2015d).
Bi_2TeI	Th: Klintenberg (2010) and P. Tang *et al.* (2014).
BiTeX (X = I, Br, Cl)	Th: Bahramy, Arita, and Nagaosa (2011), M. S. Bahramy *et al.* (2012), Eremeev *et al.* (2012b), and Landolt *et al.* (2013). Exp: Ishizaka *et al.* (2011), Chen *et al.* (2013), Landolt *et al.* (2013), Crepaldi *et al.* (2014), and Tran *et al.* (2014).
$LaBiTe_3$	Th: Yan, Zhang *et al.* (2010).
$(Bi_2)_m(Bi_2Te_3)_n$	Th: Jeffries *et al.* (2011). Exp: Jeffries *et al.* (2011), Valla *et al.* (2012), and Shirasawa *et al.* (2013).
$Bi_{14}Rh_3I_9$	Th: Rasche *et al.* (2013). Exp: Pauly *et al.* (2015).
Topological crystalline insulator (TCI): SnTe; (Pb,Sn)(S,Se,Te)	Th: Hsieh *et al.* (2012), Hota (2013), Safaei, Kacman, and Buczko (2013), Sun *et al.* (2013), Y. J. Wang *et al.* (2013), Eremeev *et al.* (2014), Fang, Gilbert, and Bernevig (2014), J. Liu *et al.* (2014), Tang and Fu (2014), J. Wang *et al.* (2014), N. Wang *et al.* (2014), and Wrasse and Schmidt (2014). Exp: Burke *et al.* (1965), Iizumi *et al.* (1975), Takafuji and Narita (1982), Littlewood *et al.* (2010), Dziawa *et al.* (2012), Tanaka *et al.* (2012), Xu *et al.* (2012a), Balakrishnan *et al.* (2013), Z. Li *et al.* (2013), Liang *et al.* (2013), Okada *et al.* (2013), Zhong *et al.* (2013), Polley *et al.* (2014), Shen *et al.* (2014), Taskin *et al.* (2014), and Zeljkovic *et al.* (2014, 2015a, 2015b).
Sn variants, Sn	Th: Fu and Kane (2007) and Küfner *et al.* (2013). Exp: Barfuss *et al.* (2013).
3D HgTe	Th: Chiu, Ghaemi, and Hughes (2012), Ortix *et al.* (2014), and Beugeling *et al.* (2015). Exp: Oostinga *et al.* (2013), Orlita *et al.* (2014), Ren *et al.* (2014), Olshanetsky *et al.* (2015), and Sochnikov *et al.* (2015).

(*Table continued*)

TABLE I. (*Continued*)

Material	References
Half Heusler	Th: Al-Sawai *et al.* (2010), Chadov *et al.* (2010), Lin, Markiewicz *et al.* (2010), and Xiao *et al.* (2010). Exp: Miyawaki *et al.* (2012) and Wang and Zhang (2013).
Li_2AgSb; $Li_2M'X$ [M = Cu, Ag, Au, or Cd and X = Sb, Bi, or Sn]	Th: Lin, Das, Wang *et al.* (2013).
Ternary chalcopyrites; famatinites; and quaternary chalcogenides	Th: Feng *et al.* (2011) and Y. J. Wang *et al.* (2011).
LiAuSe; KHgSb	Th: H. J. Zhang *et al.* (2011).
β-Ag_2Te	Th: W. Zhang *et al.* (2011). Exp: Sulaev *et al.* (2013) and Z. Zhao *et al.* (2013).
2D systems Graphene	Th: Kane and Mele (2005a), Beenakker (2008), Wunsch, Guinea, and Sols (2008), Castro Neto *et al.* (2009), Park and Louie (2009), Peres (2010), Das Sarma *et al.* (2011), Goerbig (2011), Weeks *et al.* (2011), Ghaemi, Gopalakrishnan, and Hughes (2012), Hu *et al.* (2012), Kotov *et al.* (2012), Pesin and MacDonald (2012), Diniz, Guassi, and Qu (2013), Hu *et al.* (2013), X. Kou *et al.* (2013), Lau (2013), Maher *et al.* (2013), Vaezi *et al.* (2013), and Chang *et al.* (2014). Exp: Beenakker (2008), Castro Neto *et al.* (2009), Peres (2010), Das Sarma *et al.* (2011), Goerbig (2011), and Kotov *et al.* (2012), Maher *et al.* (2013), Gomes *et al.* (2012), Kravets *et al.* (2013), Gorbachev *et al.* (2014), Young *et al.* (2014), and Ju *et al.* (2015).
Silicene; germanene	Th: Liu, Feng, and Yao (2011), Liu, Jiang, and Yao (2011), Drummond, Zólyomi, and Fal'ko (2012), Ezawa (2012, 2013), Kikutake, Ezawa, and Nagaosa (2013), Padilha *et al.* (2013), Tabert and Nicol (2013), Tahir and Schwingenschlögl (2013), Tsai *et al.* (2013), Zhang, Zhao, and Yang (2013), Gupta *et al.* (2014), and Pan *et al.* (2014).
GaAs/Ge/GaAs	Th: D. Zhang *et al.* (2013).
GaBi; InBi; TlBi	Th: Chuang *et al.* (2014) and L. Li *et al.* (2015).
Bi_4Br_4	Th: J.-J. Zhou *et al.* (2014).
GeX; SnX; PbX; BiX (X = H, I, Br, Cl, F or OH)	Th: Si *et al.* (2014) and Y. Xu *et al.* (2013).
Bi	Th: Murakami (2006), Z. Liu *et al.* (2011), Wada *et al.* (2011), Z.-Q. Huang *et al.* (2013), Wang, Chen, and Liu (2014), and Ma *et al.* (2015). Exp: Wells *et al.* (2009), Hirayama, Aoki, and Kato (2011), Hirahara *et al.* (2012), Jnawali *et al.* (2012), Lükermann *et al.* (2012), Chun-Lei *et al.* (2013), Coelho *et al.* (2013), Z. F. Wang *et al.* (2013), Drozdov *et al.* (2014), S. H. Kim *et al.* (2014), Lu *et al.* (2015), and Takayama *et al.* (2015).
Sb	Th: P. Zhang *et al.* (2012) and Chuang *et al.* (2013). Exp: Bian, Miller, and Chiang (2011) and Yao *et al.* (2013).
Bi$Te$$X$ (X = I, Br, Cl)	Th: Kou *et al.* (2014).
HgTe/CdTe	Th: Bernevig, Hughes, and Zhang (2006), Luo and Zunger (2010), and Khaymovich, Chtchelkatchev, and Vinokur (2013). Exp: König *et al.* (2007), Brüne *et al.* (2012), Zholudev *et al.* (2012), König *et al.* (2013), Nowack *et al.* (2013), Gusev *et al.* (2014), and Hart *et al.* (2014).
InAs/GaSb/AlSb	Th: Liu *et al.* (2008). Exp: Knez, Du, and Sullivan (2011), Knez *et al.* (2014), and Du *et al.* (2015).
$LaAlO_3/SrTiO_3$; $SrTiO_3/SrIrO_3$; $KTaO_3/KPtO_3$	Th: Lado, Pardo, and Baldomir (2013). Exp: Cheng *et al.* (2013).
$LaAuO_3$; $SrIrO_3$	Th: Xiao *et al.* (2011), Okamoto *et al.* (2014).
CrO_3/TiO_3	Th: Cai *et al.* (2015).
Transition metal dichalcogenides	Th: Cazalilla, Ochoa, and Guinea (2014) and Qian *et al.* (2014).
Organometallics	Th: Z. Liu *et al.* (2013), Wang, Su, and Liu (2013), Wang, Liu, and Liu (2013a), Wang, Liu, and Liu (2013b), and W. Li, Z. Liu *et al.* (2014).
Transition metal compounds	

(*Table continued*)

TABLE I. (*Continued*)

Material	References
$R_2Ir_2O_7$ (R = Nd, Sm, Eu, and Y)	Th: Pesin and Balents (2010), Yang and Kim (2010), Kargarian, Wen, and Fiete (2011), and Wan *et al.* (2011). Exp: Matsuhira *et al.* (2007) and Ueda *et al.* (2014).
$Pb_2Ir_2O_{7-x}$	Th & Exp: Hirata *et al.* (2013).
Na_2IrO_3; Li_2IrO_3	Th: Young, Lee, and Kallin (2008), Shitade *et al.* (2009), Kargarian, Langari, and Fiete (2012), and You, Kimchi, and Vishwanath (2012). Exp: Alpichshev *et al.* (2015).
$Sr_{n+1}Ir_nO_{3n+1}$; Sr_2IrO_3; Sr_2IrRhO_6	Th: Carter *et al.* (2012). Exp: Kim *et al.* (2008), Q. Li *et al.* (2013), and Ye *et al.* (2013).
AOs_2O_4 (A = Mg, Ca, Sr)	Th: Wan, Vishwanath, and Savrasov (2012).
$CeOs_4As_{12}$; $CeOs_4Sb_{12}$	Th: B. Yan, L. Müchler *et al.* (2012).
$ZrTe_5$; $HfTe_5$	Th: Weng, Dai, and Fang (2014).
Heavy f-electron materials SmB_6, YB_6, and YB_{12}	Th: Dzero *et al.* (2010, 2012), Lu *et al.* (2013), Z. H. Zhu *et al.* (2013), and Weng *et al.* (2014). Exp: Flachbart *et al.* (2001), Miyazaki *et al.* (2012), Denlinger *et al.* (2013), Frantzeskakis *et al.* (2013), Jiang *et al.* (2013), D. J. Kim *et al.* (2013), Neupane *et al.* (2013), Thomas *et al.* (2013), N. Xu *et al.* (2013), Yee *et al.* (2013), X. Zhang *et al.* (2013), Z.-H. Zhu *et al.* (2013), Kim, Xia, and Fisk (2014), G. Li *et al.* (2014), Rößler *et al.* (2014), Fuhrman *et al.* (2015), Neupane *et al.* (2015), and Syers *et al.* (2015).
SmS	Th: Z. Li *et al.* (2014) and J.-Z. Zhao *et al.* (2014).
PuB6	Th: Deng, Haule, and Kotliar (2013).
AmN and PuY	Th: X. Zhang *et al.* (2012).
URu_2Si_2	Th: Das (2012).
Weyl and 3D Dirac semimetals $HgCr_2Se_4$	Th: G. Xu *et al.* (2011) and Fang, Gilbert, Dai, and Bernevig (2012).
A_3Bi (A = Na, K, Rb)	Th: Z. Wang, Y. Sun *et al.* (2012), Narayan *et al.* (2014), and Gorbar *et al.* (2015). Exp: Z. K. Liu *et al.* (2014b) and Xu *et al.* (2015c).
BiO_2	Th: Young *et al.* (2012).
$Hg_{1-x-y}Cd_xMn_yTe$	Th: Bulmash, Liu, and Qi (2014).
Cd_3As_2	Th: Z. Wang, H. Weng *et al.* (2013). Exp: Neupane *et al.* (2014b), Ali *et al.* (2014), Borisenko *et al.* (2014), Jeon *et al.* (2014), Z. K. Liu *et al.* (2014a), Yi *et al.* (2014), and Pariari, Dutta, and Mandal (2015).
$SrMnBi_2$; $CaMnBi_2$	Exp: K. Wang *et al.* (2011) and Feng *et al.* (2014).
$LaAgSb_2$	Exp: Wang and Petrovic (2012).
TaAs, TaP, NbAs, NbP	Th: Huang *et al.* (2015) and Weng *et al.* (2015). Exp: Lv *et al.* (2015), Xu *et al.* (2015a), L. X. Yang *et al.* (2015), and Zhang *et al.* (2016).
Complex oxides $YBiO_3$	Th: Jin *et al.* (2013).
$BaBiO_3$	Th: Yan, Jansen, and Felser (2013).
Skutterudites $IrBi_3$	Th: Yang and Liu (2014).
$CoSb_3$	Th: Smith *et al.* (2011).
Antiperovskites M_3NBi (M = Ca, Sr, Ba)	Th: Sun *et al.* (2010).
Ca_3PbO	Th: Kariyado and Ogata (2011).

REFERENCES

Abrikosov, A. A., 1998, "Quantum Magnetoresistance," Phys. Rev. B **58**, 2788.

Aitani, M., Y. Sakamoto, T. Hirahara, M. Yamada, H. Miyazaki, M. Matsunami, S. Kimura, and S. Hasegawa, 2013, "Fermi-Level Tuning of Topological Insulator Thin Films," Jpn. J. Appl. Phys. **52**, 110112, No. 11R.

Alexandradinata, A., C. Fang, M. J. Gilbert, and B. A. Bernevig, 2014, "Spin-Orbit-Free Topological Insulators without Time-Reversal Symmetry," Phys. Rev. Lett. **113**, 116403.

Ali, M. N., Q. Gibson, S. Jeon, B. B. Zhou, A. Yazdani, and R. J. Cava, 2014, "The Crystal and Electronic Structures of Cd_3As_2, the Three-Dimensional Electronic Analogue of Graphene," Inorg. Chem. **53**, 4062.

Allen, J. W., B. Batlogg, and P. Wachter, 1979, "Large Low-Temperature Hall Effect and Resistivity in Mixed-Valent SmB_6," Phys. Rev. B **20**, 4807.

Alpichshev, Z., R. R. Biswas, A. V. Balatsky, J. G. Analytis, J.-H. Chu, I. R. Fisher, and A. Kapitulnik, 2012, "STM Imaging of Impurity Resonances on Bi_2Se_3," Phys. Rev. Lett. **108**, 206402.

Alpichshev, Z., F. Mahmood, G. Cao, and N. Gedik, 2015, "Confinement-Deconfinement Transition as an Indication of Spin-Liquid-Type Behavior in Na_2IrO_3," Phys. Rev. Lett. **114**, 017203.

Al-Sawai, W., H. Lin, R. S. Markiewicz, L. A. Wray, Y. Xia, S.-Y. Xu, M. Z. Hasan, and A. Bansil, 2010, "Topological Electronic Structure in Half-Heusler Topological Insulators," Phys. Rev. B **82**, 125208.

Analytis, J. G., R. D. McDonald, S. C. Riggs, J.-H. Chu, G. S. Boebinger, and I. R. Fisher, 2010, "Two-Dimensional Surface State in the Quantum Limit of a Topological Insulator," Nat. Phys. **6**, 960.

Anderson, P. W., 1958, "Absence of Diffusion in Certain Random Lattices," Phys. Rev. **109**, 1492.

Ando, Y., 2013, "Topological Insulator Materials," J. Phys. Soc. Jpn. **82**, 102001.

Ando, Y., T. Hamasaki, T. Kurokawa, K. Ichiba, F. Yang, M. Novak, S. Sasaki, K. Segawa, Y. Ando, and M. Shiraishi, 2014, "Electrical Detection of the Spin Polarization Due to Charge Flow in the Surface State of the Topological Insulator $Bi_{1.5}Sb_{0.5}Te_{1.7}Se_{1.3}$," Nano Lett. **14**, 6226.

Baasanjav, D., O. A. Tretiakov, and K. Nomura, 2014, "Magnetoelectric Effect in Topological Insulator Films beyond Linear Response Regime," Phys. Rev. B **90**, 045149.

Bahramy, M. S., R. Arita, and N. Nagaosa, 2011, "Origin of Giant Bulk Rashba Splitting: Application to BiTeI," Phys. Rev. B **84**, 041202.

Bahramy, M. S., B.-J. Yang, R. Arita, and N. Nagaosa, 2012, "Emergence of Non-Centrosymmetric Topological Insulating Phase in BiTeI under Pressure," Nat. Commun. **3**, 679.

Bahramy, M. S., *et al.*, 2012, "Emergent Quantum Confinement at Topological Insulator Surfaces," Nat. Commun. **3**, 1159.

Balakrishnan, G., L. Bawden, S. Cavendish, and M. R. Lees, 2013, "Superconducting Properties of the In-Substituted Topological Crystalline Insulator SnTe," Phys. Rev. B **87**, 140507.

Bansal, N., M. R. Cho, M. Brahlek, N. Koirala, Y. Horibe, J. Chen, W. Wu, Y. D. Park, and S. Oh, 2014, "Transferring MBE-Grown Topological Insulator Films to Arbitrary Substrates and Metal-Insulator Transition via Dirac Gap," Nano Lett. **14**, 1343.

Bansal, N., Y. S. Kim, M. Brahlek, E. Edrey, and S. Oh, 2012, "Thickness-Independent Transport Channels in Topological Insulator Bi_2Se_3 Thin Films," Phys. Rev. Lett. **109**, 116804.

Bansil, A., 1979a, "Coherent-Potential and Average T-Matrix Approximations for Disordered Muffin-Tin Alloys. I. Formalism," Phys. Rev. B **20**, 4025.

Bansil, A., 1979b, "Coherent-Potential and Average T-Matrix Approximations for Disordered Muffin-Tin Alloys. II. Application to Realistic Systems," Phys. Rev. B **20**, 4035.

Bansil, A., S. Kaprzyk, P. Mijnarends, and J. Toboła, 1999, "Electronic Structure and Magnetism of $Fe_{3-x}V_xX$ (X = Si, Ga, and Al) Alloys by the KKR-CPA Method," Phys. Rev. B **60**, 13396.

Bansil, A., and M. Lindroos, 1999, "Importance of Matrix Elements in the ARPES Spectra of BISCO," Phys. Rev. Lett. **83**, 5154.

Bansil, A., M. Lindroos, S. Sahrakorpi, and R. S. Markiewicz, 2005, "Influence of the Third Dimension of Quasi-Two-Dimensional Cuprate Superconductors on Angle-Resolved Photoemission Spectra," Phys. Rev. B **71**, 012503.

Bansil, A., R. Rao, P. Mijnarends, and L. Schwartz, 1981, "Electron Momentum Densities in Disordered Muffin-Tin Alloys," Phys. Rev. B **23**, 3608.

Bao, L., *et al.*, 2012, "Weak Anti-Localization and Quantum Oscillations of Surface States in Topological Insulator Bi_2Se_2Te," Sci. Rep. **2**, 0723.

Bardarson, J. H., and J. E. Moore, 2013, "Quantum Interference and Aharonov-Bohm Oscillations in Topological Insulators," Rep. Prog. Phys. **76**, 056501.

Barfuss, A., *et al.*, 2013, "Elemental Topological Insulator with Tunable Fermi Level: Strained α-Sn on InSb(001)," Phys. Rev. Lett. **111**, 157205.

Barreto, L., L. Kuehnemund, F. Edler, C. Tegenkamp, J. Mi, M. Bremholm, B. B. Iversen, C. Frydendahl, M. Bianchi, and P. Hofmann, 2014, "Surface-Dominated Transport on a Bulk Topological Insulator," Nano Lett. **14**, 3755.

Basak, S., H. Lin, L. A. Wray, S.-Y. Xu, L. Fu, M. Z. Hasan, and A. Bansil, 2011, "Spin Texture on the Warped Dirac-Cone Surface States in Topological Insulators," Phys. Rev. B **84**, 121401.

Beenakker, C. W. J., 2008, "*Colloquium*: Andreev Reflection and Klein Tunneling in Graphene," Rev. Mod. Phys. **80**, 1337.

Beenakker, C. W. J., 2013, "Search for Majorana Fermions in Superconductors," Annu. Rev. Condens. Matter Phys. **4**, 113.

Beidenkopf, H., P. Roushan, J. Seo, L. Gorman, I. Drozdov, Y. S. Hor, R. J. Cava, and A. Yazdani, 2011, "Spatial Fluctuations of Helical Dirac Fermions on the Surface of Topological Insulators," Nat. Phys. **7**, 939.

Bernevig, B. A., T. L. Hughes, and S.-C. Zhang, 2006, "Quantum Spin Hall Effect and Topological Phase Transition in HgTe Quantum Wells," Science **314**, 1757.

Berry, M. V., 1984, "Quantal Phase Factors Accompanying Adiabatic Changes," Proc. R. Soc. Lond. Math. Phys. Sci. **392**, 45 [http://www.jstor.org/stable/2397741].

Bestwick, A. J., E. J. Fox, X. Kou, L. Pan, K. L. Wang, and D. Goldhaber-Gordon, 2015, "Precise Quantization of the Anomalous Hall Effect near Zero Magnetic Field," Phys. Rev. Lett. **114**, 187201.

Beugeling, W., E. Kalesaki, C. Delerue, Y.-M. Niquet, D. Vanmaekelbergh, and C. M. Smith, 2015, "Topological States in Multi-Orbital HgTe Honeycomb Lattices," Nat. Commun. **6**, 6316.

Bian, G., T. Miller, and T.-C. Chiang, 2011, "Passage from Spin-Polarized Surface States to Unpolarized Quantum Well States in Topologically Nontrivial Sb Films," Phys. Rev. Lett. **107**, 036802.

Biswas, R. R., and A. Balatsky, 2009, "Quasiparticle Interference and Landau Level Spectroscopy in Graphene in the Presence of a Strong Magnetic Field," Phys. Rev. B **80**, 081412.

Black-Schaffer, A. M., and A. V. Balatsky, 2013, "Proximity-Induced Unconventional Superconductivity in Topological Insulators," Phys. Rev. B **87**, 220506.

Borisenko, S., Q. Gibson, D. Evtushinsky, V. Zabolotnyy, B. Buechner, and R. J. Cava, 2014, "Experimental Realization of a Three-Dimensional Dirac Semimetal," Phys. Rev. Lett. **113**, 027603.

Boschker, J. E., J. Momand, V. Bragaglia, R. Wang, K. Perumal, A. Giussani, B. J. Kooi, H. Riechert, and R. Calarco, 2014, "Surface Reconstruction-Induced Coincidence Lattice Formation Between Two-Dimensionally Bonded Materials and a Three-Dimensionally Bonded Substrate," Nano Lett. **14**, 3534.

Brahlek, M., N. Bansal, N. Koirala, S.-Y. Xu, M. Neupane, C. Liu, M. Z. Hasan, and S. Oh, 2012, "Topological-Metal to Band-Insulator Transition in $(Bi_{1-x}In_x)_2Se_3$ Thin Films," Phys. Rev. Lett. **109**, 186403.

Brüne, C., A. Roth, H. Buhmann, E. M. Hankiewicz, L. W. Molenkamp, J. Maciejko, X.-L. Qi, and S.-C. Zhang, 2012, "Spin Polarization of the Quantum Spin Hall Edge States," Nat. Phys. **8**, 485.

Bulmash, D., C.-X. Liu, and X.-L. Qi, 2014, "Prediction of a Weyl Semimetal in $Hg_{1-x-y}Cd_xMn_yTe$," Phys. Rev. B **89**, 081106.

Burke, J. R., R. S. Allgaier, B. B. Houston, J. Babiskin, and P. G. Siebenmann, 1965, "Shubnikov-de Haas Effect in SnTe," Phys. Rev. Lett. **14**, 360.

Burkov, A. A., and L. Balents, 2011, "Weyl Semimetal in a Topological Insulator Multilayer," Phys. Rev. Lett. **107**, 127205.

Butch, N. P., P. Syers, K. Kirshenbaum, A. P. Hope, and J. Paglione, 2011, "Superconductivity in the Topological Semimetal YPtBi," Phys. Rev. B **84**, 220504.

Butler, S. Z., *et al.*, 2013, "Progress, Challenges, and Opportunities in Two-Dimensional Materials Beyond Graphene," ACS Nano **7**, 2898.

Cacho, C., *et al.*, 2015, "Momentum-Resolved Spin Dynamics of Bulk and Surface Excited States in the Topological Insulator Bi_2Se_3," Phys. Rev. Lett. **114**, 097401.

Cai, T.-Y., X. Li, F. Wang, J. Sheng, J. Feng, and C.-D. Gong, 2015, "Single-Spin Dirac Fermion and Chern Insulator Based on Simple Oxides," Nano Lett. **15**, 6434.

Campi, D., M. Bernasconi, and G. Benedek, 2012, "Electronic Properties and Lattice Dynamics of the As(111) Surface," Phys. Rev. B **86**, 245403.

Capelle, K., and V. L. Campo, Jr., 2013, "Density Functionals and Model Hamiltonians: Pillars of Many-Particle Physics," Phys. Rep. **528**, 91.

Carter, J.-M., V. V. Shankar, M. A. Zeb, and H.-Y. Kee, 2012, "Semimetal and Topological Insulator in Perovskite Iridates," Phys. Rev. B **85**, 115105.

Castro Neto, A. H., F. Guinea, N. M. R. Peres, K. S. Novoselov, and A. K. Geim, 2009, "The Electronic Properties of Graphene," Rev. Mod. Phys. **81**, 109.

Cava, R. J., B. Batlogg, J. J. Krajewski, R. Farrow, L. W. Rupp, A. E. White, K. Short, W. F. Peck, and T. Kometani, 1988, "Superconductivity near 30 K without Copper: The $Ba_{0.6}K_{0.4}BiO_3$ Perovskite," Nature (London) **332**, 814.

Cazalilla, M. A., H. Ochoa, and F. Guinea, 2014, "Quantum Spin Hall Effect in Two-Dimensional Crystals of Transition-Metal Dichalcogenides," Phys. Rev. Lett. **113**, 077201.

Chadov, S., J. Kiss, J. Kübler, and C. Felser, 2013, "Topological Phase Transition in Bulk Materials Described by the Coherent Potential Approximation Technique," Phys. Status Solidi RRL **7**, 82.

Chadov, S., X. Qi, J. Kübler, G. H. Fecher, C. Felser, and S. C. Zhang, 2010, "Tunable Multifunctional Topological Insulators in Ternary Heusler Compounds," Nat. Mater. **9**, 541.

Chang, C.-Z., W. Zhao, D. Y. Kim, H. Zhang, B. A. Assaf, D. Heiman, S.-C. Zhang, C. Liu, M. H. W. Chan, and J. S. Moodera, 2015, "High-Precision Realization of Robust Quantum Anomalous Hall State in a Hard Ferromagnetic Topological Insulator," Nat. Mater. **14**, 473.

Chang, C.-Z., *et al.*, 2013, "Experimental Observation of the Quantum Anomalous Hall Effect in a Magnetic Topological Insulator," Science **340**, 167.

Chang, J., L. F. Register, S. K. Banerjee, and B. Sahu, 2011, "Density Functional Study of Ternary Topological Insulator Thin Films," Phys. Rev. B **83**, 235108.

Chang, P.-H., M. S. Bahramy, N. Nagaosa, and B. K. Nikolic, 2014, "Giant Thermoelectric Effect in Graphene-Based Topological Insulators with Heavy Adatoms and Nanopores," Nano Lett. **14**, 3779.

Checkelsky, J. G., J. Ye, Y. Onose, Y. Iwasa, and Y. Tokura, 2012, "Dirac-Fermion-Mediated Ferromagnetism in a Topological Insulator," Nat. Phys. **8**, 729.

Checkelsky, J. G., R. Yoshimi, A. Tsukazaki, K. S. Takahashi, Y. Kozuka, J. Falson, M. Kawasaki, and Y. Tokura, 2014, "Trajectory of the Anomalous Hall Effect towards the Quantized State in a Ferromagnetic Topological Insulator," Nat. Phys. **10**, 731.

Chen, J., *et al.*, 2010, "Gate-Voltage Control of Chemical Potential and Weak Antilocalization in Bi_2Se_3," Phys. Rev. Lett. **105**, 176602.

Chen, Y. L., *et al.*, 2009, "Experimental Realization of a Three-Dimensional Topological Insulator, Bi_2Te_3," Science **325**, 178.

Chen, Y. L., *et al.*, 2010a, "Massive Dirac Fermion on the Surface of a Magnetically Doped Topological Insulator," Science **329**, 659.

Chen, Y. L., *et al.*, 2010b, "Single Dirac Cone Topological Surface State and Unusual Thermoelectric Property of Compounds from a New Topological Insulator Family," Phys. Rev. Lett. **105**, 266401.

Chen, Y. L., *et al.*, 2013, "Discovery of a Single Topological Dirac Fermion in the Strong Inversion Asymmetric Compound BiTeCl," Nat. Phys. **9**, 704.

Cheng, G., *et al.*, 2013, "Anomalous Transport in Sketched Nanostructures at the $LaAlO_3/SrTiO_3$ Interface," Phys. Rev. X **3**, 011021.

Chis, V., I. Y. Sklyadneva, K. A. Kokh, V. A. Volodin, O. E. Tereshchenko, and E. V. Chulkov, 2012, "Vibrations in Binary and Ternary Topological Insulators: First-Principles Calculations and Raman Spectroscopy Measurements," Phys. Rev. B **86**, 174304.

Chiu, C.-K., P. Ghaemi, and T. L. Hughes, 2012, "Stabilization of Majorana Modes in Magnetic Vortices in the Superconducting Phase of Topological Insulators Using Topologically Trivial Bands," Phys. Rev. Lett. **109**, 237009.

Chiu, C.-K., H. Yao, and S. Ryu, 2013, "Classification of Topological Insulators and Superconductors in the Presence of Reflection Symmetry," Phys. Rev. B **88**, 075142.

Chiu, S.-P., and J.-J. Lin, 2013, "Weak Antilocalization in Topological Insulator Bi_2Te_3 Microflakes," Phys. Rev. B **87**, 035122.

Cho, S., N. P. Butch, J. Paglione, and M. S. Fuhrer, 2011, "Insulating Behavior in Ultrathin Bismuth Selenide Field Effect Transistors," Nano Lett. **11**, 1925.

Chou, B.-H., Z.-Q. Huang, C.-H. Hsu, F.-C. Chuang, Y.-T. Liu, H. Lin, and A. Bansil, 2014, "Hydrogenated Ultra-Thin Tin Films Predicted as Two-Dimensional Topological Insulators.," New J. Phys. **16**, 115008.

Chuang, F.-C., C.-H. Hsu, C.-Y. Chen, Z.-Q. Huang, V. Ozolins, H. Lin, and A. Bansil, 2013, "Tunable Topological Electronic Structures in Sb(111) Bilayers: A First-Principles Study," Appl. Phys. Lett. **102**, 022424.

Chuang, F.-C., L.-Z. Yao, Z.-Q. Huang, Y.-T. Liu, C.-H. Hsu, T. Das, H. Lin, and A. Bansil, 2014, "Prediction of Large-Gap Two-Dimensional Topological Insulators Consisting of Bilayers of Group III Elements with Bi," Nano Lett. **14**, 2505.

Chung, S. B., and S.-C. Zhang, 2009, "Detecting the Majorana Fermion Surface State of He^3-B through Spin Relaxation," Phys. Rev. Lett. **103**, 235301.

Chun-Lei, G., Q. Dong, L. Can-Hua, J. Jin-Feng, and L. Feng, 2013, "Topological Edge States and Electronic Structures of a 2D Topological Insulator: Single-Bilayer Bi (111)," Chin. Phys. B **22**, 067304.

Ciftci, Y. O., K. Colakoglu, and E. Deligoz, 2008, "A First-Principles Studies on TlX (X=P, As)," Open Physics **6**, 802.

Coelho, P. M., G. A. S. Ribeiro, A. Malachias, V. L. Pimentel, W. S. Silva, D. D. Reis, M. S. C. Mazzoni, and R. Magalhaes-Paniago, 2013, "Temperature-Induced Coexistence of a Conducting Bilayer and the Bulk-Terminated Surface of the Topological Insulator Bi_2Te_3," Nano Lett. **13**, 4517.

Coh, S., D. Vanderbilt, A. Malashevich, and I. Souza, 2011, "Chern-Simons Orbital Magnetoelectric Coupling in Generic Insulators," Phys. Rev. B **83**, 085108.

Cooley, J. C., M. C. Aronson, Z. Fisk, and P. C. Canfield, 1995, "SmB_6: Kondo Insulator or Exotic Metal?," Phys. Rev. Lett. **74**, 1629.

Crepaldi, A., B. Ressel, F. Cilento, M. Zacchigna, C. Grazioli, H. Berger, P. Bugnon, K. Kern, M. Grioni, and F. Parmigiani, 2012, "Ultrafast Photodoping and Effective Fermi-Dirac Distribution of the Dirac Particles in Bi_2Se_3," Phys. Rev. B **86**, 205133.

Crepaldi, A., *et al.*, 2014, "Momentum and Photon Energy Dependence of the Circular Dichroic Photoemission in the Bulk Rashba Semiconductors BiTeX (X=I, Br, Cl)," Phys. Rev. B **89**, 125408.

Dalven, R., 1966, "Fundamental Optical Absorption in β-Silver Telluride," Phys. Rev. Lett. **16**, 311.

Dalven, R., and R. Gill, 1967, "Energy Gap in β-Ag_2Se," Phys. Rev. **159**, 645.

Das, T., 2012, "Spin-Orbit Density Wave Induced Hidden Topological Order in URu_2Si_2," Sci. Rep. **2**, 596.

Das, T., 2013, "Weyl Semimetal and Superconductor Designed in an Orbital-Selective Superlattice," Phys. Rev. B **88**, 035444.

Das, T., and A. V. Balatsky, 2013, "Engineering Three-Dimensional Topological Insulators in Rashba-Type Spin-Orbit Coupled Heterostructures," Nat. Commun. **4**, 1972.

Das, T., T. Durakiewicz, J.-X. Zhu, J. J. Joyce, J. L. Sarrao, and M. J. Graf, 2012, "Imaging the Formation of High-Energy Dispersion Anomalies in the Actinide $UCoGa_5$," Phys. Rev. X **2**, 041012.

Das, T., R. S. Markiewicz, and A. Bansil, 2014, "Intermediate Coupling Model of Cuprates," Adv. Phys. **63**, 151.

Das, T., J.-X. Zhu, and M. J. Graf, 2012, "Spin Fluctuations and the Peak-Dip-Hump Feature in the Photoemission Spectrum of Actinides," Phys. Rev. Lett. **108**, 017001.

Das Sarma, S., S. Adam, E. H. Hwang, and E. Rossi, 2011, "Electronic Transport in Two-Dimensional Graphene," Rev. Mod. Phys. **83**, 407.

Deng, X., K. Haule, and G. Kotliar, 2013, "Plutonium Hexaboride Is a Correlated Topological Insulator," Phys. Rev. Lett. **111**, 176404.

Denlinger, J. D., J. W. Allen, J.-S. Kang, K. Sun, B.-I. Min, D.-J. Kim, and Z. Fisk, 2013, "SmB_6 Photoemission: Past and Present," arXiv:1312.6636.

Deshpande, M. P., S. V. Bhatt, V. Sathe, R. Rao, and S. H. Chaki, 2014, "Pressure and Temperature Dependence of Raman Spectra and Their Anharmonic Effects in Bi_2Se_3 Single Crystal," Physica B (Amsterdam) **433**, 72.

Diniz, G. S., M. R. Guassi, and F. Qu, 2013, "Engineering the Quantum Anomalous Hall Effect in Graphene with Uniaxial Strains," J. Appl. Phys. **114**, 243701.

Dóra, B., J. Cayssol, F. Simon, and R. Moessner, 2012, "Optically Engineering the Topological Properties of a Spin Hall Insulator," Phys. Rev. Lett. **108**, 056602.

Doung, L. Q., H. Lin, W. F. Tsai, and Y. P. Feng, 2015, "Quantum anomalous Hall effect with field-tunable Chern number near Z_2 topological critical point," Phys. Rev. B **92**, 115205.

Drozdov, I. K., A. Alexandradinata, S. Jeon, S. Nadj-Perge, H. Ji, R. J. Cava, B. A. Bernevig, and A. Yazdani, 2014, "One-Dimensional Topological Edge States of Bismuth Bilayers," Nat. Phys. **10**, 664.

Drummond, N. D., V. Zólyomi, and V. I. Fal'ko, 2012, "Electrically Tunable Band Gap in Silicene," Phys. Rev. B **85**, 075423.

Du, L., I. Knez, G. Sullivan, and R.-R. Du, 2015, "Robust Helical Edge Transport in Gated InAs/GaSb Bilayers," Phys. Rev. Lett. **114**, 096802.

Dzero, M., and V. Galitski, 2013, "A New Exotic State in an Old Material: A Tale of SmB_6," J. Exp. Theor. Phys. **117**, 499.

Dzero, M., K. Sun, P. Coleman, and V. Galitski, 2012, "Theory of Topological Kondo Insulators," Phys. Rev. B **85**, 045130.

Dzero, M., K. Sun, V. Galitski, and P. Coleman, 2010, "Topological Kondo Insulators," Phys. Rev. Lett. **104**, 106408.

Dziawa, P., *et al.*, 2012, "Topological Crystalline Insulator States in $Pb_{1-x}Sn_xSe$," Nat. Mater. **11**, 1023.

Ebihara, K., K. Yada, A. Yamakage, and Y. Tanaka, 2012, "Finite Size Effects of the Surface States in a Lattice Model of Topological Insulator," Physica E (Amsterdam) **44**, 885.

Edmonds, M. T., J. T. Hellerstedt, A. Tadich, A. Schenk, K. M. O'Donnell, J. Tosado, N. P. Butch, P. Syers, J. Paglione, and M. S. Fuhrer, 2014, "Air-Stable Electron Depletion of Bi_2Se_3 Using Molybdenum Trioxide into the Topological Regime," ACS Nano **8**, 6400.

Elliott, S. R., and M. Franz, 2015, "*Colloquium*: Majorana Fermions in Nuclear, Particle and Solid-State Physics," Rev. Mod. Phys. **87**, 137.

Eremeev, S. V., G. Bihlmayer, M. Vergniory, Y. M. Koroteev, T. V. Menshchikova, J. Henk, A. Ernst, and E. V. Chulkov, 2011, "Ab Initio Electronic Structure of Thallium-Based Topological Insulators," Phys. Rev. B **83**, 205129.

Eremeev, S. V., Y. M. Koroteev, and E. V. Chulkov, 2010, "Ternary Thallium-Based Semimetal Chalcogenides Tl-V-VI2 as a New Class of Three-Dimensional Topological Insulators," JETP Lett. **91**, 594.

Eremeev, S. V., Y. M. Koroteev, I. A. Nechaev, and E. V. Chulkov, 2014, "Role of Surface Passivation in the Formation of Dirac States at Polar Surfaces of Topological Crystalline Insulators: The Case of SnTe(111)," Phys. Rev. B **89**, 165424.

Eremeev, S. V., V. N. Men'shov, V. V. Tugushev, P. M. Echenique, and E. V. Chulkov, 2013, "Magnetic Proximity Effect at the Three-Dimensional Topological Insulator/magnetic Insulator Interface," Phys. Rev. B **88**, 144430.

Eremeev, S. V., I. A. Nechaev, Y. M. Koroteev, P. M. Echenique, and E. V. Chulkov, 2012a, "Ideal Two-Dimensional Electron Systems with a Giant Rashba-Type Spin Splitting in Real Materials: Surfaces of Bismuth Tellurohalides," Phys. Rev. Lett. **108**, 246802.

Eremeev, S. V., *et al.*, 2012b, "Atom-Specific Spin Mapping and Buried Topological States in a Homologous Series of Topological Insulators," Nat. Commun. **3**, 635.

Essin, A. M., and V. Gurarie, 2011, "Bulk-Boundary Correspondence of Topological Insulators from Their Respective Green's Functions," Phys. Rev. B **84**, 125132.

Essin, A. M., J. E. Moore, and D. Vanderbilt, 2009, "Magnetoelectric Polarizability and Axion Electrodynamics in Crystalline Insulators," Phys. Rev. Lett. **102**, 146805.

Ezawa, M., 2012, "Spin-Valley Optical Selection Rule and Strong Circular Dichroism in Silicene," Phys. Rev. B **86**, 161407.

Ezawa, M., 2013, "Photoinduced Topological Phase Transition and a Single Dirac-Cone State in Silicene," Phys. Rev. Lett. **110**, 026603.

Fan, Y., *et al.*, 2014, "Magnetization Switching through Giant Spin-Orbit Torque in a Magnetically Doped Topological Insulator Heterostructure," Nat. Mater. **13**, 699.

Fang, C., M. J. Gilbert, and B. A. Bernevig, 2012, "Bulk Topological Invariants in Noninteracting Point Group Symmetric Insulators," Phys. Rev. B **86**, 115112.

Fang, C., M. J. Gilbert, and B. A. Bernevig, 2014, "Large-Chern-Number Quantum Anomalous Hall Effect in Thin-Film Topological Crystalline Insulators," Phys. Rev. Lett. **112**, 046801.

Fang, C., M. J. Gilbert, X. Dai, and B. A. Bernevig, 2012, "Multi-Weyl Topological Semimetals Stabilized by Point Group Symmetry," Phys. Rev. Lett. **108**, 266802.

Fang, L., C. C. Stoumpos, Y. Jia, A. Glatz, D. Y. Chung, H. Claus, U. Welp, W. K. Kwok, and M. G. Kanatzidis, 2014, "Dirac Fermions and Superconductivity in Homologous Structures $(Ag_xPb_{1-x}Se)_5(Bi_2Se_3)_{3m}$, (m=1, 2)," Phys. Rev. B **90**, 020504.

Fauqué, B., N. P. Butch, P. Syers, J. Paglione, S. Wiedmann, A. Collaudin, B. Grena, U. Zeitler, and K. Behnia, 2013, "Magneto-thermoelectric Properties of Bi_2Se_3," Phys. Rev. B **87**, 035133.

Feng, B., Z. Ding, S. Meng, Y. Yao, X. He, P. Cheng, L. Chen, and K. Wu, 2012, "Evidence of Silicene in Honeycomb Structures of Silicon on Ag(111)," Nano Lett. **12**, 3507.

Feng, W., D. Xiao, J. Ding, and Y. Yao, 2011, "Three-Dimensional Topological Insulators in I-III-VI2 and II-IV-V2 Chalcopyrite Semiconductors," Phys. Rev. Lett. **106**, 016402.

Feng, W., and Y. Yao, 2012, "Three-Dimensional Topological Insulators: A Review on Host Materials," Sci. China Phys. Mech. Astron. **55**, 2199.

Feng, Y., *et al.*, 2014, "Strong Anisotropy of Dirac Cone in $SrMnBi_2$ and $CaMnBi_2$ Revealed by Angle-Resolved Photoemission Spectroscopy," Sci. Rep. **4**, 5385.

Flachbart, K., K. Gloos, E. Konovalova, Y. Paderno, M. Reiffers, P. Samuely, and P. Švec, 2001, "Energy Gap of Intermediate-Valent SmB_6 Studied by Point-Contact Spectroscopy," Phys. Rev. B **64**, 085104.

Fleurence, A., R. Friedlein, T. Ozaki, H. Kawai, Y. Wang, and Y. Yamada-Takamura, 2012, "Experimental Evidence for Epitaxial Silicene on Diboride Thin Films," Phys. Rev. Lett. **108**, 245501.

Fradkin, E., E. Dagotto, and D. Boyanovsky, 1986, "Physical Realization of the Parity Anomaly in Condensed Matter Physics," Phys. Rev. Lett. **57**, 2967.

Frantzeskakis, E., *et al.*, 2013, "Kondo Hybridization and the Origin of Metallic States at the (001) Surface of SmB_6," Phys. Rev. X **3**, 041024.

Fruchart, M., and D. Carpentier, 2013, "An Introduction to Topological Insulators," C.R. Phys. **14**, 779.

Fu, L., 2009, "Hexagonal Warping Effects in the Surface States of the Topological Insulator Bi_2Te_3," Phys. Rev. Lett. **103**, 266801.

Fu, L., 2011, "Topological Crystalline Insulators," Phys. Rev. Lett. **106**, 106802.

Fu, L., and E. Berg, 2010, "Odd-Parity Topological Superconductors: Theory and Application to $Cu_xBi_2Se_3$," Phys. Rev. Lett. **105**, 097001.

Fu, L., and C. L. Kane, 2006, "Time Reversal Polarization and a Z_2 Adiabatic Spin Pump," Phys. Rev. B **74**, 195312.

Fu, L., and C. L. Kane, 2007, "Topological Insulators with Inversion Symmetry," Phys. Rev. B **76**, 045302.

Fu, L., and C. L. Kane, 2008, "Superconducting Proximity Effect and Majorana Fermions at the Surface of a Topological Insulator," Phys. Rev. Lett. **100**, 096407.

Fu, L., C. L. Kane, and E. J. Mele, 2007, "Topological Insulators in Three Dimensions," Phys. Rev. Lett. **98**, 106803.

Fu, Y.-S., M. Kawamura, K. Igarashi, H. Takagi, T. Hanaguri, and T. Sasagawa, 2014, "Imaging the Two-Component Nature of Dirac-Landau Levels in the Topological Surface State of Bi_2Se_3," Nat. Phys. **10**, 815.

Fuhrman, W. T., *et al.*, 2015, "Interaction Driven Subgap Spin Exciton in the Kondo Insulator SmB_6," Phys. Rev. Lett. **114**, 036401.

Fukui, T., and Y. Hatsugai, 2007, "Quantum Spin Hall Effect in Three Dimensional Materials: Lattice Computation of Z_2 Topological Invariants and Its Application to Bi and Sb," J. Phys. Soc. Jpn. **76**, 053702.

Gardner, J. S., M. J. P. Gingras, and J. E. Greedan, 2010, "Magnetic Pyrochlore Oxides," Rev. Mod. Phys. **82**, 53.

Gehring, P., H. M. Benia, Y. Weng, R. Dinnebier, C. R. Ast, M. Burghard, and K. Kern, 2013, "A Natural Topological Insulator," Nano Lett. **13**, 1179.

Ghaemi, P., S. Gopalakrishnan, and T. L. Hughes, 2012, "Designer Quantum Spin Hall Phase Transition in Molecular Graphene," Phys. Rev. B **86**, 201406.

Glinka, Y. D., S. Babakiray, T. A. Johnson, A. D. Bristow, M. B. Holcomb, and D. Lederman, 2013, "Ultrafast Carrier Dynamics in Thin-Films of the Topological Insulator Bi_2Se_3," Appl. Phys. Lett. **103**, 151903.

Goerbig, M. O., 2011, "Electronic Properties of Graphene in a Strong Magnetic Field," Rev. Mod. Phys. **83**, 1193.

Gomes, K. K., W. Ko, W. Mar, Y. Chen, Z.-X. Shen, and H. C. Manoharan, 2009, "Quantum Imaging of Topologically Unpaired Spin-Polarized Dirac Fermions," arXiv:0909.0921, http://arxiv.org/abs/0909.0921.

Gomes, K. K., W. Mar, W. Ko, F. Guinea, and H. C. Manoharan, 2012, "Designer Dirac Fermions and Topological Phases in Molecular Graphene," Nature (London) **483**, 306.

Gorbachev, R. V., *et al.*, 2014, "Detecting Topological Currents in Graphene Superlattices," Science **346**, 448.

Gorbar, E. V., V. A. Miransky, I. A. Shovkovy, and P. O. Sukhachov, 2015, "Dirac Semimetals A_3Bi $(A = \mathrm{Na}, \mathrm{K}, \mathrm{Rb})$ as Z_2 Weyl Semimetals," Phys. Rev. B **91**, 121101.

Gorshunov, B., N. Sluchanko, A. Volkov, M. Dressel, G. Knebel, A. Loidl, and S. Kunii, 1999, "Low-Energy Electrodynamics of SmB_6," Phys. Rev. B **59**, 1808.

Grushin, A. G., T. Neupert, C. Chamon, and C. Mudry, 2012, "Enhancing the Stability of a Fractional Chern Insulator against Competing Phases," Phys. Rev. B **86**, 205125.

Gu, Z., H. A. Fertig, D. P. Arovas, and A. Auerbach, 2011, "Floquet Spectrum and Transport through an Irradiated Graphene Ribbon," Phys. Rev. Lett. **107**, 216601.

Guo, H. *et al.*, 2011, "Evolution of Surface States in $Bi_{1-x}Sb_x$ Alloys across the Topological Phase Transition," Phys. Rev. B **83**, 201104.

Guo, H.-M., G. Rosenberg, G. Refael, and M. Franz, 2010, "Topological Anderson Insulator in Three Dimensions," Phys. Rev. Lett. **105**, 216601.

Gupta, G., H. Lin, A. Bansil, M. B. A. Jalil, C.-Y. Huang, W.-F. Tsai, and G. Liang, 2014, "Y-Shape Spin-Separator for Two-Dimensional Group-IV Nanoribbons Based on Quantum Spin Hall Effect," Appl. Phys. Lett. **104**, 032410.

Gusev, G. M., Z. D. Kvon, E. B. Olshanetsky, A. D. Levin, Y. Krupko, J. C. Portal, N. N. Mikhailov, and S. A. Dvoretsky, 2014, "Temperature Dependence of the Resistance of a Two-Dimensional Topological Insulator in a HgTe Quantum Well," Phys. Rev. B **89**, 125305.

Hajlaoui, M., *et al.*, 2014, "Tuning a Schottky Barrier in a Photoexcited Topological Insulator with Transient Dirac Cone Electron-Hole Asymmetry," Nat. Commun. **5**, 3003.

Haldane, F. D. M., 1988, "Model for a Quantum Hall Effect without Landau Levels: Condensed-Matter Realization of the 'Parity Anomaly'," Phys. Rev. Lett. **61**, 2015.

Haldane, F. D. M., 2004, "Berry Curvature on the Fermi Surface: Anomalous Hall Effect as a Topological Fermi-Liquid Property," Phys. Rev. Lett. **93**, 206602.

Harrison, S. E., *et al.*, 2014, "Study of Gd-Doped Bi_2Te_3 Thin Films: Molecular Beam Epitaxy Growth and Magnetic Properties," J. Appl. Phys. **115**, 023904.

Hart, S., H. Ren, T. Wagner, P. Leubner, M. Muehlbauer, C. Bruene, H. Buhmann, L. Molenkamp, and A. Yacoby, 2014, "Induced Superconductivity in the Quantum Spin Hall Edge," Nat. Phys. **10**, 638.

Hasan, M. Z., and C. L. Kane, 2010, "*Colloquium*: Topological Insulators," Rev. Mod. Phys. **82**, 3045.

Hasan, M. Z., H. Lin, and A. Bansil, 2009, "Warping the Cone on a Topological Insulator," Physics **2**, 108.

Heber, J., 2009, "Materials Science: Enter the Oxides," Nature (London) **459**, 28.

Heimes, A., P. Kotetes, and G. Schön, 2014, "Majorana Fermions from Shiba States in an Antiferromagnetic Chain on Top of a Superconductor," Phys. Rev. B **90**, 060507.

Held, K., I. A. Nekrasov, G. Keller, V. Eyert, N. Blümer, A. K. McMahan, R. T. Scalettar, T. Pruschke, V. I. Anisimov, and D. Vollhardt, 2006, "Realistic Investigations of Correlated Electron Systems with LDA+DMFT," Phys. Status Solidi B **243**, 2599.

Henk, J., A. Ernst, S. V. Eremeev, E. V. Chulkov, I. V. Maznichenko, and I. Mertig, 2012, "Complex Spin Texture in the Pure and Mn-Doped Topological Insulator Bi_2Te_3," Phys. Rev. Lett. **108**, 206801.

Henk, J., M. Flieger, I. V. Maznichenko, I. Mertig, A. Ernst, S. V. Eremeev, and E. V. Chulkov, 2012, "Topological Character and Magnetism of the Dirac State in Mn-Doped Bi_2Te_3," Phys. Rev. Lett. **109**, 076801.

Hinsche, N. F., B. Y. Yavorsky, M. Gradhand, M. Czerner, M. Winkler, J. König, H. Böttner, I. Mertig, and P. Zahn, 2012, "Thermoelectric Transport in Bi_2Te_3/Sb_2Te_3 Superlattices," Phys. Rev. B **86**, 085323.

Hinsche, N. F., S. Zastrow, J. Gooth, L. Pudewill, R. Zierold, F. Rittweger, T. Rauch, J. Henk, K. Nielsch, and I. Mertig, 2015, "Impact of the Topological Surface State on the Thermoelectric Transport in Sb_2Te_3 Thin Films," ACS Nano **9**, 4406.

Hirahara, T., *et al.*, 2012, "Atomic and Electronic Structure of Ultrathin Bi(111) Films Grown on $Bi_2Te_3(111)$ Substrates: Evidence for a Strain-Induced Topological Phase Transition," Phys. Rev. Lett. **109**, 227401.

Hirata, Y., *et al.*, 2013, "Mechanism of Enhanced Optical Second-Harmonic Generation in the Conducting Pyrochlore-Type $Pb_2Ir_2O_{7-x}$ Oxide Compound," Phys. Rev. Lett. **110**, 187402.

Hirayama, H., Y. Aoki, and C. Kato, 2011, "Quantum Interference of Rashba-Type Spin-Split Surface State Electrons," Phys. Rev. Lett. **107**, 027204.

Hoefer, K., C. Becker, D. Rata, J. Swanson, P. Thalmeier, and L. H. Tjeng, 2014, "Intrinsic Conduction through Topological Surface States of Insulating Bi_2Te_3 Epitaxial Thin Films," Proc. Natl. Acad. Sci. U.S.A. **111**, 14979.

Hofmann, P., 2006, "The Surfaces of Bismuth: Structural and Electronic Properties," Prog. Surf. Sci. **81**, 191.

Hohenberg, P., and W. Kohn, 1964, "Inhomogeneous Electron Gas," Phys. Rev. **136**, B864.

Hong, S. S., Y. Zhang, J. J. Cha, X.-L. Qi, and Y. Cui, 2014, "One-Dimensional Helical Transport in Topological Insulator Nanowire Interferometers," Nano Lett. **14**, 2815.

Hor, Y. S., A. Richardella, P. Roushan, Y. Xia, J. G. Checkelsky, A. Yazdani, M. Z. Hasan, N. P. Ong, and R. J. Cava, 2009, "P-Type Bi_2Se_3 for Topological Insulator and Low-Temperature Thermoelectric Applications," Phys. Rev. B **79**, 195208.

Hor, Y. S., *et al.*, 2010, "Development of Ferromagnetism in the Doped Topological Insulator $Bi_{2-x}Mn_xTe_3$," Phys. Rev. B **81**, 195203.

Hota, R. L., 2013, "Theory of Anisotropic Lattice Diamagnetism in N-Type $Pb_{1-x}Mn_xS$," J. Magn. Magn. Mater. **345**, 236.

Hsieh, D., D. Qian, L. Wray, Y. Xia, Y. S. Hor, R. J. Cava, and M. Z. Hasan, 2008, "A Topological Dirac Insulator in a Quantum Spin Hall Phase," Nature (London) **452**, 970.

Hsieh, D., *et al.*, 2009a, "A Tunable Topological Insulator in the Spin Helical Dirac Transport Regime," Nature (London) **460**, 1101.

Hsieh, D., *et al.*, 2009b, "Observation of Time-Reversal-Protected Single-Dirac-Cone Topological-Insulator States in Bi_2Te_3 and Sb_2Te_3," Phys. Rev. Lett. **103**, 146401.

Hsieh, D., *et al.*, 2009c, "Observation of Unconventional Quantum Spin Textures in Topological Insulators," Science **323**, 919.

Hsieh, T. H., H. Lin, J. Liu, W. Duan, A. Bansil, and L. Fu, 2012, "Topological Crystalline Insulators in the SnTe Material Class," Nat. Commun. **3**, 982.

Hsu, C.-H., and S. Chakravarty, 2014, "Superconductivity from Fractionalized Excitations in URu_2Si_2," Phys. Rev. B **90**, 134507.

Hu, F. M., T. O. Wehling, J. E. Gubernatis, T. Frauenheim, and R. M. Nieminen, 2013, "Magnetic Impurity Affected by Spin-Orbit Coupling: Behavior near a Topological Phase Transition," Phys. Rev. B **88**, 045106.

Hu, J., J. Alicea, R. Wu, and M. Franz, 2012, "Giant Topological Insulator Gap in Graphene with 5d Adatoms," Phys. Rev. Lett. **109**, 266801.

Huang, S.-M., *et al.*, 2015, "An Inversion Breaking Weyl Semimetal State in the TaAs Material Class," Nat. Commun. **6**, 7373.

Huang, X., X. Zhang, Y. Liu, Y. Wu, B. Sa, M. Ma, Z. Sun, and R. Liu, 2013, "Different Topological Insulating Behavior in β-GaS and GaS-II under Uniaxial Tension," Phys. Rev. B **88**, 235301.

Huang, Z.-Q., F.-C. Chuang, C.-H. Hsu, Y.-T. Liu, H.-R. Chang, H. Lin, and A. Bansil, 2013, "Nontrivial Topological Electronic Structures in a Single Bi(111) Bilayer on Different Substrates: A First-Principles Study," Phys. Rev. B **88**, 165301.

Hughes, T. L., E. Prodan, and B. A. Bernevig, 2011, "Inversion-Symmetric Topological Insulators," Phys. Rev. B **83**, 245132.

Huisman, L., D. Nicholson, L. Schwartz, and A. Bansil, 1981, "Effective-Medium Theory of Electronic States in Structurally Disordered Metals: Application to Liquid Cu," Phys. Rev. B **24**, 1824.

Huotari, S., K. Hämäläinen, S. Manninen, W. Caliebe, T. Buslaps, V. Honkimäki, and P. Suortti, 2000, "Energy Dependence of Experimental Be Compton Profiles," Phys. Rev. B **62**, 7956.

Iizumi, M., Y. Hamaguchi, K. F. Komatsubara, and Y. Kato, 1975, "Phase Transition in SnTe with Low Carrier Concentration," J. Phys. Soc. Jpn. **38**, 443.

Imada, M., A. Fujimori, and Y. Tokura, 1998, "Metal-Insulator Transitions," Rev. Mod. Phys. **70**, 1039.

Inoue, J., and A. Tanaka, 2010, "Photoinduced Transition between Conventional and Topological Insulators in Two-Dimensional Electronic Systems," Phys. Rev. Lett. **105**, 017401.

Ishizaka, K., *et al.*, 2011, "Giant Rashba-Type Spin Splitting in Bulk BiTeI," Nat. Mater. **10**, 521.

Jeffries, J. R., A. L. Lima Sharma, P. A. Sharma, C. D. Spataru, S. K. McCall, J. D. Sugar, S. T. Weir, and Y. K. Vohra, 2011, "Distinct Superconducting States in the Pressure-Induced Metallic Structures of the Nominal Semimetal Bi_4Te_3," Phys. Rev. B **84**, 092505.

Jenkins, G. S., A. B. Sushkov, D. C. Schmadel, N. P. Butch, P. Syers, J. Paglione, and H. D. Drew, 2010, "Terahertz Kerr and Reflectivity Measurements on the Topological Insulator Bi_2Se_3," Phys. Rev. B **82**, 125120.

Jenkins, G. S., A. B. Sushkov, D. C. Schmadel, M.-H. Kim, M. Brahlek, N. Bansal, S. Oh, and H. D. Drew, 2012, "Giant Plateau in the Terahertz Faraday Angle in Gated Bi_2Se_3," Phys. Rev. B **86**, 235133.

Jeon, S., B. B. Zhou, A. Gyenis, B. E. Feldman, I. Kimchi, A. C. Potter, Q. D. Gibson, R. J. Cava, A. Vishwanath, and A. Yazdani, 2014, "Landau Quantization and Quasiparticle Interference in the Three-Dimensional Dirac Semimetal Cd_3As_2," Nat. Mater. **13**, 851.

Ji, H., J. M. Allred, M. K. Fuccillo, M. E. Charles, M. Neupane, L. A. Wray, M. Z. Hasan, and R. J. Cava, 2012, "$Bi_2Te_{1.6}S_{1.4}$: A Topological Insulator in the Tetradymite Family," Phys. Rev. B **85**, 201103.

Jiang, J., *et al.*, 2013, "Observation of Possible Topological in-Gap Surface States in the Kondo Insulator SmB_6 by Photoemission," Nat. Commun. **4**, 3010.

Jiang, Y., Z. Li, C. Song, M. Chen, R. L. Greene, K. He, L. Wang, X. Chen, X. Ma, and Q.-K. Xue, 2015, "Mass Acquisition of Dirac Fermions in Cr-Doped Topological Insulator Sb_2Te_3 Films," Phys. Rev. B **92**, 195418.

Jin, H., S. H. Rhim, J. Im, and A. J. Freeman, 2013, "Topological Oxide Insulator in Cubic Perovskite Structure," Sci. Rep. **3**, 1651.

Jin, H., J.-H. Song, A. J. Freeman, and M. G. Kanatzidis, 2011, "Candidates for Topological Insulators: Pb-Based Chalcogenide Series," Phys. Rev. B **83**, 041202.

Jnawali, G., C. Klein, T. Wagner, H. Hattab, P. Zahl, D. P. Acharya, P. Sutter, A. Lorke, and M. Horn-von Hoegen, 2012, "Manipulation of Electronic Transport in the Bi(111) Surface State," Phys. Rev. Lett. **108**, 266804.

Jozwiak, C., *et al.*, 2013, "Photoelectron Spin-Flipping and Texture Manipulation in a Topological Insulator," Nat. Phys. **9**, 293.

Ju, L., *et al.*, 2015, "Topological Valley Transport at Bilayer Graphene Domain Walls," Nature (London) **520**, 650.

Junod, P., H. Hediger, B. Kilchör, and J. Wullschleger, 1977, "Metal-Non-Metal Transition in Silver Chalcogenides," Philos. Mag. **36**, 941.

Kane, C. L., and E. J. Mele, 2005a, "Quantum Spin Hall Effect in Graphene," Phys. Rev. Lett. **95**, 226801.

Kane, C. L., and E. J. Mele, 2005b, "Z_2 Topological Order and the Quantum Spin Hall Effect," Phys. Rev. Lett. **95**, 146802.

Kane, C. L., and E. J. Mele, 2006, "A New Spin on the Insulating State," Science **314**, 1692.

Kargarian, M., A. Langari, and G. A. Fiete, 2012, "Unusual Magnetic Phases in the Strong Interaction Limit of Two-Dimensional Topological Band Insulators in Transition Metal Oxides," Phys. Rev. B **86**, 205124.

Kargarian, M., J. Wen, and G. A. Fiete, 2011, "Competing Exotic Topological Insulator Phases in Transition-Metal Oxides on the Pyrochlore Lattice with Distortion," Phys. Rev. B **83**, 165112.

Kariyado, T., and M. Ogata, 2011, "Three-Dimensional Dirac Electrons at the Fermi Energy in Cubic Inverse Perovskites: Ca_3PbO and Its Family," J. Phys. Soc. Jpn. **80**, 083704.

Kastl, C., C. Karnetzky, H. Karl, and A. W. Holleitner, 2015, "Ultrafast Helicity Control of Surface Currents in Topological Insulators with near-Unity Fidelity," Nat. Commun. **6**, 6617.

Katan, Y. T., and D. Podolsky, 2013, "Modulated Floquet Topological Insulators," Phys. Rev. Lett. **110**, 016802.

Khanna, S., A. Ibrahim, S. McKnight, and A. Bansil, 1985, "D-Band Filling in Ni-P Metallic Glasses," Solid State Commun. **55**, 223.

Khaymovich, I. M., N. M. Chtchelkatchev, and V. M. Vinokur, 2013, "Interplay of Superconductivity and Topological Order in HgTe Quantum Wells," J. Supercond. Novel Magn. **26**, 2881.

Kikutake, K., M. Ezawa, and N. Nagaosa, 2013, "Edge States in Silicene Nanodisks," Phys. Rev. B **88**, 115432.

Kim, B. J., *et al.*, 2008, "Novel $J_{\mathrm{eff}} = 1/2$ Mott State Induced by Relativistic Spin-Orbit Coupling in Sr_2IrO_4," Phys. Rev. Lett. **101**, 076402.

Kim, D., S. Cho, N. P. Butch, P. Syers, K. Kirshenbaum, S. Adam, J. Paglione, and M. S. Fuhrer, 2012, "Surface Conduction of Topological Dirac Electrons in Bulk Insulating Bi_2Se_3," Nat. Phys. **8**, 459.

Kim, D., P. Syers, N. P. Butch, J. Paglione, and M. S. Fuhrer, 2013, "Coherent Topological Transport on the Surface of Bi_2Se_3," Nat. Commun. **4**, 2040.

Kim, D., P. Syers, N. P. Butch, J. Paglione, and M. S. Fuhrer, 2014, "Ambipolar Surface State Thermoelectric Power of Topological Insulator Bi_2Se_3," Nano Lett. **14**, 1701.

Kim, D. J., S. Thomas, T. Grant, J. Botimer, Z. Fisk, and J. Xia, 2013, "Surface Hall Effect and Nonlocal Transport in SmB_6: Evidence for Surface Conduction," Sci. Rep. **3**, 3150.

Kim, D. J., J. Xia, and Z. Fisk, 2014, "Topological Surface State in the Kondo Insulator Samarium Hexaboride," Nat. Mater. **13**, 466.

Kim, J., J. Kim, and S.-H. Jhi, 2010, "Prediction of Topological Insulating Behavior in Crystalline Ge-Sb-Te," Phys. Rev. B **82**, 201312.

Kim, N., P. Lee, Y. Kim, J. S. Kim, Y. Kim, D. Y. Noh, S. U. Yu, J. Chung, and K. S. Kim, 2014, "Persistent Topological Surface State at the Interface of Bi_2Se_3 Film Grown on Patterned Graphene," ACS Nano **8**, 1154.

Kim, S., *et al.*, 2011, "Surface Scattering via Bulk Continuum States in the 3D Topological Insulator Bi_2Se_3," Phys. Rev. Lett. **107**, 056803.

Kim, S. H., K.-H. Jin, J. Park, J. S. Kim, S.-H. Jhi, T.-H. Kim, and H. W. Yeom, 2014, "Edge and Interfacial States in a Two-Dimensional Topological Insulator: Bi(111) Bilayer on Bi_2Te_2Se," Phys. Rev. B **89**, 155436.

Kim, Y. S., M. Brahlek, N. Bansal, E. Edrey, G. A. Kapilevich, K. Iida, M. Tanimura, Y. Horibe, S.-W. Cheong, and S. Oh, 2011, "Thickness-Dependent Bulk Properties and Weak Antilocalization Effect in Topological Insulator Bi_2Se_3," Phys. Rev. B **84**, 073109.

Kirshenbaum, K., P. S. Syers, A. P. Hope, N. P. Butch, J. R. Jeffries, S. T. Weir, J. J. Hamlin, M. B. Maple, Y. K. Vohra, and J. Paglione, 2013, "Pressure-Induced Unconventional Superconducting Phase in the Topological Insulator Bi_2Se_3," Phys. Rev. Lett. **111**, 087001.

Kitaev, A., 2009, "Periodic Table for Topological Insulators and Superconductors," in *AIP Conference Proceedings* (AIP Publishing, New York), Vol. 1134, pp. 22.

Kitagawa, T., E. Berg, M. Rudner, and E. Demler, 2010, "Topological Characterization of Periodically Driven Quantum Systems," Phys. Rev. B **82**, 235114.

Klintenberg, M., 2010, "The Search for Strong Topological Insulators," arXiv:1007.4838, http://arxiv.org/abs/1007.4838.

Knez, I., R.-R. Du, and G. Sullivan, 2011, "Evidence for Helical Edge Modes in Inverted InAs/GaSb Quantum Wells," Phys. Rev. Lett. **107**, 136603.

Knez, I., C. T. Rettner, S.-H. Yang, S. S. P. Parkin, L. Du, R.-R. Du, and G. Sullivan, 2014, "Observation of Edge Transport in the Disordered Regime of Topologically Insulating InAs/GaSb Quantum Wells," Phys. Rev. Lett. **112**, 026602.

Kohn, W., and L. J. Sham, 1965, "Self-Consistent Equations Including Exchange and Correlation Effects," Phys. Rev. **140**, A1133.

Koleini, M., T. Frauenheim, and B. Yan, 2013, "Gas Doping on the Topological Insulator Bi_2Se_3 Surface," Phys. Rev. Lett. **110**, 016403.

Kong, D., *et al.*, 2011, "Ambipolar Field Effect in the Ternary Topological Insulator $(Bi_xSb_{1-x})_2Te_3$ by Composition Tuning," Nat. Nanotechnol. **6**, 705.

Kong, P. P., *et al.*, 2013, "Superconductivity of the Topological Insulator Bi_2Se_3 at High Pressure," J. Phys. Condens. Matter **25**, 362204.

König, M., S. Wiedmann, C. Brüne, A. Roth, H. Buhmann, L. W. Molenkamp, X.-L. Qi, and S.-C. Zhang, 2007, "Quantum Spin Hall Insulator State in HgTe Quantum Wells," Science **318**, 766.

König, M., *et al.*, 2013, "Spatially Resolved Study of Backscattering in the Quantum Spin Hall State," Phys. Rev. X **3**, 021003.

Kotliar, G., S. Y. Savrasov, K. Haule, V. S. Oudovenko, O. Parcollet, and C. A. Marianetti, 2006, "Electronic Structure Calculations with Dynamical Mean-Field Theory," Rev. Mod. Phys. **78**, 865.

Kotov, V. N., B. Uchoa, V. M. Pereira, F. Guinea, and A. H. Castro Neto, 2012, "Electron-Electron Interactions in Graphene: Current Status and Perspectives," Rev. Mod. Phys. **84**, 1067.

Kou, L., S.-C. Wu, C. Felser, T. Frauenheim, C. Chen, and B. Yan, 2014, "Robust 2D Topological Insulators in van Der Waals Heterostructures," ACS Nano **8**, 10448.

Kou, L., B. Yan, F. Hu, S.-C. Wu, T. O. Wehling, C. Felser, C. Chen, and T. Frauenheim, 2013, "Graphene-Based Topological Insulator with an Intrinsic Bulk Band Gap above Room Temperature," Nano Lett. **13**, 6251.

Kou, X., *et al.*, 2013, "Manipulating Surface-Related Ferromagnetism in Modulation-Doped Topological Insulators," Nano Lett. **13**, 4587.

Kravets, V. G., *et al.*, 2013, "Singular Phase Nano-Optics in Plasmonic Metamaterials for Label-Free Single-Molecule Detection," Nat. Mater. **12**, 304.

Kriener, M., K. Segawa, S. Sasaki, and Y. Ando, 2012, "Anomalous Suppression of the Superfluid Density in the $Cu_xBi_2Se_3$ Superconductor upon Progressive Cu Intercalation," Phys. Rev. B **86**, 180505.

Küfner, S., J. Furthmüller, L. Matthes, M. Fitzner, and F. Bechstedt, 2013, "Structural and Electronic Properties of α-Tin Nanocrystals from First Principles," Phys. Rev. B **87**, 235307.

Kundu, A., and B. Seradjeh, 2013, "Transport Signatures of Floquet Majorana Fermions in Driven Topological Superconductors," Phys. Rev. Lett. **111**, 136402.

Kuroda, K., *et al.*, 2010a, "Hexagonally Deformed Fermi Surface of the 3D Topological Insulator Bi_2Se_3," Phys. Rev. Lett. **105**, 076802.

Kuroda, K., *et al.*, 2010b, "Experimental Realization of a Three-Dimensional Topological Insulator Phase in Ternary Chalcogenide $TlBiSe_2$," Phys. Rev. Lett. **105**, 146801.

Lado, J. L., V. Pardo, and D. Baldomir, 2013, "Ab Initio Study of Z_2 Topological Phases in Perovskite (111) $(SrTiO_3)_7/(SrIrO_3)_2$ and $(KTaO_3)_7/(KPtO_3)_2$ Multilayers," Phys. Rev. B **88**, 155119.

Landolt, G., *et al.*, 2013, "Bulk and Surface Rashba Splitting in Single Termination BiTeCl," New J. Phys. **15**, 085022.

Lang, M., *et al.*, 2014, "Proximity Induced High-Temperature Magnetic Order in Topological Insulator—Ferrimagnetic Insulator Heterostructure," Nano Lett. **14**, 3459.

Lau, C. N. (Jeanie), 2013, "Condensed Matter: Graphene's Topological Insulation," Nat. Phys. **9**, 135.

Lawson, B. J., Y. S. Hor, and L. Li, 2012, "Quantum Oscillations in the Topological Superconductor Candidate $Cu_{0.25}Bi_2Se_3$," Phys. Rev. Lett. **109**, 226406.

Lee, I., *et al.*, 2015, "Imaging Dirac-Mass Disorder from Magnetic Dopant Atoms in the Ferromagnetic Topological Insulator $Cr_x(Bi_{0.1}Sb_{0.9})_{2-x}Te_3$," Proc. Natl. Acad. Sci. U.S.A. **112**, 1316.

Lee, J. H., G.-H. Lee, J. Park, J. Lee, S.-G. Nam, Y.-S. Shin, J. S. Kim, and H.-J. Lee, 2014, "Local and Non Local Fraunhofer-like Pattern from an Edge-Stepped Topological Surface Josephson Current Distribution," Nano Lett. **14**, 5029.

Lee, W.-C., C. Wu, D. P. Arovas, and S.-C. Zhang, 2009, "Quasiparticle Interference on the Surface of the Topological Insulator Bi_2Te_3," Phys. Rev. B **80**, 245439.

Li, C. H., O. M. J. van 't Erve, J. T. Robinson, Y. Liu, L. Li, and B. T. Jonker, 2014, "Electrical Detection of Charge-Current-Induced Spin Polarization due to Spin-Momentum Locking in Bi_2Se_3," Nat. Nanotechnol. **9**, 218.

Li, G., *et al.*, 2014, "Two-Dimensional Fermi Surfaces in Kondo Insulator SmB_6," Science **346**, 1208.

Li, J., R.-L. Chu, J. K. Jain, and S.-Q. Shen, 2009, "Topological Anderson Insulator," Phys. Rev. Lett. **102**, 136806.

Li, L., X. Zhang, X. Chen, and M. Zhao, 2015, "Giant Topological Nontrivial Band Gaps in Chloridized Gallium Bismuthide," Nano Lett. **15**, 1296.

Li, M., C.-Z. Chang, L. Wu, J. Tao, W. Zhao, M. H. W. Chan, J. S. Moodera, J. Li, and Y. Zhu, 2015, "Experimental Verification of the Van Vleck Nature of Long-Range Ferromagnetic Order in the Vanadium-Doped Three-Dimensional Topological Insulator Sb_2Te_3," Phys. Rev. Lett. **114**, 146802.

Li, Q., *et al.*, 2013, "Atomically Resolved Spectroscopic Study of Sr_2IrO_4: Experiment and Theory," Sci. Rep. **3**, 3037.

Li, R., J. Wang, X.-L. Qi, and S.-C. Zhang, 2010, "Dynamical Axion Field in Topological Magnetic Insulators," Nat. Phys. **6**, 284.

Li, W., Z. Liu, Y.-S. Wu, and Y. Chen, 2014, "Exotic Fractional Topological States in a Two-Dimensional Organometallic Material," Phys. Rev. B **89**, 125411.

Li, W., X.-Y. Wei, J.-X. Zhu, C. S. Ting, and Y. Chen, 2014, "Pressure-Induced Topological Quantum Phase Transition in Sb_2Se_3," Phys. Rev. B **89**, 035101.

Li, Z., J. Li, P. Blaha, and N. Kioussis, 2014, "Predicted Topological Phase Transition in the SmS Kondo Insulator under Pressure," Phys. Rev. B **89**, 121117.

Li, Z., S. Shao, N. Li, K. McCall, J. Wang, and S. X. Zhang, 2013, "Single Crystalline Nanostructures of Topological Crystalline Insulator SnTe with Distinct Facets and Morphologies," Nano Lett. **13**, 5443.

Liang, T., Q. Gibson, J. Xiong, M. Hirschberger, S. P. Koduvayur, R. J. Cava, and N. P. Ong, 2013, "Evidence for Massive Bulk Dirac Fermions in $Pb_{1-x}Sn_xSe$ from Nernst and Thermopower Experiments," Nat. Commun. **4**, 2696.

Lin, H., T. Das, Y. J. Wang, L. A. Wray, S.-Y. Xu, M. Z. Hasan, and A. Bansil, 2013, "Adiabatic Transformation as a Search Tool for New Topological Insulators: Distorted Ternary Li_2AgSb-Class Semiconductors and Related Compounds," Phys. Rev. B **87**, 121202.

Lin, H., T. Das, L. A. Wray, S.-Y. Xu, M. Z. Hasan, and A. Bansil, 2011, "An Isolated Dirac Cone on the Surface of Ternary Tetradymite-like Topological Insulators," New J. Phys. **13**, 095005.

Lin, H., R. S. Markiewicz, L. A. Wray, L. Fu, M. Z. Hasan, and A. Bansil, 2010, "Single-Dirac-Cone Topological Surface States in the $TlBiSe_2$ Class of Topological Semiconductors," Phys. Rev. Lett. **105**, 036404.

Lin, H., S. Sahrakorpi, R. S. Markiewicz, and A. Bansil, 2006, "Raising Bi-O Bands above the Fermi Energy Level of Hole-Doped $Bi_2Sr_2CaCu_2O_{8+\delta}$ and Other Cuprate Superconductors," Phys. Rev. Lett. **96**, 097001.

Lin, H., L. A. Wray, Y. Xia, S. Xu, S. Jia, R. J. Cava, A. Bansil, and M. Z. Hasan, 2010, "Half-Heusler Ternary Compounds as New Multifunctional Experimental Platforms for Topological Quantum Phenomena," Nat. Mater. **9**, 546.

Lin, H., *et al.*, 2013, "Topological Dangling Bonds with Large Spin Splitting and Enhanced Spin Polarization on the Surfaces of Bi_2Se_3," Nano Lett. **13**, 1915.

Lindner, N. H., G. Refael, and V. Galitski, 2011, "Floquet Topological Insulator in Semiconductor Quantum Wells," Nat. Phys. **7**, 490.

Lindroos, M., and A. Bansil, 1996, "A Novel Direct Method of Fermi Surface Determination Using Constant Initial Energy Angle-Scanned Photoemission Spectroscopy," Phys. Rev. Lett. **77**, 2985.

Littlewood, P. B., *et al.*, 2010, "Band Structure of SnTe Studied by Photoemission Spectroscopy," Phys. Rev. Lett. **105**, 086404.

Liu, C., T. L. Hughes, X.-L. Qi, K. Wang, and S.-C. Zhang, 2008, "Quantum Spin Hall Effect in Inverted Type-II Semiconductors," Phys. Rev. Lett. **100**, 236601.

Liu, C.-C., W. Feng, and Y. Yao, 2011, "Quantum Spin Hall Effect in Silicene and Two-Dimensional Germanium," Phys. Rev. Lett. **107**, 076802.

Liu, C.-C., H. Jiang, and Y. Yao, 2011, "Low-Energy Effective Hamiltonian Involving Spin-Orbit Coupling in Silicene and Two-Dimensional Germanium and Tin," Phys. Rev. B **84**, 195430.

Liu, C.-X., H. Zhang, B. Yan, X.-L. Qi, T. Frauenheim, X. Dai, Z. Fang, and S.-C. Zhang, 2010, "Oscillatory Crossover from Two-Dimensional to Three-Dimensional Topological Insulators," Phys. Rev. B **81**, 041307.

Liu, F., C.-C. Liu, K. Wu, F. Yang, and Y. Yao, 2013, "$D + id'$ Chiral Superconductivity in Bilayer Silicene," Phys. Rev. Lett. **111**, 066804.

Liu, J., T. H. Hsieh, P. Wei, W. Duan, J. Moodera, and L. Fu, 2014, "Spin-Filtered Edge States with an Electrically Tunable Gap in a Two-Dimensional Topological Crystalline Insulator," Nat. Mater. **13**, 178.

Liu, Y., Y. Y. Li, S. Rajput, D. Gilks, L. Lari, P. L. Galindo, M. Weinert, V. K. Lazarov, and L. Li, 2014, "Tuning Dirac States by Strain in the Topological Insulator Bi_2Se_3," Nat. Phys. **10**, 294.

Liu, Z., C.-X. Liu, Y.-S. Wu, W.-H. Duan, F. Liu, and J. Wu, 2011, "Stable Nontrivial Z_2 Topology in Ultrathin Bi (111) Films: A First-Principles Study," Phys. Rev. Lett. **107**, 136805.

Liu, Z., Z.-F. Wang, J.-W. Mei, Y.-S. Wu, and F. Liu, 2013, "Flat Chern Band in a Two-Dimensional Organometallic Framework," Phys. Rev. Lett. **110**, 106804.

Liu, Z. K., *et al.*, 2014a, "A Stable Three-Dimensional Topological Dirac Semimetal Cd_3As_2," Nat. Mater. **13**, 677.

Liu, Z. K., *et al.*, 2014b, "Discovery of a Three-Dimensional Topological Dirac Semimetal, Na_3Bi," Science **343**, 864.

Lu, F., J. Zhao, H. Weng, Z. Fang, and X. Dai, 2013, "Correlated Topological Insulators with Mixed Valence," Phys. Rev. Lett. **110**, 096401.

Lu, Y., *et al.*, 2015, "Topological Properties Determined by Atomic Buckling in Self-Assembled Ultrathin Bi(110)," Nano Lett. **15**, 80.

Lükermann, D., S. Sologub, H. Pfnür, C. Klein, M. Horn-von Hoegen, and C. Tegenkamp, 2012, "Scattering at Magnetic and Nonmagnetic Impurities on Surfaces with Strong Spin-Orbit Coupling," Phys. Rev. B **86**, 195432.

Luo, C. W., *et al.*, 2013, "Snapshots of Dirac Fermions near the Dirac Point in Topological Insulators," Nano Lett. **13**, 5797.

Luo, J.-W., and A. Zunger, 2010, "Design Principles and Coupling Mechanisms in the 2D Quantum Well Topological Insulator HgTe/CdTe," Phys. Rev. Lett. **105**, 176805.

Luo, W., and X.-L. Qi, 2013, "Massive Dirac Surface States in Topological Insulator/magnetic Insulator Heterostructures," Phys. Rev. B **87**, 085431.

Luo, X., M. B. Sullivan, and S. Y. Quek, 2012, "First-Principles Investigations of the Atomic, Electronic, and Thermoelectric Properties of Equilibrium and Strained Bi_2Se_3 and Bi_2Te_3 Including van Der Waals Interactions," Phys. Rev. B **86**, 184111.

Lv, B. Q., *et al.*, 2015, "Observation of Weyl Nodes in TaAs," Nat. Phys. **11**, 724.

Ma, Y., Y. Dai, L. Kou, T. Frauenheim, and T. Heine, 2015, "Robust Two-Dimensional Topological Insulators in Methyl-Functionalized Bismuth, Antimony, and Lead Bilayer Films," Nano Lett. **15**, 1083.

Mackenzie, A. P., and Y. Maeno, 2003, "The Superconductivity of Sr_2RuO_4 and the Physics of Spin-Triplet Pairing," Rev. Mod. Phys. **75**, 657.

Mader, J., S. Berko, H. Krakauer, and A. Bansil, 1976, "Electronic Momentum Densities by Two-Dimensional Angular Correlation of Annihilation Radiation in Aluminum," Phys. Rev. Lett. **37**, 1232.

Maher, P., C. R. Dean, A. F. Young, T. Taniguchi, K. Watanabe, K. L. Shepard, J. Hone, and P. Kim, 2013, "Evidence for a Spin Phase Transition at Charge Neutrality in Bilayer Graphene," Nat. Phys. **9**, 154.

Maier, T., M. Jarrell, T. Pruschke, and M. H. Hettler, 2005, "Quantum Cluster Theories," Rev. Mod. Phys. **77**, 1027.

Marcinkova, A., J. K. Wang, C. Slavonic, A. H. Nevidomskyy, K. F. Kelly, Y. Filinchuk, and E. Morosan, 2013, "Topological Metal Behavior in $GeBi_2Te_4$ Single Crystals," Phys. Rev. B **88**, 165128.

Martin, R. M., and J. W. Allen, 1979, "Theory of Mixed Valence: Metals or Small Gap Insulators (invited)," J. Appl. Phys. **50**, 7561.

Marzari, N., and D. Vanderbilt, 1997, "Maximally Localized Generalized Wannier Functions for Composite Energy Bands," Phys. Rev. B **56**, 12847.

Mas-Ballesté, R., C. Gómez-Navarro, J. Gómez-Herrero, and F. Zamora, 2011, "2D Materials: To Graphene and beyond," Nanoscale **3**, 20.

Matsuhira, K., M. Wakeshima, R. Nakanishi, T. Yamada, A. Nakamura, W. Kawano, S. Takagi, and Y. Hinatsu, 2007, "Metal-Insulator Transition in Pyrochlore Iridates $Ln_2Ir_2O_7$ (Ln=Nd, Sm, and Eu)," J. Phys. Soc. Jpn. **76**, 043706.

Mellnik, A. R., *et al.*, 2014, "Spin-Transfer Torque Generated by a Topological Insulator," Nature (London) **511**, 449.

Meng, L., *et al.*, 2013, "Buckled Silicene Formation on Ir(111)," Nano Lett. **13**, 685.

Meng, T., and L. Balents, 2012, "Weyl Superconductors," Phys. Rev. B **86**, 054504.

Menshchikova, T. V., S. V. Eremeev, and E. V. Chulkov, 2011, "On the Origin of Two-Dimensional Electron Gas States at the Surface of Topological Insulators," JETP Lett. **94**, 106.

Menshchikova, T. V., M. M. Otrokov, S. S. Tsirkin, D. A. Samorokov, V. V. Bebneva, A. Ernst, V. M. Kuznetsov, and E. V. Chulkov, 2013, "Band Structure Engineering in Topological Insulator Based Heterostructures," Nano Lett. **13**, 6064.

Mijnarends, P., and A. Bansil, 1976, "Momentum Density for Compton Scattering from Random Alloys," Phys. Rev. B **13**, 2381.

Miyamoto, K., *et al.*, 2012, "Topological Surface States with Persistent High Spin Polarization across the Dirac Point in Bi_2Te_2Se and Bi_2Se_2Te," Phys. Rev. Lett. **109**, 166802.

Miyawaki, T., N. Sugimoto, N. Fukatani, T. Yoshihara, K. Ueda, N. Tanaka, and H. Asano, 2012, "Structural and Electrical Properties of Half-Heusler La-Pt-Bi Thin Films Grown by 3-Source Magnetron Co-Sputtering," J. Appl. Phys. **111**, 07E327.

Miyazaki, H., T. Hajiri, T. Ito, S. Kunii, and S. Kimura, 2012, "Momentum-Dependent Hybridization Gap and Dispersive in-Gap State of the Kondo Semiconductor SmB_6," Phys. Rev. B **86**, 075105.

Mong, R. S. K., A. M. Essin, and J. E. Moore, 2010, "Antiferromagnetic Topological Insulators," Phys. Rev. B **81**, 245209.

Moore, J. E., and L. Balents, 2007, "Topological Invariants of Time-Reversal-Invariant Band Structures," Phys. Rev. B **75**, 121306.

Muff, S., F. von Rohr, G. Landolt, B. Slomski, A. Schilling, R. J. Cava, J. Osterwalder, and J. H. Dil, 2013, "Separating the Bulk and Surface N- to P-Type Transition in the Topological Insulator $GeBi_{4-x}Sb_xTe_7$," Phys. Rev. B **88**, 035407.

Murakami, S., 2006, "Quantum Spin Hall Effect and Enhanced Magnetic Response by Spin-Orbit Coupling," Phys. Rev. Lett. **97**, 236805.

Murakami, S., 2007, "Phase Transition between the Quantum Spin Hall and Insulator Phases in 3D: Emergence of a Topological Gapless Phase," New J. Phys. **9**, 356.

Murakami, S., N. Nagaosa, and S.-C. Zhang, 2004, "Spin-Hall Insulator," Phys. Rev. Lett. **93**, 156804.

Nadj-Perge, S., I. K. Drozdov, J. Li, H. Chen, S. Jeon, J. Seo, A. H. MacDonald, B. A. Bernevig, and A. Yazdani, 2014, "Observation of Majorana Fermions in Ferromagnetic Atomic Chains on a Superconductor," Science **346**, 602.

Nakahara, M., 1990, *Geometry, Topology and Physics* (Hilger, Bristol).

Nakayama, K., K. Eto, Y. Tanaka, T. Sato, S. Souma, T. Takahashi, K. Segawa, and Y. Ando, 2012, "Manipulation of Topological States and the Bulk Band Gap Using Natural Heterostructures of a Topological Insulator," Phys. Rev. Lett. **109**, 236804.

Nandkishore, R., L. S. Levitov, and A. V. Chubukov, 2012, "Chiral Superconductivity from Repulsive Interactions in Doped Graphene," Nat. Phys. **8**, 158.

Narayan, A., D. Di Sante, S. Picozzi, and S. Sanvito, 2014, "Topological Tuning in Three-Dimensional Dirac Semimetals," Phys. Rev. Lett. **113**, 256403.

Neupane, M., *et al.*, 2012, "Topological Surface States and Dirac Point Tuning in Ternary Topological Insulators," Phys. Rev. B **85**, 235406.

Neupane, M., *et al.*, 2013, "Surface Electronic Structure of the Topological Kondo-Insulator Candidate Correlated Electron System SmB_6," Nat. Commun. **4**, 2991.

Neupane, M., *et al.*, 2014a, "Observation of Quantum-Tunnelling-Modulated Spin Texture in Ultrathin Topological Insulator Bi_2Se_3 Films," Nat. Commun. **5**, 3841.

Neupane, M., *et al.*, 2014b, "Observation of a Topological 3D Dirac Semimetal Phase in High-Mobility Cd_3As_2 and Related Materials," Nat. Commun. **5**, 3786.

Neupane, M., *et al.*, 2015, "Non-Kondo-like Electronic Structure in the Correlated Rare-Earth Hexaboride YbB_6," Phys. Rev. Lett. **114**, 016403.

Nieminen, J., H. Lin, R. Markiewicz, and A. Bansil, 2009, "Origin of the Electron-Hole Asymmetry in the Scanning Tunneling Spectrum of the High-Temperature $Bi_2Sr_2CaCu_2O_{8+\delta}$ Superconductor," Phys. Rev. Lett. **102**, 037001.

Nieminen, J., I. Suominen, T. Das, R. S. Markiewicz, and A. Bansil, 2012, "Evidence of Strong Correlations at the van Hove Singularity in the Scanning Tunneling Spectra of Superconducting $Bi_2Sr_2CaCu_2O_{8+\delta}$ Single Crystals," Phys. Rev. B **85**, 214504.

Niesner, D., *et al.*, 2012, "Unoccupied Topological States on Bismuth Chalcogenides," Phys. Rev. B **86**, 205403.

Niesner, D., *et al.*, 2014, "Bulk and Surface Electron Dynamics in a P-Type Topological Insulator $SnSb_2Te_4$," Phys. Rev. B **89**, 081404.

Ning, W., H. Du, F. Kong, J. Yang, Y. Han, M. Tian, and Y. Zhang, 2013, "One-Dimensional Weak Antilocalization in Single-Crystal Bi_2Te_3 Nanowires," Sci. Rep. **3**, 1564.

Nishide, A., A. A. Taskin, Y. Takeichi, T. Okuda, A. Kakizaki, T. Hirahara, K. Nakatsuji, F. Komori, Y. Ando, and I. Matsuda, 2010, "Direct Mapping of the Spin-Filtered Surface Bands of a Three-Dimensional Quantum Spin Hall Insulator," Phys. Rev. B **81**, 041309.

Niu, C., Y. Dai, Y. Zhu, J. Lu, Y. Ma, and B. Huang, 2012, "Topological Phase Transition and Unexpected Mass Acquisition of Dirac Fermion in $TlBi(S_{1-x}Se_x)_2$," Appl. Phys. Lett. **101**, 182101.

Niu, C., Y. Dai, Y. Zhu, Y. Ma, L. Yu, S. Han, and B. Huang, 2012, "Realization of Tunable Dirac Cone and Insulating Bulk States in Topological Insulators $(Bi_{1-x}Sb_x)_2Te_3$," Sci. Rep. **2**, 976.

Nomura, M., S. Souma, A. Takayama, T. Sato, T. Takahashi, K. Eto, K. Segawa, and Y. Ando, 2014, "Relationship between Fermi Surface Warping and out-of-Plane Spin Polarization in Topological Insulators: A View from Spin- and Angle-Resolved Photoemission," Phys. Rev. B **89**, 045134.

Novak, M., S. Sasaki, M. Kriener, K. Segawa, and Y. Ando, 2013, "Unusual Nature of Fully Gapped Superconductivity in In-Doped SnTe," Phys. Rev. B **88**, 140502.

Novak, M., S. Sasaki, K. Segawa, and Y. Ando, 2015, "Large Linear Magnetoresistance in the Dirac Semimetal TlBiSSe," Phys. Rev. B **91**, 041203.

Nowack, K. C., *et al.*, 2013, "Imaging Currents in HgTe Quantum Wells in the Quantum Spin Hall Regime," Nat. Mater. **12**, 787.

Ojanen, T., 2012, "Magnetoelectric Effects in Superconducting Nanowires with Rashba Spin-Orbit Coupling," Phys. Rev. Lett. **109**, 226804.

Ojanen, T., 2013, "Helical Fermi Arcs and Surface States in Time-Reversal Invariant Weyl Semimetals," Phys. Rev. B **87**, 245112.

Okada, Y., W. Zhou, D. Walkup, C. Dhital, S. D. Wilson, and V. Madhavan, 2012, "Ripple-Modulated Electronic Structure of a 3D Topological Insulator," Nat. Commun. **3**, 1158.

Okada, Y., *et al.*, 2011, "Direct Observation of Broken Time-Reversal Symmetry on the Surface of a Magnetically Doped Topological Insulator," Phys. Rev. Lett. **106**, 206805.

Okada, Y., *et al.*, 2013, "Observation of Dirac Node Formation and Mass Acquisition in a Topological Crystalline Insulator," Science **341**, 1496.

Okamoto, K., *et al.*, 2012, "Observation of a Highly Spin-Polarized Topological Surface State in $GeBi_2Te_4$," Phys. Rev. B **86**, 195304.

Okamoto, S., W. Zhu, Y. Nomura, R. Arita, D. Xiao, and N. Nagaosa, 2014, "Correlation Effects in (111) Bilayers of Perovskite Transition-Metal Oxides," Phys. Rev. B **89**, 195121.

Okuda, T., and A. Kimura, 2013, "Spin- and Angle-Resolved Photoemission of Strongly Spin-Orbit Coupled Systems," J. Phys. Soc. Jpn. **82**, 021002.

Okuda, T., *et al.*, 2013, "Experimental Evidence of Hidden Topological Surface States in $PbBi_4Te_7$," Phys. Rev. Lett. **111**, 206803.

Olshanetsky, E. B., Z. D. Kvon, G. M. Gusev, A. D. Levin, O. E. Raichev, N. N. Mikhailov, and S. A. Dvoretsky, 2015, "Persistence of a Two-Dimensional Topological Insulator State in Wide HgTe Quantum Wells," Phys. Rev. Lett. **114**, 126802.

Onoda, M., and N. Nagaosa, 2003, "Quantized Anomalous Hall Effect in Two-Dimensional Ferromagnets: Quantum Hall Effect in Metals," Phys. Rev. Lett. **90**, 206601.

Oostinga, J. B., L. Maier, P. Schüffelgen, D. Knott, C. Ames, C. Brüne, G. Tkachov, H. Buhmann, and L. W. Molenkamp, 2013, "Josephson Supercurrent through the Topological Surface States of Strained Bulk HgTe," Phys. Rev. X **3**, 021007.

Orlita, M., *et al.*, 2014, "Observation of Three-Dimensional Massless Kane Fermions in a Zinc-Blende Crystal," Nat. Phys. **10**, 233.

Oroszlány, L., and A. Cortijo, 2012, "Gap Generation in Topological Insulator Surface States by Nonferromagnetic Magnets," Phys. Rev. B **86**, 195427.

Ortix, C., J. W. F. Venderbos, R. Hayn, and J. van den Brink, 2014, "Absence of Helical Surface States in Bulk Semimetals with Broken Inversion Symmetry," Phys. Rev. B **89**, 121408.

Ou, J.-Y., J.-K. So, G. Adamo, A. Sulaev, L. Wang, and N. I. Zheludev, 2014, "Ultraviolet and Visible Range Plasmonics in the Topological Insulator $Bi_{1.5}Sb_{0.5}Te_{1.8}Se_{1.2}$," Nat. Commun. **5**, 5139.

Padilha, J. E., L. Seixas, R. B. Pontes, A. J. R. da Silva, and A. Fazzio, 2013, "Quantum Spin Hall Effect in a Disordered Hexagonal Si_xGe_{1-x} Alloy," Phys. Rev. B **88**, 201106.

Pan, H., Z. Li, C.-C. Liu, G. Zhu, Z. Qiao, and Y. Yao, 2014, "Valley-Polarized Quantum Anomalous Hall Effect in Silicene," Phys. Rev. Lett. **112**, 106802.

Pariari, A., P. Dutta, and P. Mandal, 2015, "Probing the Fermi Surface of Three-Dimensional Dirac Semimetal Cd_3As_2 through the de Haas-van Alphen Technique," Phys. Rev. B **91**, 155139.

Park, B. C., T.-H. Kim, K. I. Sim, B. Kang, J. W. Kim, B. Cho, K.-H. Jeong, M.-H. Cho, and J. H. Kim, 2015, "Terahertz Single Conductance Quantum and Topological Phase Transitions in Topological Insulator Bi_2Se_3 Ultrathin Films," Nat. Commun. **6**, 6552.

Park, C.-H., and S. G. Louie, 2009, "Making Massless Dirac Fermions from a Patterned Two-Dimensional Electron Gas," Nano Lett. **9**, 1793.

Pathak, S., V. B. Shenoy, and G. Baskaran, 2010, "Possible High-Temperature Superconducting State with a D+id Pairing Symmetry in Doped Graphene," Phys. Rev. B **81**, 085431.

Pauly, C., *et al.*, 2012, "Probing Two Topological Surface Bands of Sb_2Te_3 by Spin-Polarized Photoemission Spectroscopy," Phys. Rev. B **86**, 235106.

Pauly, C., *et al.*, 2015, "Subnanometre-Wide Electron Channels Protected by Topology," Nat. Phys. **11**, 338.

Peres, N. M. R., 2010, "*Colloquium*: The Transport Properties of Graphene: An Introduction," Rev. Mod. Phys. **82**, 2673.

Perez-Piskunow, P. M., G. Usaj, C. A. Balseiro, and L. E. F. F. Torres, 2014, "Floquet Chiral Edge States in Graphene," Phys. Rev. B **89**, 121401.

Pesin, D., and L. Balents, 2010, "Mott Physics and Band Topology in Materials with Strong Spin-orbit Interaction," Nat. Phys. **6**, 376.

Pesin, D., and A. H. MacDonald, 2012, "Spintronics and Pseudospintronics in Graphene and Topological Insulators," Nat. Mater. **11**, 409.

Peverati, R., and D. G. Truhlar, 2014, "Quest for a Universal Density Functional: The Accuracy of Density Functionals across a Broad Spectrum of Databases in Chemistry and Physics," Phil. Trans. R. Soc. A **372**, 20120476.

Pickett, W. E., 1989, "Electronic Structure of the High-Temperature Oxide Superconductors," Rev. Mod. Phys. **61**, 433.

Pientka, F., L. I. Glazman, and F. von Oppen, 2013, "Topological Superconducting Phase in Helical Shiba Chains," Phys. Rev. B **88**, 155420.

Polley, C. M., *et al.*, 2014, "Observation of Topological Crystalline Insulator Surface States on (111)-Oriented $Pb_{1-x}Sn_xSe$ Films," Phys. Rev. B **89**, 075317.

Qi, X.-L., T. L. Hughes, S. Raghu, and S.-C. Zhang, 2009, "Time-Reversal-Invariant Topological Superconductors and Superfluids in Two and Three Dimensions," Phys. Rev. Lett. **102**, 187001.

Qi, X.-L., T. L. Hughes, and S.-C. Zhang, 2008, "Topological Field Theory of Time-Reversal Invariant Insulators," Phys. Rev. B **78**, 195424.

Qi, X.-L., R. Li, J. Zang, and S.-C. Zhang, 2009, "Inducing a Magnetic Monopole with Topological Surface States," Science **323**, 1184.

Qi, X.-L., Y.-S. Wu, and S.-C. Zhang, 2006, "Topological Quantization of the Spin Hall Effect in Two-Dimensional Paramagnetic Semiconductors," Phys. Rev. B **74**, 085308.

Qi, X.-L., and S.-C. Zhang, 2011, "Topological Insulators and Superconductors," Rev. Mod. Phys. **83**, 1057.

Qian, X., J. Liu, L. Fu, and J. Li, 2014, "Quantum Spin Hall Effect in Two-Dimensional Transition Metal Dichalcogenides," Science **346**, 1344.

Qu, D.-X., Y. S. Hor, and R. J. Cava, 2012, "Quantum Oscillations in Magnetothermopower Measurements of the Topological Insulator Bi_2Te_3," Phys. Rev. Lett. **109**, 246602.

Qu, D.-X., Y. S. Hor, J. Xiong, R. J. Cava, and N. P. Ong, 2010, "Quantum Oscillations and Hall Anomaly of Surface States in the Topological Insulator Bi_2Te_3," Science **329**, 821.

Rasche, B., A. Isaeva, M. Ruck, S. Borisenko, V. Zabolotnyy, B. Büchner, K. Koepernik, C. Ortix, M. Richter, and J. van den Brink, 2013, "Stacked Topological Insulator Built from Bismuth-Based Graphene Sheet Analogues," Nat. Mater. **12**, 422.

Rechtsman, M. C., J. M. Zeuner, Y. Plotnik, Y. Lumer, D. Podolsky, F. Dreisow, S. Nolte, M. Segev, and A. Szameit, 2013, "Photonic Floquet Topological Insulators," Nature (London) **496**, 196.

Ren, J., *et al.*, 2014, "Electronic Structure of the Quantum Spin Hall Parent Compound CdTe and Related Topological Issues," Phys. Rev. B **90**, 205211.

Ren, Z., A. A. Taskin, S. Sasaki, K. Segawa, and Y. Ando, 2010, "Large Bulk Resistivity and Surface Quantum Oscillations in the Topological Insulator Bi_2Te_2Se," Phys. Rev. B **82**, 241306.

Ren, Z., A. A. Taskin, S. Sasaki, K. Segawa, and Y. Ando, 2012, "Fermi Level Tuning and a Large Activation Gap Achieved in the Topological Insulator Bi_2Te_2Se by Sn Doping," Phys. Rev. B **85**, 155301.

Rischau, C. W., B. Leridon, B. Fauqué, V. Metayer, and C. J. van der Beek, 2013, "Doping of Bi_2Te_3 Using Electron Irradiation," Phys. Rev. B **88**, 205207.

Rößler, S., T.-H. Jang, D. J. Kim, L. H. Tjeng, Z. Fisk, F. Steglich, and S. Wirth, 2014, "Hybridization Gap and Fano Resonance in SmB_6," Proc. Natl. Acad. Sci. U.S.A. **111**, 4798.

Roushan, P., J. Seo, C. V. Parker, Y. S. Hor, D. Hsieh, D. Qian, A. Richardella, M. Z. Hasan, R. J. Cava, and A. Yazdani, 2009, "Topological Surface States Protected from Backscattering by Chiral Spin Texture," Nature (London) **460**, 1106.

Roy, R., 2009, "Topological Phases and the Quantum Spin Hall Effect in Three Dimensions," Phys. Rev. B **79**, 195322.
Roy, R., and C. Kallin, 2008, "Collective Modes and Electromagnetic Response of a Chiral Superconductor," Phys. Rev. B **77**, 174513.
Sa, B., J. Zhou, R. Ahuja, and Z. Sun, 2014, "First-Principles Investigations of Electronic and Mechanical Properties for Stable $Ge_2Sb_2Te_5$ with van Der Waals Corrections," Comput. Mater. Sci. **82**, 66.
Sa, B., J. Zhou, Z. Song, Z. Sun, and R. Ahuja, 2011, "Pressure-Induced Topological Insulating Behavior in the Ternary Chalcogenide $Ge_2Sb_2Te_5$," Phys. Rev. B **84**, 085130.
Saari, T., C.-Y. Huang, J. Nieminen, W.-F. Tsai, H. Lin, and A. Bansil, 2014, "Electrically Tunable Localized Tunneling Channels in Silicene Nanoribbons," Appl. Phys. Lett. **104**, 173104.
Safaei, S., P. Kacman, and R. Buczko, 2013, "Topological Crystalline Insulator (Pb,Sn)Te: Surface States and Their Spin Polarization," Phys. Rev. B **88**, 045305.
Sahin, C., and M. E. Flatte, 2015, "Tunable Giant Spin Hall Conductivities in a Strong Spin-Orbit Semimetal: $Bi_{1-x}Sb_x$," Phys. Rev. Lett. **114**, 107201.
Sahrakorpi, S., M. Lindroos, R. S. Markiewicz, and A. Bansil, 2005, "Evolution of Midgap States and Residual Three Dimensionality in $La_{2-x}Sr_xCuO_4$," Phys. Rev. Lett. **95**, 157601.
Sasaki, S., K. Segawa, and Y. Ando, 2014, "New Superconductor Derived from A Topological Insulator Heterostructure," Phys. Rev. B **90**, 220504.
Sato, M., 2009, "Topological Properties of Spin-Triplet Superconductors and Fermi Surface Topology in the Normal State," Phys. Rev. B **79**, 214526.
Sato, T., K. Segawa, H. Guo, K. Sugawara, S. Souma, T. Takahashi, and Y. Ando, 2010, "Direct Evidence for the Dirac-Cone Topological Surface States in the Ternary Chalcogenide $TlBiSe_2$," Phys. Rev. Lett. **105**, 136802.
Sato, T., K. Segawa, K. Kosaka, S. Souma, K. Nakayama, K. Eto, T. Minami, Y. Ando, and T. Takahashi, 2011, "Unexpected Mass Acquisition of Dirac Fermions at the Quantum Phase Transition of a Topological Insulator," Nat. Phys. **7**, 840.
Schlenk, T., *et al.*, 2013, "Controllable Magnetic Doping of the Surface State of a Topological Insulator," Phys. Rev. Lett. **110**, 126804.
Schnyder, A. P., S. Ryu, A. Furusaki, and A. W. W. Ludwig, 2008, "Classification of Topological Insulators and Superconductors in Three Spatial Dimensions," Phys. Rev. B **78**, 195125.
Schwartz, L., and A. Bansil, 1974, "Total and Component Densities of States in Substitutional Alloys," Phys. Rev. B **10**, 3261.
Seibel, C., H. Bentmann, J. Braun, J. Minar, H. Maass, K. Sakamoto, M. Arita, K. Shimada, H. Ebert, and F. Reinert, 2015, "Connection of a Topological Surface State with the Bulk Continuum in $Sb_2Te_3(0001)$," Phys. Rev. Lett. **114**, 066802.
Sessi, P., T. Bathon, K. A. Kokh, O. E. Tereshchenko, and M. Bode, 2014, "Probing the Electronic Properties of Individual MnPc Molecules Coupled to Topological States," Nano Lett. **14**, 5092.
Sessi, P., F. Reis, T. Bathon, K. A. Kokh, O. E. Tereshchenko, and M. Bode, 2014, "Signatures of Dirac Fermion-Mediated Magnetic Order," Nat. Commun. **5**, 5349.
Shen, J., Y. Jung, A. S. Disa, F. J. Walker, C. H. Ahn, and J. J. Cha, 2014, "Synthesis of SnTe Nanoplates with {100} and {111} Surfaces," Nano Lett. **14**, 4183.
Shikin, A. M., *et al.*, 2014, "Electronic and Spin Structure of the Topological Insulator $Bi_2Te_{2.4}Se_{0.6}$," Phys. Rev. B **89**, 125416.
Shiozaki, K., and M. Sato, 2014, "Topology of Crystalline Insulators and Superconductors," Phys. Rev. B **90**, 165114.
Shirasawa, T., J. Tsunoda, T. Hirahara, and T. Takahashi, 2013, "Structure of a Bi/Bi_2Te_3 Heteroepitaxial Film Studied by X-Ray Crystal Truncation Rod Scattering," Phys. Rev. B **87**, 075449.
Shitade, A., H. Katsura, J. Kuneš, X.-L. Qi, S.-C. Zhang, and N. Nagaosa, 2009, "Quantum Spin Hall Effect in a Transition Metal Oxide Na_2IrO_3," Phys. Rev. Lett. **102**, 256403.
Shoman, T., A. Takayama, T. Sato, S. Souma, T. Takahashi, T. Oguchi, K. Segawa, and Y. Ando, 2015, "Topological Proximity Effect in a Topological Insulator Hybrid," Nat. Commun. **6**, 6547.
Si, C., J. Liu, Y. Xu, J. Wu, B.-L. Gu, and W. Duan, 2014, "Functionalized Germanene as a Prototype of Large-Gap Two-Dimensional Topological Insulators," Phys. Rev. B **89**, 115429.
Singh, B., H. Lin, R. Prasad, and A. Bansil, 2013, "Topological Phase Transition and Two-Dimensional Topological Insulators in Ge-Based Thin Films," Phys. Rev. B **88**, 195147.
Singh, B., A. Sharma, H. Lin, M. Z. Hasan, R. Prasad, and A. Bansil, 2012, "Topological Electronic Structure and Weyl Semimetal in the $TlBiSe_2$ Class of Semiconductors," Phys. Rev. B **86**, 115208.
Sinova, J., D. Culcer, Q. Niu, N. A. Sinitsyn, T. Jungwirth, and A. H. MacDonald, 2004, "Universal Intrinsic Spin Hall Effect," Phys. Rev. Lett. **92**, 126603.
Slager, R.-J., A. Mesaros, V. Juričić, and J. Zaanen, 2013, "The Space Group Classification of Topological Band-Insulators," Nat. Phys. **9**, 98.
Sleight, A. W., J. L. Gillson, and P. E. Bierstedt, 1975, "High-Temperature Superconductivity in the $BaPb_{1-x}Bi_xO_3$ Systems," Solid State Commun. **17**, 27.
Smedskjaer, L. C., A. Bansil, U. Welp, Y. Fang, and K. G. Bailey, 1991, "Positron Studies of Metallic $YBa_2Cu_3O_{7-x}$," J. Phys. Chem. Solids **52**, 1541.
Smith, J. C., S. Banerjee, V. Pardo, and W. E. Pickett, 2011, "Dirac Point Degenerate with Massive Bands at a Topological Quantum Critical Point," Phys. Rev. Lett. **106**, 056401.
Sochnikov, I., *et al.*, 2015, "Nonsinusoidal Current-Phase Relationship in Josephson Junctions from the 3D Topological Insulator HgTe," Phys. Rev. Lett. **114**, 066801.
Song, Z., C.-C. Liu, J. Yang, J. Han, M. Ye, B. Fu, Y. Yang, Q. Niu, J. Lu, and Y. Yao, 2014, "Quantum Spin Hall Insulators and Quantum Valley Hall Insulators of BiX/SbX (X = H, F, Cl, and Br) Monolayers with a Record Bulk Band Gap," NPG Asia Mater. **6**, e147.
Soumyanarayanan, A., M. M. Yee, Y. He, H. Lin, D. R. Gardner, A. Bansil, Y. S. Lee, and J. E. Hoffman, 2013, "Imaging the Nanoscale Band Structure of Topological Sb," arXiv:1311.1758, http://arxiv.org/abs/1311.1758.
Steinberg, H., D. R. Gardner, Y. S. Lee, and P. Jarillo-Herrero, 2010, "Surface State Transport and Ambipolar Electric Field Effect in Bi_2Se_3 Nanodevices," Nano Lett. **10**, 5032.
Stocks, G. M., W. M. Temmerman, and B. L. Gyorffy, 1978, "Complete Solution of the Korringa-Kohn-Rostoker Coherent-Potential-Approximation Equations: Cu-Ni Alloys," Phys. Rev. Lett. **41**, 339.
Sulaev, A., *et al.*, 2013, "Experimental Evidences of Topological Surface States of β-Ag_2Te," AIP Adv. **3**, 032123.
Sun, Y., X.-Q. Chen, C. Franchini, D. Li, S. Yunoki, Y. Li, and Z. Fang, 2011, "Strain-Driven Onset of Nontrivial Topological Insulating States in Zintl Sr_2X Compounds (X = Pb, Sn)," Phys. Rev. B **84**, 165127.
Sun, Y., X.-Q. Chen, S. Yunoki, D. Li, and Y. Li, 2010, "New Family of Three-Dimensional Topological Insulators with Antiperovskite Structure," Phys. Rev. Lett. **105**, 216406.
Sun, Y., Z. Zhong, T. Shirakawa, C. Franchini, D. Li, Y. Li, S. Yunoki, and X.-Q. Chen, 2013, "Rocksalt SnS and SnSe: Native Topological Crystalline Insulators," Phys. Rev. B **88**, 235122.

Sung, J. H., H. Heo, I. Hwang, M. Lim, D. Lee, K. Kang, H. C. Choi, J.-H. Park, S.-H. Jhi, and M.-H. Jo, 2014, "Atomic Layer-by-Layer Thermoelectric Conversion in Topological Insulator Bismuth/Antimony Tellurides," Nano Lett. **14**, 4030.

Syers, P., D. Kim, M. S. Fuhrer, and J. Paglione, 2015, "Tuning Bulk and Surface Conduction in the Proposed Topological Kondo Insulator SmB_6," Phys. Rev. Lett. **114**, 096601.

Tabert, C. J., and E. J. Nicol, 2013, "AC/DC Spin and Valley Hall Effects in Silicene and Germanene," Phys. Rev. B **87**, 235426.

Tahir, M., and U. Schwingenschlögl, 2013, "Valley Polarized Quantum Hall Effect and Topological Insulator Phase Transitions in Silicene," Sci. Rep. **3**, 1075.

Takafuji, Y., and S. Narita, 1982, "Shubnikov-de Haas Measurements in N-Type $Pb_{1-x}Sn_xTe$," Jpn. J. Appl. Phys. **21**, 1315.

Takayama, A., T. Sato, S. Souma, T. Oguchi, and T. Takahashi, 2015, "One-Dimensional Edge States with Giant Spin Splitting in a Bismuth Thin Film," Phys. Rev. Lett. **114**, 066402.

Tanaka, Y., Z. Ren, T. Sato, K. Nakayama, S. Souma, T. Takahashi, K. Segawa, and Y. Ando, 2012, "Experimental Realization of a Topological Crystalline Insulator in SnTe," Nat. Phys. **8**, 800.

Tang, E., and L. Fu, 2014, "Strain-Induced Partially Flat Band, Helical Snake States and Interface Superconductivity in Topological Crystalline Insulators," Nat. Phys. **10**, 964.

Tang, J., *et al.*, 2014, "Electrical Detection of Spin-Polarized Surface States Conduction in $(Bi_{0.5}Sb_{0.47})_2Te_3$ Topological Insulator," Nano Lett. **14**, 5423.

Tang, P., B. Yan, W. Cao, S.-C. Wu, C. Felser, and W. Duan, 2014, "Weak Topological Insulators Induced by the Interlayer Coupling: A First-Principles Study of Stacked Bi_2TeI," Phys. Rev. B **89**, 041409.

Taskin, A. A., Z. Ren, S. Sasaki, K. Segawa, and Y. Ando, 2011, "Observation of Dirac Holes and Electrons in a Topological Insulator," Phys. Rev. Lett. **107**, 016801.

Taskin, A. A., F. Yang, S. Sasaki, K. Segawa, and Y. Ando, 2014, "Topological Surface Transport in Epitaxial SnTe Thin Films Grown on Bi_2Te_3," Phys. Rev. B **89**, 121302.

Teague, M. L., H. Chu, F.-X. Xiu, L. He, K.-L. Wang, and N.-C. Yeh, 2012, "Observation of Fermi-Energy Dependent Unitary Impurity Resonances in a Strong Topological Insulator Bi_2Se_3 with Scanning Tunneling Spectroscopy," Solid State Commun. **152**, 747.

Teo, J. C. Y., L. Fu, and C. L. Kane, 2008, "Surface States and Topological Invariants in Three-Dimensional Topological Insulators: Application to $Bi_{1-x}Sb_x$," Phys. Rev. B **78**, 045426.

Teo, J. C. Y., and C. L. Kane, 2014, "From Luttinger Liquid to Non-Abelian Quantum Hall States," Phys. Rev. B **89**, 085101.

Thomas, S., D. J. Kim, S. B. Chung, T. Grant, Z. Fisk, and J. Xia, 2013, "Weak Antilocalization and Linear Magnetoresistance in The Surface State of SmB_6," arXiv:1307.4133, http://arxiv.org/abs/1307.4133.

Thouless, D. J., M. Kohmoto, M. P. Nightingale, and M. den Nijs, 1982, "Quantized Hall Conductance in a Two-Dimensional Periodic Potential," Phys. Rev. Lett. **49**, 405.

Tian, M., W. Ning, Z. Qu, H. Du, J. Wang, and Y. Zhang, 2013, "Dual Evidence of Surface Dirac States in Thin Cylindrical Topological Insulator Bi_2Te_3 Nanowires," Sci. Rep. **3**, 1212.

Tian, M., J. Wang, W. Ning, T. E. Mallouk, and M. H. W. Chan, 2015, "Surface Superconductivity in Thin Cylindrical Bi Nanowire," Nano Lett. **15**, 1487.

Tokura, Y., and H. Y. Hwang, 2008, "Condensed-Matter Physics: Complex Oxides on Fire," Nat. Mater. **7**, 694.

Tran, M. K., *et al.*, 2014, "Infrared- and Raman-Spectroscopy Measurements of a Transition in the Crystal Structure and a Closing of the Energy Gap of BiTeI under Pressure," Phys. Rev. Lett. **112**, 047402.

Tsai, W.-F., C.-Y. Huang, T.-R. Chang, H. Lin, H.-T. Jeng, and A. Bansil, 2013, "Gated Silicene as a Tunable Source of Nearly 100% Spin-Polarized Electrons," Nat. Commun. **4**, 1500.

Tsipas, P., *et al.*, 2014, "Observation of Surface Dirac Cone in High-Quality Ultrathin Epitaxial Bi_2Se_3 Topological Insulator on AlN (0001) Dielectric," ACS Nano **8**, 6614.

Tsutsumi, Y., M. Ishikawa, T. Kawakami, T. Mizushima, M. Sato, M. Ichioka, and K. Machida, 2013, "UPt_3 as a Topological Crystalline Superconductor," J. Phys. Soc. Jpn. **82**, 113707.

Turner, A. M., and A. Vishwanath, 2013, "Beyond Band Insulators: Topology of Semi-Metals and Interacting Phases," arXiv:1301.0330, http://arxiv.org/abs/1301.0330.

Ueda, K., J. Fujioka, Y. Takahashi, T. Suzuki, S. Ishiwata, Y. Taguchi, M. Kawasaki, and Y. Tokura, 2014, "Anomalous Domain-Wall Conductance in Pyrochlore-Type $Nd_2Ir_2O_7$ on the Verge of the Metal-Insulator Transition," Phys. Rev. B **89**, 075127.

Vaezi, A., Y. Liang, D. H. Ngai, L. Yang, and E.-A. Kim, 2013, "Topological Edge States at a Tilt Boundary in Gated Multilayer Graphene," Phys. Rev. X **3**, 021018.

Vafek, O., and A. Vishwanath, 2014, "Dirac Fermions in Solids: From High-Tc Cuprates and Graphene to Topological Insulators and Weyl Semimetals," Annu. Rev. Condens. Matter Phys. **5**, 83.

Valdés Aguilar, R., *et al.*, 2012, "Terahertz Response and Colossal Kerr Rotation from the Surface States of the Topological Insulator Bi_2Se_3," Phys. Rev. Lett. **108**, 087403.

Valla, T., *et al.*, 2012, "Topological Semimetal in a Bi-Bi_2Se_3 Infinitely Adaptive Superlattice Phase," Phys. Rev. B **86**, 241101.

Vargas, A., S. Basak, F. Liu, B. Wang, E. Panaitescu, H. Lin, R. Markiewicz, A. Bansil, and S. Kar, 2014, "The Changing Colors of a Quantum-Confined Topological Insulator," ACS Nano **8**, 1222.

Vogt, P., P. De Padova, C. Quaresima, J. Avila, E. Frantzeskakis, M. C. Asensio, A. Resta, B. Ealet, and G. Le Lay, 2012, "Silicene: Compelling Experimental Evidence for Graphenelike Two-Dimensional Silicon," Phys. Rev. Lett. **108**, 155501.

Volovik, G. E., 1988, "Quantized Hall Effect in Superfluid Helium-3 Film," Phys. Lett. A **128**, 277.

Wada, M., S. Murakami, F. Freimuth, and G. Bihlmayer, 2011, "Localized Edge States in Two-Dimensional Topological Insulators: Ultrathin Bi Films," Phys. Rev. B **83**, 121310.

Wan, X., and S. Y. Savrasov, 2014, "Turning a Band Insulator into an Exotic Superconductor," Nat. Commun. **5**, 4144.

Wan, X., A. M. Turner, A. Vishwanath, and S. Y. Savrasov, 2011, "Topological Semimetal and Fermi-Arc Surface States in the Electronic Structure of Pyrochlore Iridates," Phys. Rev. B **83**, 205101.

Wan, X., A. Vishwanath, and S. Y. Savrasov, 2012, "Computational Design of Axion Insulators Based on 5d Spinel Compounds," Phys. Rev. Lett. **108**, 146601.

Wang, E., *et al.*, 2013, "Fully Gapped Topological Surface States in Bi_2Se_3 Films Induced by a D-Wave High-Temperature Superconductor," Nat. Phys. **9**, 621.

Wang, J., J. Liu, Y. Xu, J. Wu, B.-L. Gu, and W. Duan, 2014, "Structural Stability and Topological Surface States of the SnTe (111) Surface," Phys. Rev. B **89**, 125308.

Wang, K., D. Graf, H. Lei, S. W. Tozer, and C. Petrovic, 2011, "Quantum Transport of Two-Dimensional Dirac Fermions in $SrMnBi_2$," Phys. Rev. B **84**, 220401.

Wang, K., D. Graf, and C. Petrovic, 2014, "Large Magnetothermopower and Fermi Surface Reconstruction in Sb_2Te_2Se," Phys. Rev. B **89**, 125202.

Wang, K., and C. Petrovic, 2012, "Multiband Effects and Possible Dirac States in $LaAgSb_2$," Phys. Rev. B **86**, 155213.
Wang, L.-L., and D. D. Johnson, 2011, "Ternary Tetradymite Compounds as Topological Insulators," Phys. Rev. B **83**, 241309.
Wang, M.-X., *et al.*, 2012, "The Coexistence of Superconductivity and Topological Order in the Bi_2Se_3 Thin Films," Science **336**, 52.
Wang, N., D. West, J. Liu, J. Li, Q. Yan, B.-L. Gu, S. B. Zhang, and W. Duan, 2014, "Microscopic Origin of the P-Type Conductivity of the Topological Crystalline Insulator SnTe and the Effect of Pb Alloying," Phys. Rev. B **89**, 045142.
Wang, Q.-H., D. Wang, and F.-C. Zhang, 2010, "Electronic Structure near an Impurity and Terrace on the Surface of a Three-Dimensional Topological Insulator," Phys. Rev. B **81**, 035104.
Wang, R., B. Wang, R. Shen, L. Sheng, and D. Y. Xing, 2014, "Floquet Weyl Semimetal Induced by off-Resonant Light," Europhys. Lett. **105**, 17004.
Wang, W., Y. Du, G. Xu, X. Zhang, E. Liu, Z. Liu, Y. Shi, J. Chen, G. Wu, and X. Zhang, 2013, "Large Linear Magnetoresistance and Shubnikov-de Hass Oscillations in Single Crystals of YPdBi Heusler Topological Insulators," Sci. Rep. **3**, 2181.
Wang, X., G. Bian, P. Wang, and T.-C. Chiang, 2015, "Dirac Semimetal Films as Spin Conductors on Topological Substrates," Phys. Rev. B **91**, 125103.
Wang, X., and T.-C. Chiang, 2014, "Topological States in Bi_2Se_3 Surfaces Created by Cleavage within a Quintuple Layer: Analysis in Terms of the Shockley Criterion," Phys. Rev. B **89**, 125109.
Wang, Y., *et al.*, 2012, "Gate-Controlled Surface Conduction in Na-Doped Bi_2Te_3 Topological Insulator Nanoplates," Nano Lett. **12**, 1170.
Wang, Y. H., H. Steinberg, P. Jarillo-Herrero, and N. Gedik, 2013, "Observation of Floquet-Bloch States on the Surface of a Topological Insulator," Science **342**, 453.
Wang, Y. J., H. Lin, T. Das, M. Z. Hasan, and A. Bansil, 2011, "Topological Insulators in the Quaternary Chalcogenide Compounds and Ternary Famatinite Compounds," New J. Phys. **13**, 085017.
Wang, Y. J., W.-F. Tsai, H. Lin, S.-Y. Xu, M. Neupane, M. Z. Hasan, and A. Bansil, 2013, "Nontrivial Spin Texture of the Coaxial Dirac Cones on the Surface of Topological Crystalline Insulator SnTe," Phys. Rev. B **87**, 235317.
Wang, Z., Y. Sun, X.-Q. Chen, C. Franchini, G. Xu, H. Weng, X. Dai, and Z. Fang, 2012, "Dirac Semimetal and Topological Phase Transitions in A_3Bi ($A = Na, K, Rb$)," Phys. Rev. B **85**, 195320.
Wang, Z., H. Weng, Q. Wu, X. Dai, and Z. Fang, 2013, "Three-Dimensional Dirac Semimetal and Quantum Transport in Cd_3As_2," Phys. Rev. B **88**, 125427.
Wang, Z., and S.-C. Zhang, 2012, "Simplified Topological Invariants for Interacting Insulators," Phys. Rev. X **2**, 031008.
Wang, Z., and S.-C. Zhang, 2013, "Chiral Anomaly, Charge Density Waves, and Axion Strings from Weyl Semimetals," Phys. Rev. B **87**, 161107.
Wang, Z. F., L. Chen, and F. Liu, 2014, "Tuning Topological Edge States of Bi(111) Bilayer Film by Edge Adsorption," Nano Lett. **14**, 2879.
Wang, Z. F., Z. Liu, and F. Liu, 2013a, "Organic Topological Insulators in Organometallic Lattices," Nat. Commun. **4**, 1471.
Wang, Z. F., Z. Liu, and F. Liu, 2013b, "Quantum Anomalous Hall Effect in 2D Organic Topological Insulators," Phys. Rev. Lett. **110**, 196801.
Wang, Z. F., N. Su, and F. Liu, 2013, "Prediction of a Two-Dimensional Organic Topological Insulator," Nano Lett. **13**, 2842.
Wang, Z. F., M.-Y. Yao, W. Ming, L. Miao, F. Zhu, C. Liu, C. L. Gao, D. Qian, J.-F. Jia, and F. Liu, 2013, "Creation of Helical Dirac Fermions by Interfacing Two Gapped Systems of Ordinary Fermions," Nat. Commun. **4**, 1384.
Weeks, C., J. Hu, J. Alicea, M. Franz, and R. Wu, 2011, "Engineering a Robust Quantum Spin Hall State in Graphene via Adatom Deposition," Phys. Rev. X **1**, 021001.
Wehling, T. O., A. M. Black-Schaffer, and A. V. Balatsky, 2014, "Dirac Materials," Adv. Phys. **63**, 1.
Wei, P., F. Katmis, B. A. Assaf, H. Steinberg, P. Jarillo-Herrero, D. Heiman, and J. S. Moodera, 2013, "Exchange-Coupling-Induced Symmetry Breaking in Topological Insulators," Phys. Rev. Lett. **110**, 186807.
Wells, J. W., *et al.*, 2009, "Nondegenerate Metallic States on Bi(114): A One-Dimensional Topological Metal," Phys. Rev. Lett. **102**, 096802.
Wen, X.-G., 1995, "Topological Orders and Edge Excitations in Fractional Quantum Hall States," Adv. Phys. **44**, 405.
Weng, H., X. Dai, and Z. Fang, 2014, "Transition-Metal Pentatelluride $ZrTe_5$ and $HfTe_5$: A Paradigm for Large-Gap Quantum Spin Hall Insulators," Phys. Rev. X **4**, 011002.
Weng, H., C. Fang, Z. Fang, B. A. Bernevig, and X. Dai, 2015, "Weyl Semimetal Phase in Noncentrosymmetric Transition-Metal Monophosphides," Phys. Rev. X **5**, 011029.
Weng, H., J. Zhao, Z. Wang, Z. Fang, and X. Dai, 2014, "Topological Crystalline Kondo Insulator in Mixed Valence Ytterbium Borides," Phys. Rev. Lett. **112**, 016403.
Weyl, H., 1929, "Elektron Und Gravitation I," Z. Phys. **56**, 330.
Wilczek, F., 1987, "Two Applications of Axion Electrodynamics," Phys. Rev. Lett. **58**, 1799.
Wrasse, E. O., and T. M. Schmidt, 2014, "Prediction of Two-Dimensional Topological Crystalline Insulator in PbSe Mono Layer," Nano Lett. **14**, 5717.
Wray, L. A., S.-Y. Xu, Y. Xia, Y. S. Hor, D. Qian, A. V. Fedorov, H. Lin, A. Bansil, R. J. Cava, and M. Z. Hasan, 2010, "Observation of Topological Order in a Superconducting Doped Topological Insulator," Nat. Phys. **6**, 855.
Wray, L. A., S.-Y. Xu, Y. Xia, D. Hsieh, A. V. Fedorov, Y. S. Hor, R. J. Cava, A. Bansil, H. Lin, and M. Z. Hasan, 2011, "A Topological Insulator Surface under Strong Coulomb, Magnetic and Disorder Perturbations," Nat. Phys. **7**, 32.
Wu, G., H. Chen, Y. Sun, X. Li, P. Cui, C. Franchini, J. Wang, X.-Q. Chen, and Z. Zhang, 2013, "Tuning the Vertical Location of Helical Surface States in Topological Insulator Heterostructures via Dual-Proximity Effects," Sci. Rep. **3**, 1233.
Wu, L., M. Brahlek, R. Valdés Aguilar, A. V. Stier, C. M. Morris, Y. Lubashevsky, L. S. Bilbro, N. Bansal, S. Oh, and N. P. Armitage, 2013, "A Sudden Collapse in the Transport Lifetime across the Topological Phase Transition in $(Bi_{1-x}In_x)_2Se_3$," Nat. Phys. **9**, 410.
Wunsch, B., F. Guinea, and F. Sols, 2008, "Dirac-Point Engineering and Topological Phase Transitions in Honeycomb Optical Lattices," New J. Phys. **10**, 103027.
Xia, Y., *et al.*, 2009, "Observation of a Large-Gap Topological-Insulator Class with a Single Dirac Cone on the Surface," Nat. Phys. **5**, 398.
Xiao, D., M.-C. Chang, and Q. Niu, 2010, "Berry Phase Effects on Electronic Properties," Rev. Mod. Phys. **82**, 1959.
Xiao, D., Y. Yao, W. Feng, J. Wen, W. Zhu, X.-Q. Chen, G. M. Stocks, and Z. Zhang, 2010, "Half-Heusler Compounds as a New Class of Three-Dimensional Topological Insulators," Phys. Rev. Lett. **105**, 096404.
Xiao, D., W. Zhu, Y. Ran, N. Nagaosa, and S. Okamoto, 2011, "Interface Engineering of Quantum Hall Effects in Digital Transition Metal Oxide Heterostructures," Nat. Commun. **2**, 596.

Xiong, J., A. C. Petersen, D. Qu, Y. S. Hor, R. J. Cava, and N. P. Ong, 2012, "Quantum Oscillations in a Topological Insulator Bi_2Te_2Se with Large Bulk Resistivity," Physica E (Amsterdam) **44**, 917.

Xu, G., H. Weng, Z. Wang, X. Dai, and Z. Fang, 2011, "Chern Semimetal and the Quantized Anomalous Hall Effect in $HgCr_2Se_4$," Phys. Rev. Lett. **107**, 186806.

Xu, N., *et al.*, 2013, "Surface and Bulk Electronic Structure of the Strongly Correlated System SmB_6 and Implications for a Topological Kondo Insulator," Phys. Rev. B **88**, 121102.

Xu, R., A. Husmann, T. F. Rosenbaum, M.-L. Saboungi, J. E. Enderby, and P. B. Littlewood, 1997, "Large Magnetoresistance in Non-Magnetic Silver Chalcogenides," Nature (London) **390**, 57.

Xu, S.-Y., *et al.*, 2010, "Discovery of Several Large Families of Topological Insulator Classes with Backscattering-Suppressed Spin-Polarized Single-Dirac-Cone on the Surface," arXiv:1007.5111, http://arxiv.org/abs/1007.5111.

Xu, S.-Y., *et al.*, 2011, "Topological Phase Transition and Texture Inversion in a Tunable Topological Insulator," Science **332**, 560.

Xu, S.-Y., *et al.*, 2012a, "Observation of a Topological Crystalline Insulator Phase and Topological Phase Transition in $Pb_{1-x}Sn_xTe$," Nat. Commun. **3**, 1192.

Xu, S.-Y., *et al.*, 2012b, "Hedgehog Spin Texture and Berry's Phase Tuning in a Magnetic Topological Insulator," Nat. Phys. **8**, 616.

Xu, S.-Y., *et al.*, 2015a, "Discovery of A Weyl Fermion State with Fermi Arcs in Niobium Arsenide," Nat. Phys. **11**, 748.

Xu, S.-Y., *et al.*, 2015b, "Discovery of a Weyl Fermion semimetal and topological Fermi arcs," Science **349**, 613.

Xu, S.-Y., *et al.*, 2015c, "Observation of Fermi Arc Surface States in a Topological Metal," Science **347**, 294.

Xu, S.-Y., *et al.*, 2015d, "Unconventional Transformation of Spin Dirac Phase across a Topological Quantum Phase Transition," Nat. Commun. **6**, 6870.

Xu, Y., I. Miotkowski, C. Liu, J. Tian, H. Nam, N. Alidoust, J. Hu, C.-K. Shih, M. Z. Hasan, and Y. P. Chen, 2014, "Observation of Topological Surface State Quantum Hall Effect in an Intrinsic Three-Dimensional Topological Insulator," Nat. Phys. **10**, 956.

Xu, Y., B. Yan, H.-J. Zhang, J. Wang, G. Xu, P. Tang, W. Duan, and S.-C. Zhang, 2013, "Large-Gap Quantum Spin Hall Insulators in Tin Films," Phys. Rev. Lett. **111**, 136804.

Yan, B., M. Jansen, and C. Felser, 2013, "A Large-Energy-Gap Oxide Topological Insulator Based on the Superconductor $BaBiO_3$," Nat. Phys. **9**, 709.

Yan, B., C.-X. Liu, H.-J. Zhang, C.-Y. Yam, X.-L. Qi, T. Frauenheim, and S.-C. Zhang, 2010, "Theoretical Prediction of Topological Insulators in Thallium-Based III-V-VI2 Ternary Chalcogenides," Europhys. Lett. **90**, 37002.

Yan, B., L. Müchler, X.-L. Qi, S.-C. Zhang, and C. Felser, 2012, "Topological Insulators in Filled Skutterudites," Phys. Rev. B **85**, 165125.

Yan, B., H.-J. Zhang, C.-X. Liu, X.-L. Qi, T. Frauenheim, and S.-C. Zhang, 2010, "Theoretical Prediction of Topological Insulator in Ternary Rare Earth Chalcogenides," Phys. Rev. B **82**, 161108.

Yan, B., and S.-C. Zhang, 2012, "Topological Materials," Rep. Prog. Phys. **75**, 096501.

Yan, Y., Z.-M. Liao, Y.-B. Zhou, H.-C. Wu, Y.-Q. Bie, J.-J. Chen, J. Meng, X.-S. Wu, and D.-P. Yu, 2013, "Synthesis and Quantum Transport Properties of Bi_2Se_3 Topological Insulator Nanostructures," Sci. Rep. **3**, 1264.

Yan, Y., *et al.*, 2014, "Topological Surface State Enhanced Photothermoelectric Effect in Bi_2Se_3 Nanoribbons," Nano Lett. **14**, 4389.

Yang, B.-J., and Y. B. Kim, 2010, "Topological Insulators and Metal-Insulator Transition in the Pyrochlore Iridates," Phys. Rev. B **82**, 085111.

Yang, F., A. A. Taskin, S. Sasaki, K. Segawa, Y. Ohno, K. Matsumoto, and Y. Ando, 2015, "Dual-Gated Topological Insulator Thin-Film Device for Efficient Fermi-Level Tuning," ACS Nano **9**, 4050.

Yang, K., W. Setyawan, S. Wang, M. Buongiorno Nardelli, and S. Curtarolo, 2012, "A Search Model for Topological Insulators with High-Throughput Robustness Descriptors," Nat. Mater. **11**, 614.

Yang, K.-Y., Y.-M. Lu, and Y. Ran, 2011, "Quantum Hall Effects in a Weyl Semimetal: Possible Application in Pyrochlore Iridates," Phys. Rev. B **84**, 075129.

Yang, L. X., *et al.*, 2015, "Weyl Semimetal Phase in the Non-Centrosymmetric Compound TaAs," Nat. Phys. **11**, 728.

Yang, M., and W.-M. Liu, 2014, "The D-P Band-Inversion Topological Insulator in Bismuth-Based Skutterudites," Sci. Rep. **4**, 5131.

Yao, G., Z. Luo, F. Pan, W. Xu, Y. P. Feng, and X. Wang, 2013, "Evolution of Topological Surface States in Antimony Ultra-Thin Films," Sci. Rep. **3**, 2010.

Ye, F., S. Chi, B. C. Chakoumakos, J. A. Fernandez-Baca, T. Qi, and G. Cao, 2013, "Magnetic and Crystal Structures of Sr_2IrO_4: A Neutron Diffraction Study," Phys. Rev. B **87**, 140406.

Yee, M. M., Y. He, A. Soumyanarayanan, D.-J. Kim, Z. Fisk, and J. E. Hoffman, 2013, "Imaging the Kondo Insulating Gap on SmB_6," arXiv:1308.1085, http://arxiv.org/abs/1308.1085.

Yi, H., *et al.*, 2014, "Evidence of Topological Surface State in Three-Dimensional Dirac Semimetal Cd_3As_2," Sci. Rep. **4**, 6106.

Yoshimi, R., A. Tsukazaki, K. Kikutake, J. G. Checkelsky, K. S. Takahashi, M. Kawasaki, and Y. Tokura, 2014, "Dirac Electron States Formed at the Heterointerface between a Topological Insulator and a Conventional Semiconductor," Nat. Mater. **13**, 253.

Yoshimi, R., A. Tsukazaki, Y. Kozuka, J. Falson, K. S. Takahashi, J. G. Checkelsky, N. Nagaosa, M. Kawasaki, and Y. Tokura, 2015, "Quantum Hall Effect on Top and Bottom Surface States of Topological Insulator $(Bi_{1-x}Sb_x)_2Te_3$ Films," Nat. Commun. **6**, 6627.

You, Y.-Z., I. Kimchi, and A. Vishwanath, 2012, "Doping a Spin-Orbit Mott Insulator: Topological Superconductivity from the Kitaev-Heisenberg Model and Possible Application to $(Na_2/Li_2)IrO_3$," Phys. Rev. B **86**, 085145.

Young, A. F., J. D. Sanchez-Yamagishi, B. Hunt, S. H. Choi, K. Watanabe, T. Taniguchi, R. C. Ashoori, and P. Jarillo-Herrero, 2014, "Tunable Symmetry Breaking and Helical Edge Transport in a Graphene Quantum Spin Hall State," Nature (London) **505**, 528.

Young, M. W., S.-S. Lee, and C. Kallin, 2008, "Fractionalized Quantum Spin Hall Effect," Phys. Rev. B **78**, 125316.

Young, S. M., S. Zaheer, J. C. Y. Teo, C. L. Kane, E. J. Mele, and A. M. Rappe, 2012, "Dirac Semimetal in Three Dimensions," Phys. Rev. Lett. **108**, 140405.

Yu, R., W. Zhang, H.-J. Zhang, S.-C. Zhang, X. Dai, and Z. Fang, 2010, "Quantized Anomalous Hall Effect in Magnetic Topological Insulators," Science **329**, 61.

Zeljkovic, I., *et al.*, 2014, "Mapping the Unconventional Orbital Texture in Topological Crystalline Insulators," Nat. Phys. **10**, 572.

Zeljkovic, I., *et al.*, 2015a, "Dirac Mass Generation from Crystal Symmetry Breaking on the Surfaces of Topological Crystalline Insulators," Nat. Mater. **14**, 318.

Zeljkovic, I., *et al.*, 2015b, "Nanoscale Determination of the Mass Enhancement Factor in the Lightly Doped Bulk Insulator Lead Selenide," Nat. Commun. **6**, 6559.

Zhang, C., *et al.*, 2016, "Signatures of the Adler-Bell-Jackiw Chiral Anomaly in a Weyl Fermion Semimetal," Nat. Commun. **7**, 10735.
Zhang, D., W. Lou, M. Miao, S. Zhang, and K. Chang, 2013, "Interface-Induced Topological Insulator Transition in GaAs/Ge/GaAs Quantum Wells," Phys. Rev. Lett. **111**, 156402.
Zhang, D., *et al.*, 2012, "Interplay between Ferromagnetism, Surface States, and Quantum Corrections in a Magnetically Doped Topological Insulator," Phys. Rev. B **86**, 205127.
Zhang, F., C. L. Kane, and E. J. Mele, 2013, "Topological Mirror Superconductivity," Phys. Rev. Lett. **111**, 056403.
Zhang, H., C.-X. Liu, X.-L. Qi, X. Dai, Z. Fang, and S.-C. Zhang, 2009, "Topological Insulators in Bi_2Se_3, Bi_2Te_3 and Sb_2Te_3 with a Single Dirac Cone on the Surface," Nat. Phys. **5**, 438.
Zhang, H., and S.-C. Zhang, 2013, "Topological Insulators from the Perspective of First-Principles Calculations," Phys. Status Solidi RRL **7**, 72.
Zhang, H. B., H. L. Yu, D. H. Bao, S. W. Li, C. X. Wang, and G. W. Yang, 2012, "Weak Localization Bulk State in a Topological Insulator Bi_2Te_3 Film," Phys. Rev. B **86**, 075102.
Zhang, H.-J., S. Chadov, L. Müchler, B. Yan, X.-L. Qi, J. Kübler, S.-C. Zhang, and C. Felser, 2011, "Topological Insulators in Ternary Compounds with a Honeycomb Lattice," Phys. Rev. Lett. **106**, 156402.
Zhang, J., B. Zhao, and Z. Yang, 2013, "Abundant Topological States in Silicene with Transition Metal Adatoms," Phys. Rev. B **88**, 165422.
Zhang, J., *et al.*, 2011, "Band Structure Engineering in $(Bi_{1-x}Sb_x)_2Te_3$ Ternary Topological Insulators," Nat. Commun. **2**, 574.
Zhang, J., *et al.*, 2013, "Topology-Driven Magnetic Quantum Phase Transition in Topological Insulators," Science **339**, 1582.
Zhang, J.-M., W. Zhu, Y. Zhang, D. Xiao, and Y. Yao, 2012, "Tailoring Magnetic Doping in the Topological Insulator Bi_2Se_3," Phys. Rev. Lett. **109**, 266405.
Zhang, P., Z. Liu, W. Duan, F. Liu, and J. Wu, 2012, "Topological and Electronic Transitions in a Sb(111) Nanofilm: The Interplay between Quantum Confinement and Surface Effect," Phys. Rev. B **85**, 201410.
Zhang, Q., Z. Zhang, Z. Zhu, U. Schwingenschlögl, and Y. Cui, 2012, "Exotic Topological Insulator States and Topological Phase Transitions in Sb_2Se_3-Bi_2Se_3 Heterostructures," ACS Nano **6**, 2345.
Zhang, S. J., *et al.*, 2012, "The Comprehensive Phase Evolution for Bi_2Te_3 Topological Compound as Function of Pressure," J. Appl. Phys. **111**, 112630.
Zhang, S.-C., and J. Hu, 2001, "A Four-Dimensional Generalization of the Quantum Hall Effect," Science **294**, 823.
Zhang, T., *et al.*, 2009, "Experimental Demonstration of Topological Surface States Protected by Time-Reversal Symmetry," Phys. Rev. Lett. **103**, 266803.
Zhang, W., R. Yu, W. Feng, Y. Yao, H. Weng, X. Dai, and Z. Fang, 2011, "Topological Aspect and Quantum Magnetoresistance of $\beta - Ag_2Te$," Phys. Rev. Lett. **106**, 156808.
Zhang, X., N. P. Butch, P. Syers, S. Ziemak, R. L. Greene, and J. Paglione, 2013, "Hybridization, Inter-Ion Correlation, and Surface States in the Kondo Insulator SmB_6," Phys. Rev. X **3**, 011011.
Zhang, X., H. Zhang, J. Wang, C. Felser, and S.-C. Zhang, 2012, "Actinide Topological Insulator Materials with Strong Interaction," Science **335**, 1464.
Zhang, Y. *et al.*, 2010, "Crossover of the Three-Dimensional Topological Insulator Bi_2Se_3 to the Two-Dimensional Limit," Nat. Phys. **6**, 584.
Zhao, J.-Z., F. Lu, H. Weng, Z. Fang, and X. Dai, 2014, "SmS: A Mixed Valence Semi-Metal with Topological Band Structure," in *Bulletin of the American Physical Society* (American Physical Society), Vol. 59, No. 1, http://meetings.aps.org/link/BAPS.2014.MAR.D43.5.
Zhao, L., H. Deng, I. Korzhovska, Z. Chen, M. Konczykowski, A. Hruban, V. Oganesyan, and L. Krusin-Elbaum, 2014, "Singular Robust Room-Temperature Spin Response from Topological Dirac Fermions," Nat. Mater. **13**, 580.
Zhao, L., P. Tang, B.-L. Gu, and W. Duan, 2013, "Field-Effect Birefringent Spin Lens in Ultrathin Film of Magnetically Doped Topological Insulators," Phys. Rev. Lett. **111**, 116601.
Zhao, Y., *et al.*, 2014, "Crossover from 3D to 2D Quantum Transport in Bi_2Se_3/In_2Se_3 Superlattices," Nano Lett. **14**, 5244.
Zhao, Z., S. Wang, H. Zhang, and W. L. Mao, 2013, "Pressure-Induced Structural Transitions and Metallization in Ag_2Te," Phys. Rev. B **88**, 024120.
Zholudev, M., *et al.*, 2012, "Magnetospectroscopy of Two-Dimensional HgTe-Based Topological Insulators around the Critical Thickness," Phys. Rev. B **86**, 205420.
Zhong, R. D., J. A. Schneeloch, X. Y. Shi, Z. J. Xu, C. Zhang, J. M. Tranquada, Q. Li, and G. D. Gu, 2013, "Optimizing the Superconducting Transition Temperature and Upper Critical Field of $Sn_{1-x}In_xTe$," Phys. Rev. B **88**, 020505.
Zhou, J.-J., W. Feng, C.-C. Liu, S. Guan, and Y. Yao, 2014, "Large-Gap Quantum Spin Hall Insulator in Single Layer Bismuth Monobromide Bi_4Br_4," Nano Lett. **14**, 4767.
Zhou, M., W. Ming, Z. Liu, Z. Wang, P. Li, and F. Liu, 2014, "Epitaxial Growth of Large-Gap Quantum Spin Hall Insulator on Semiconductor Surface," Proc. Natl. Acad. Sci. U.S.A. **111**, 14378.
Zhou, X., C. Fang, W.-F. Tsai, and J. Hu, 2009, "Theory of Quasiparticle Scattering in a Two-Dimensional System of Helical Dirac Fermions: Surface Band Structure of a Three-Dimensional Topological Insulator," Phys. Rev. B **80**, 245317.
Zhu, H., *et al.*, 2013, "Topological Insulator Bi_2Se_3 Nanowire High Performance Field-Effect Transistors," Sci. Rep. **3**, 1757.
Zhu, J., *et al.*, 2013, "Superconductivity in Topological Insulator Sb_2Te_3 Induced by Pressure," Sci. Rep. **3**, 2016.
Zhu, L., H. Wang, Y. Wang, J. Lv, Y. Ma, Q. Cui, Y. Ma, and G. Zou, 2011, "Substitutional Alloy of Bi and Te at High Pressure," Phys. Rev. Lett. **106**, 145501.
Zhu, X., L. Santos, R. Sankar, S. Chikara, C. Howard, F. C. Chou, C. Chamon, and M. El-Batanouny, 2011, "Interaction of Phonons and Dirac Fermions on the Surface of Bi_2Se_3: A Strong Kohn Anomaly," Phys. Rev. Lett. **107**, 186102.
Zhu, X.-G., and P. Hofmann, 2014, "Topological Surface States on $Bi_{1-x}Sb_x$: Dependence on Surface Orientation, Termination, and Stability," Phys. Rev. B **89**, 125402.
Zhu, X.-G., M. Stensgaard, L. Barreto, W. S. e Silva, S. Ulstrup, M. Michiardi, M. Bianchi, M. Dendzik, and P. Hofmann, 2013, "Three Dirac Points on the (110) Surface of the Topological Insulator $Bi_{1-x}Sb_x$," New J. Phys. **15**, 103011.
Zhu, Z.-H., A. Nicolaou, G. Levy, N. P. Butch, P. Syers, X. F. Wang, J. Paglione, G. A. Sawatzky, I. S. Elfimov, and A. Damascelli, 2013, "Polarity-Driven Surface Metallicity in SmB_6," Phys. Rev. Lett. **111**, 216402.